Die approbierte Originalversion dieser Dissertation ist an der Hauptbibliothek der Technischen Universität Wien aufgestellt (http://www.ub.tuwien.ac.at).

The approved original version of this thesis is available at the main library of the Vienna University of Technology (http://www.ub.tuwien.ac.at/englweb/).

TECHNISCHE UNIVERSITÄT WIEN
Vienna University of Technology

DISSERTATION

From Chip Surface to Signal Amplification: Protein Microarrays for Disease Biomarker Detection

ausgeführt zum Zwecke der Erlangung des akademischen Grades eines Doktors der technischen Wissenschaften unter der Leitung von

Univ.Doz. Dipl.-Ing. Dr.techn. Georg Haberhauer, MBA

Vizerektorat für Strategische Entwicklung der Universität für Bodenkultur Wien

und

Dipl.-Ing. Dr.techn. Claudia Preininger

AIT Austrian Institute of Technology GmbH, Health & Environment / Bioresources

eingereicht an der Technischen Universität Wien
Fakultät für Technische Chemie

von

DI Patrick Domnanich

Matr. Nr. 0125518
Arakawastr. 6/2/25
A-1220 Wien

Wien, am 28.09.2010

Kurzfassung der Dissertation

Protein Microarrays sind eine zukunftsträchtige Technologie mit zahlreichen Anwendungen in der klinischen Forschung und Diagnostik. Sie erlauben die gleichzeitige Analyse ganzer Sets von Biomarkern, die Rückschlüsse auf Krankheitsstadium und Verlauf zulassen. Dies ermöglicht einen weiteren Schritt in Richtung personalisierter Medizin, in der auf den Patienten abgestimmte, verträglichere Therapien Anwendung finden.

Das Melanom, eine besonders aggressive Form des Hautkrebses, zeichnet sich durch einen auffallend unberechenbaren klinischen Verlauf aus, der durch die derzeitigen Bewertungskriterien nur ungenügend erfasst wird.

Um die Prognosestellung zu erleichtern wurde in dieser Arbeit ein Protein Microarray zur simultanen und parallelen Analyse von fünf Melanom-Markern in Patientenblut entwickelt. Der Chip quantifiziert sowohl die spezifischen Prognose- und Staging-Faktoren S100B und Vascular Endothelial Growth Factor A (VEGF-A), als auch die krankheitsrelevanten Entzündungsmediatoren und Immunfaktoren C-reaktives Protein (CRP), Interleukin 6 (IL6) und Interleukin 10 (IL10). Die einzelnen Tests sind als Sandwich Immunoassays implementiert und werden mittels Fluoreszenzmessung ausgelesen. Die Optimierung von Druckpuffer, Antikörperkonzentration, Assaypuffer und Inkubationszeit führte zu einer hohen Reproduzierbarkeit (Variabilitätskoeffizient < 20%) und niedrigen Cross-Reaktivität (< 0,5% mit anti IL10). Des Weiteren wurden Testsensitivitäten erreicht, die in der Größenordnung kommerzieller ELISA (enzyme-linked immunosorbent assay) Einzeltests liegen.

Während Interleukine in Konzentrationen von pg/mL detektiert werden müssen, liegen CRP Serum Konzentrationen normalerweise unter 3 mg/L und können im Fall einer Entzündung auf das Tausendfache ansteigen. Der CRP Antikörper Sandwich-Test weist jedoch nur einen Arbeitsbereich von 0.4 µg/L – 0.2 mg/L CRP auf. Um die parallele Messung von CRP zu ermöglichen, wurden RNA Aptamere als alternative Erkennungsmoleküle untersucht. Tatsächlich zeigten Aptamer-Antikörper Sandwichtests breitere Arbeitsbereiche (10 µg/L – 100 mg/L) und eine bessere Erfassung physiologischer CRP Konzentrationen.

Zur Sensitivitätssteigerung in Bezug auf niedrig konzentrierte Analyten, die nur schwache Fluoreszenzsignale liefern, wurde ein reflektierender Goldchip entwickelt, der mit Polyelektrolytmultilayern aus Xanthan und Chitosan beschichtet war. Auf diesen Signalverstärkungssubstraten waren die gemessenen Fluoreszenzintensitäten bis zu 50-mal so hoch wie auf Glaschips. In Bezug auf kommerzielle Chips wurde das Signal-Rausch-Verhältnis um bis zu Faktor 11 verbessert. Auch die Sensitivität stieg bis zu 38-fach an.

Schließlich werden in dieser Arbeit Metall-Affinitäts-Slides präsentiert, die auf Derivaten von Aminosäuren basieren. Diese Substrate ermöglichen die Immobilisierung von poly-Histidin-markierten Proteinen mittels Nickel-Chelat-Komplexbildung und erleichtern so den Aufbau von Assays mit gleichmäßig orientierten Proteinen. Die Slides wurden mit Hilfe der Photoelektronenspektroskopie charakterisiert und wiesen Selektivitäten > 95% für hexa-Histidin-markierte Proteine auf. Außerdem waren die Signalstärken bis zu sechsmal so hoch wie auf kommerziellen Substraten.

Abstract

Protein microarrays are an emerging technology in clinical diagnostics. They permit the analysis of an entire set of biomarkers reflecting disease stage and likelihood of progression. Thus they could give raise to new, less toxic therapies on an individual patient's basis.

Melanoma, a form of skin cancer, features a highly variable clinical course that is not predictable by current staging criteria. To facilitate establishment of a prognosis a protein microarray for the simultaneous and highly parallel analysis of five melanoma biomarkers in patients' blood serum was developed. The chip quantifies specific prognostic and staging factors S100B and Vascular Endothelial Growth Factor A (VEGF-A) as well as disease-related inflammatory and immunomodulatory parameters – C-reactive Protein (CRP), interleukins IL6 and IL10. Individual tests are implemented as sandwich immunoassays with streptavidin-biotin chemistry and fluorescence detection. Optimization of parameters such as print buffer composition, antibody concentrations, assay binding buffer and incubation time led to high reproducibility (coefficient of variation < 20%), weak cross-reactivity (<0.5% with anti-IL-10) and excellent sensitivities that are perfectly comparable to classical single-analyte enzyme-linked immunosorbent assay (ELISA) tests.

While interleukins have to be detected at the pg/mL scale, CRP serum concentrations are normally below 3 mg/L and rise by a factor of 1000 in response to an inflammatory stimulus. The CRP antibody sandwich assay features a working range of 0.4 µg/L – 0.2 mg/L CRP. To render possible the parallel analyte determination, in this thesis RNA aptamers were investigated as alternative binding elements. In fact aptamer-antibody sandwiches yielded broader working ranges (10 µg/L – 100 mg/L) and showed improved coverage of elevated physiological CRP concentrations.

To furthermore enhance the sensitivity for low abundant target proteins which only produce low fluorescence signals strengths, a reflective gold chip coated with xanthan chitosan polyelectrolyte multilayers is introduced. On this amplification substrate fluorescence signals are up to 50 times higher than on glass slides and in comparison to commercial substrates the signal to noise ratio is enhanced by up to factor 11. Also sensitivity increases up to 38 fold.

Finally this thesis reports on metal affinity slides based on amino acid derived ligands. These substrates enable the immobilisation of poly-histidine-tagged proteins via nickel-chelate complexes and thus facilitate the set-up of assays with uniformly oriented probe molecules. The slides are characterized by X-ray photoelectron spectroscopy (XPS) and show a

selectivity > 95% for tagged proteins in functional tests. Signal strengths are up to six times higher than on commercial products.

Acknowledgements

I am greatly indebted to Dr. Claudia Preininger for the possibility to write my PhD thesis at her group, for her considerable support, for the freedom I had to realize my own ideas and for the many possibilities to present my results here in Austria and abroad.

I also acknowledge my University Supervisor, Prof. Georg Haberhauer, for his advice and support.

I thank Ursula Sauer for encouragement and many fruitful discussions.

I would also like to thank my former and current PhD room colleagues Claudia, Stefan, Markus, Marlies, Milica, Kathi, Michi, Gudrun, Kuheli and Valerie for the good cooperation, the excellent working atmosphere, cookies and all the activities beyond the lab.

I acknowledge Melanie for endless discussions, for making me laugh and for the many trips in the company bus.

I also thank Dacimoneida Brito Peña, Katharina Drochter and Victoria Dorrer for their enthusiastic collaboration during their internships.

I am deeply indebted to my parents Brigitta and Friedrich for their continuous support without which this work would not have been possible.

Furthermore I thank Daniel and all other friends, who have contributed in their own manner to the materialization of this work, for their patience and support.

Contents

General Introduction **1**

1 Scope of the thesis 1

2 Protein Microarrays 3
2.1 History 3
2.2 Assay principles 4
2.2.1 Forward-phase microarrays 4
2.2.2 Reverse-phase microarrays 9
2.2.3 Functional protein arrays 10
2.3 Biomarkers 12

3 Chip fabrication 14
3.1 Microarray substrates 15
3.1.1 Binding principles 16
3.1.2 Coating techniques 22
3.1.3 Surface characterisation 23
3.2 Microarray printing 29
3.3 Probes 30
3.3.1 Antibodies 30
3.3.2 Aptamers 33
3.3.3 Other binding elements 35

4 Microarray processing 37

5 Detection 39
5.1 Optical label-free techniques 39
5.1.1 Surface plasmon resonance 39
5.1.2 Reflectometric interference spectroscopy 40
5.2 Optical label-based techniques 41
5.2.1 Fluorescence scanners 41
5.2.2 Fluorescence signal amplification techniques 43

6 References 47

Chapter 1 **54**

Protein microarray for the analysis of human melanoma biomarkers

Chapter 2 **62**

Aptamer-antibody on-chip sandwich immunoassay for detection of CRP in spiked serum

Chapter 3 **69**

Xanthan/chitosan gold chip for metal enhanced protein biomarker detection

Chapter 4 **89**

Iminodiacetic acid and carboxymethyl amino acids as metal chelate affinity ligands in protein microarrays

Chapter 5 **109**

Conference presentations

Final conclusions **117**

GENERAL INTRODUCTION

1 Scope of the thesis

Protein microarrays represent an increasingly powerful technology that has many advantages over the traditional enzyme linked immunoassay method. The chips are amenable to assay miniaturization and multiplexing and thus allow for a significant reduction in sample volume and processing time. Protein microarrays have been widely applied for high though-put drug screens, they have been used to study protein-protein interactions, and they have great potential for disease diagnosis.

In this thesis a protein microarray for biomarkers of melanoma, a highly malignant form of skin caner, is presented. The system quantifies five relevant serum proteins (S100B, VEGF-A, CRP, IL-6 and IL-10) in parallel. The influence of assay incubation time, spotting solution, probe concentration and assay binding buffer is investigated. Additionally, the manuscript highlights the importance of data analysis using a four-parameter logistic model. Parameters such as data reproducibility (% CV), slope of the calibration curves and coefficient of determination (R^2) are valuable guides in optimizing the chip system. The results of this study are presented in "Protein microarray for the analysis of human melanoma biomarkers" (Sensors and Actuators B: Chemical 139(1): 2-8).

In a second study a sandwich immunoassay which employs an RNA aptamer is used to attain an extended assay range for CRP. Low, high and medium physiological analyte levels can be determined from a single sample dilution as demonstrated in "Aptamer-antibody on-chip sandwich immunoassay for detection of CRP in spiked serum" (Biosensors and Bioelectronics 24(5): 1456-1461).

To increase immunoassay sensitivity for the detection of low abundant analytes such as cytokines, a reflective gold chip substrate coated with polyelectrolyte multilayers (PEM) was developed for metal enhanced signal amplification. Several (semi)natural polysaccharides are tested for PEM construction and thickness of the coating is optimized in respect to fluorescence signal strengths. Also performance of the substrates in comparison to commercial microarray slides is reported in "Xanthan/chitosan gold chip for metal enhanced protein biomarker detection" (submitted to Biosensors and Bioelectronics).

In the fourth paper affinity microarray surfaces for the orientation-specific presentation of protein probes were developed. Correct probe orientation assures exposure of the active protein site and is thus a valuable tool in the design of more sensitive assays. Surface chemistry is based on iminodiacetic acid and amino acid derivates that chelate nickel ions. Binding selectivity for hexa-histidine tagged proteins and the use of optimized spotting buffers are discussed in “Iminodiacetic acid and carboxymethyl amino acids as metal chelate affinity ligands in protein microarrays” (to be submitted to Anal. Biochem.).

1 Protein Microarrays

1.1 History

The completion of the human genome sequence by the Human Genome Project and Celera in 2000 has led to an unprecedented boost in biological information which has already proven useful in medical diagnosis and risk assessment [1]. In parallel biomedical research has rapidly advanced with the availability of technologies such as DNA arrays [2]. DNA array technology is based on the ability of one strand of DNA to bind a second strand in a specific and complementary way. This technique was successfully applied in genome-wide screenings of cellular gene expression profiles associated with conditions like cancer, heart disease [3], Alzheimer [4] and Crohn's disease [5]. Notwithstanding the great potential of DNA array technology, this approach has several limitations: Apart from the obvious fact that not nucleic acids but the encoded proteins carry out cellular functions it was found that messenger RNA levels do not always correlate with protein abundance levels [1]. Moreover the diversity of proteins generated from a single gene via post-translational modification and differential gene splicing leads to additional complexity in eukaryotes. It has also been found that some genes are never translated into proteins but rather function as RNAs [6]. Most notably changes in protein levels and other protein alterations hold important diagnostic clues as they may result from or foster specific diseases, or are induced by various external factors like toxic agents.

Until recently, analysis of global protein changes was almost exclusively performed using two-dimensional gel electrophoresis. Although this technique was applied in numerous studies investigating different cell lines and human bodily fluids, the approach is labor intensive, insensitive and proved resistant to high-throughput automation [1].

Proteomic research, which attempts to grasp the ensemble of proteins in a cell or organism at a certain time point, now begins to focus on protein chip technology. Traditionally applied methods encompass sequencing techniques, mass spectrometry for protein identification, X-ray scattering and nuclear magnetic resonance for the study of proteins' 3D-structure, the yeast two-hybrid system for investigating protein interactions and gel electrophoresis for elucidating protein expression. In this context protein microarrays have the potential to overcome some of the limitations of two-dimensional gel electrophoresis for expression studies. This new technology is addressable in a highly parallel fashion requiring only minimal sample amount. In general terms protein microarrays can be described as a collection

of biomolecules immobilized on a carrier substrate in a spatially defined manner (e.g. in arrays) [7]. In principle forward phase, reverse phase and functional protein microarrays have been described.

1.2 Assay principles

1.2.1 Forward-phase microarrays

In forward phase microarrays antibodies or other recognition elements are immobilised on the chip surface capturing the analyte of interest from the solution phase. In this kind of array each spot consists of one type of immobilized recognition element. Each array is incubated with one test sample and multiple analytes in that sample are analyzed simultaneously (Fig. 1). In the next sections a selection of assay types, which can be implemented on-chip, is outlined. In the examples antibodies serve as capture elements. Though the most common biorecognition element, in principle other capture elements can be used as well. Whatever the nature of the capture element, it must be assured that it is both specific for the target analyte and exhibits no cross-reaction with the other assay components.

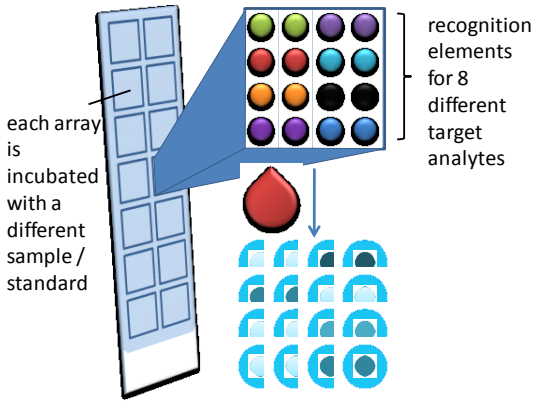

Fig. 1 Scheme of a forward-phase microarray

1.2.1.1 Direct immunoassay

The direct immunoassay is a very simple assay format which involves the direct binding of the antigen to the immobilized antibody. The approach requires that the antigen is detectable. Either the antigen features intrinsic fluorescence, all proteins of a sample are labelled, or label-free methods such as surface plasmon resonance or atomic force microscopy is applied.

A study by Knezevic and coworkers identifies critical changes in protein expression of progressing oral cavity cancer [8]. They developed a microarray on nitrocellulose slides containing 368 antibodies specific to different cellular proteins. Carcinoma cells of different disease stages were obtained by laser capture microdissection of tissue samples. Cell lysates were biotinylated, applied to the protein chips and detected via streptavidin-coupled luminescence chemistry. The authors showed that quantitative, and potentially qualitative, differences in expression patterns of multiple proteins within epithelial cells correlated reproducibly with oral-cavity tumour progression.

In an interesting twist on the issue of sample labelling Zhou et al. [21] measured the relative levels of proteins from serum samples of patients with liver cancer or cirrhosis compared to the samples from healthy controls. Two serum samples, which should be compared, were labeled with biotin and digoxigenin respectively, and were captured on antibody microarrays. Antibodies targeting the biotin tag and the digoxigenin tag were coupled to Cy3 or Cy5 labelled rolling circle amplification. Produced fluorescence was up to 30-fold higher than in alternative direct-labelling or in indirect detection methods.

Generating similar profiles of the relative abundance of a multiplicity of protein species is desirable in many research areas. These include studies in embryonic development, immunobiology, drug responses, cancer biology and the discovery of biomarkers [9].

Ivanov and coworkers [10] developed a biosensor system for registration of social disease markers using an optical label-free surface plasmon resonance platform. They detect hepatitis B and C markers in real time. The hepatitis B marker HBsAg was revealed in patient serum with a biosensor based on immobilized anti-HBsAg. Advantages of the optical biosensor are the rapid detection of the antigen (within 5–8 min) and the repeated use of the cuvette. A similar approach was taken for the revelation of antibodies to HCVcore antigen in serum.

As another label-free detection method, atomic force microscopy (AFM) uses a sharp micron-scale tip to scan surface features. The methodology enables imaging in solution, providing real-time data acquisition under physiologically relevant conditions. Huff et al. [11] report on the development of a platform which combines the surface profiling capabilities of AFM with fixed immuno-capture using antibodies immobilized in a nanoarray format. This approach provides a distinctive platform for direct, label-free detection and characterization of viral particles and other pathogens.

1.2.1.2 Sandwich immunoassay

For a typical sandwich immunoassay a capture antibody is immobilized on the chip surface (Fig. 2a). In a next step the test sample is added and the antibody binds the target antigen. Finally a detection antibody binds to the target analyte at an epitope (binding site) distinct from the capture antibody. Therefore an antigen sandwich is formed between the two antibodies. The detection antibody carries a label that generates a detectable signal. Due to the assay design the signal from the detection antibody increases with increasing analyte concentration. When the logarithmic signal strength is plotted against the logarithmic analyte concentration a sigmoidal dose-response curve is obtained. An example for a typical

sandwich immunoassay calibration curve (for the interleukin 10) is shown in Fig. 2b. The sandwich immunoassay combines high selectivity with high sensitivity. Selectivity is inferred by the use of two different antibodies which both have to specifically bind to the target analyte. High sensitivity is achieved through the use of a capture antibody in the first step, which pre-concentrates the analyte at the solid phase before detection.

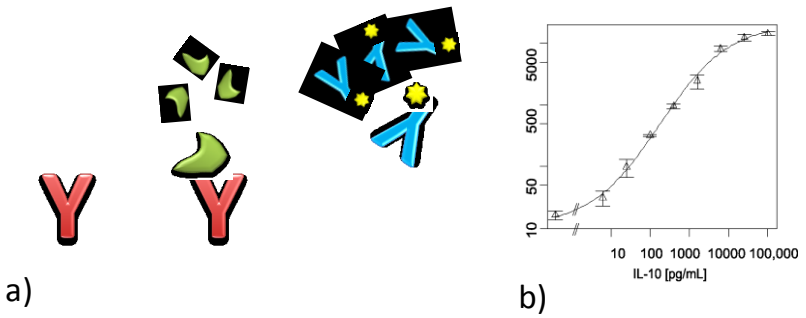

Fig. 2 Sandwich immunoassay. a) Schematic assay principle b) Typical calibration curve (for interleukin 10)

Sandwich immunoassays can be used to analyze protein levels or biomarkers in research areas covering clinical diagnosis, environmental analysis and food safety. The majority of studies have applied antibodies as capture elements. A broad body of literature is dealing with the detection of cytokines in patients' sera and bodily fluids (e.g. [12-14]).

Cytokines are involved in local and systemic events of the immune response, inflammation, hemopoiesis, healing, and the response to injury. They also play a prominent role in conditions such as cancer, sepsis and cardiovascular diseases. Therefore measuring cytokine levels has a high potential for diagnosis and disease management [15].

One of the largest cytokine arrays fabricated so far was reported by Schweitzer and co-workers [16] who arrayed 75 antibodies on chemically derivatized glass slides. The authors used the platform in a sandwich approach to study cytokine secretion from human dentritic cells induced by lipopolysaccharide or tumor necrosis factor-alpha. Rolling circle amplification which retains the high spatial resolution of the assay (not afforded by enzyme-catalyzed chemiluminiscence) was used for enhanced detection sensitivity. As cross-reactivity becomes an issue at this high number of analyzed antigens antibody probes were subdivided into groups of roughly the same size. They were spotted on different proportions of the glass slides separated by teflon barriers which avoided signals generated by cross-reactivity.

Protein arrays with a smaller panel of cytokines are marketed by a number of companies. The systems are either based on polymer membranes (e.g. Panomics, GE Healthcare, RayBiotech) or modified glass slides (e.g. R&D Systems). Detection is performed either via fluorescence or chemiluminescence.

Matsunaga et al. [17] used a cytokine chip by RayBiotech to investigate the upregulation of inflammatory molecules in the exhaled breath condensate of asthma patients as compared to healthy volunteers. They concluded that measurements of cytokine levels in exhaled breath condensate may be used to monitor the asthmatic airway condition and the effect of therapeutic interventions.

Biosite Inc. (http://www.biosite.com) has developed a portfolio of multianalyte assays for cardiovascular diseases as well as a drug screening test. The technology termed "Triage system" integrates a protein array in a microcapillary fluidics device. The test design allows for precisely timed immunoreactions to occur in predetermined assay zones along the length of the device. The analytical process begins as soon as the blood or urine sample is added to the sample port, which filters out blood cells and particulates. Next the sample is mixed with fluorescently labelled antibodies or antigens (depending on the test) that bind to the analytes. As sample flows through the device, it encounters the protein array composed of analyte-specific antibodies. Labelled bound analyte is subsequently detected via a laser-excited fluorescent signal. The amount of fluorescent signal can be quantified with an electronically stored calibration curve.

1.2.1.3 Competitive Immunoassay

In comparison to sandwich immunoassays the competitive immunoassay only requires one antibody. This is an advantage as two selective antibodies that bind to different non-overlapping epitopes on the analyte may be difficult to obtain. Additionally small analyte molecules do not permit two antibodies to bind in a sandwich fashion due to steric hindrance.

In a competitive immunoassay a capture antibody is immobilized on the chip substrate (Fig. 3). In a first step a mixture of unlabeled analyte (from the sample) and labelled analyte is added to the microarray. Both compete simultaneously for the binding site on the capture antibody. Thus the amount of bound labelled analyte is inversely proportional to the unlabeled analyte concentration in the sample. Accordingly lower signal levels indicate higher target analyte levels.

Fig. 3 Principle of the competitive immunoassay

1.2.1.4 Binding inhibition immunoassay

In a binding inhibition immunoassay, the analyte, rather than the antibody, is immobilized on the chip surface (Fig. 4a). The sample is mixed with a defined concentration of labelled detection antibody. The detection antibody binds to the target analyte in the sample. When the mixture is subsequently applied to the chip only excess target antibody, that has not yet bound to sample analyte, is free to bind to the immobilized on-chip analyte probe. The more analyte in the sample, the less detection antibody is available for the last binding step. Therefore the signal generated in this type of assay decreases with increasing analyte concentration. A typical response curve for the analyte SPARC (secreted protein, acidic, cysteine-rich) is shown in Fig. 4b.

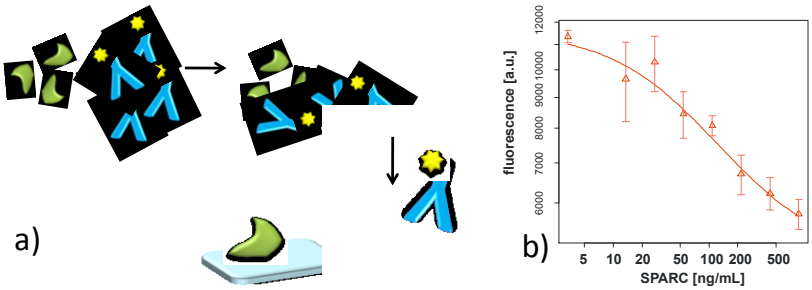

Fig. 4 Binding inhibition immunoassay. a) Schematic assay principle b) Typical calibration curve (for SPARC)

Binding inhibition assays are typically less sensitive than sandwich assays. Yet this property may be useful for detecting highly abundant target proteins as the working range of the assays can be adjusted via the detection antibody concentration: More detection antibody shifts the standard curve to higher target protein concentrations. An obstacle in the set-up of binding inhibition assays may be the immobilization of small, fragile analyte molecules which are

prone to denaturation. This effect can be prevented by conjugating the analyte to a carrier protein like bovine serum albumin (BSA).

Using this assay principle Du and co-workers [18] developed a chip for high throughput urine screening of athletes for prohibited substances. Substrates modified with aldehyde groups were used to bind 16 different BSA-conjugated drug molecules. Chips were incubated with mixtures of an urine sample and anti-drug mouse monoclonal antibodies. Detection was performed with a fluorescently labelled anti-mouse antibody.

1.2.2 Reverse-phase microarrays

In contrast to forward-phase microarrays, in the reverse-phase approach each immobilized spot contains an individual complex test sample [19] [20]. Thus an array can contain hundreds of different samples (e.g. cell lysates or patient samples). Each array is probed with a labelled detection protein directed against a specific analyte. The obtained signal can be directly compared across multiple samples. Therefore the function of a single protein or pathway may be studied. Compared to western blotting, a traditional technique for probing the proteome, the amount of required biological sample material is reduced by more than factor thousand. This enables researchers to analyze more proteins from each sample. Furthermore cell populations that are present in low numbers (e.g. stem cells) can be targeted [21].

Reverse-phase microarrays were used by Paweletz et al. [22] to longitudinally analyze pro-survival checkpoint proteins at the transition stage from histologically normal prostate epithelium to prostate intraepithelial neoplasia and to invasive prostate cancer. Methodically they obtained epithelial cells by laser capture microdissection, arrayed the lysates onto nitrocellulose slides at distinct positions and probed with different antibodies. The authors found that the level of phosphorylated Erk decreased during disease progression, whereas the abundance of phosphorylated Akt tended to increase.

Another use of reverse phase arrays is based on a technique termed surface enhanced laser desorption ionization (SELDI). It is implemented by the ProteinChip technology of Ciphergen, in which the surface is a MALDI-TOF style mass spectrometer target [23]. The system uses arrays that contain chemically (hydrophobic, hydrophilic, anionic, cationic) or biochemically (receptor, DNA, antibody) treated surfaces [24]. A crude sample such as whole cell lysate or a bodily fluid is applied and subclasses of sample proteins are captured selectively based on their specific physical or biochemical characteristics. The chip is subsequently washed and the molecular size and quantity of individual bound proteins are

directly assessed by a time of flight mass spectrometer. The resulting quantitative protein mass profiles can be directly compared to uncover relevant changes in the patterns of underlying protein expression. Apart from being very sensitive (the lower limit of detection is 10 fmol) the SELDI technology is quantitative and highly reproducible [25].

Pettricoin and co-workers used this technology with a hydrophobic chip surface for the detection of ovarian cancer [26]. The experimental setup included a pattern-discovery and a pattern-matching stage conducted using a bioinformatic program. Serum samples of 50 healthy women and of 50 women with different stages of ovarian cancer served as the training set. The authors identified a proteomic pattern which distinguished cancer cases from non-cancer cases. This pattern was subsequently used to classify ovarian cancer cases and non-malignant cases in a blinded test set of 116 masked samples with a sensitivity of 100% and a specificity of 95%.

In the field of breast cancer research, where no effective serological assays are available, the SELDI TOF-MS platform has proven an extremely useful diagnostic tool: Li et al. [30] have applied a Ni chip surface for analyzing serum samples of women at different clinical stages of breast cancer. The resulting pattern discriminated healthy from breast cancer serum with 93% sensitivity and 91% specificity.

Similar approaches were successfully applied for diagnosing prostate cancer [27], HIV-1 associated cognitive impairment [28] and Alzheimer's disease [29].

1.2.3 Functional protein arrays

Functional protein arrays have been extensively applied in discovery research and drug screening [30]. Bearing a large set of purified proteins of interest they can be used to screen for molecular interactions (Fig. 5): Those include the study of interactions between proteins and proteins, peptides, small ligands, DNA and lipids. Furthermore chips were applied for the identification of kinase substrates and for immune profiling.

For instance Kim et al. [31] have developed an allergy chip which consists of spotted protein extracts of Dermatophagoides pteronyssinus, egg white, milk and soybean on a nitrocellulose chip. The chip was incubated with patients' sera. Bound IgE antibodies, that mediate type I allergy, were detected with biotinylated anti lgE antibodies and streptavidin coupled fluorescence dye.

Another clinically relevant application is the identification of proteins that induce an antibody response in autoimmune disorders [32-33]. Microarrays of autoantigens were fabricated by immobilizing several hundred proteins and peptides to the surface of a derivatized glass slide. After incubating arrays with patient serum, fluorescent labels were used to detect antibodies that play a role in autoimmune diseases including systemic lupus erythematosus and reheumatoid arthritis [34].

Similar approaches were applied to serodiagnose people with parasitic or viral infections including SARS [35], herpes simplex virus [36] and hepatitis C virus [37].

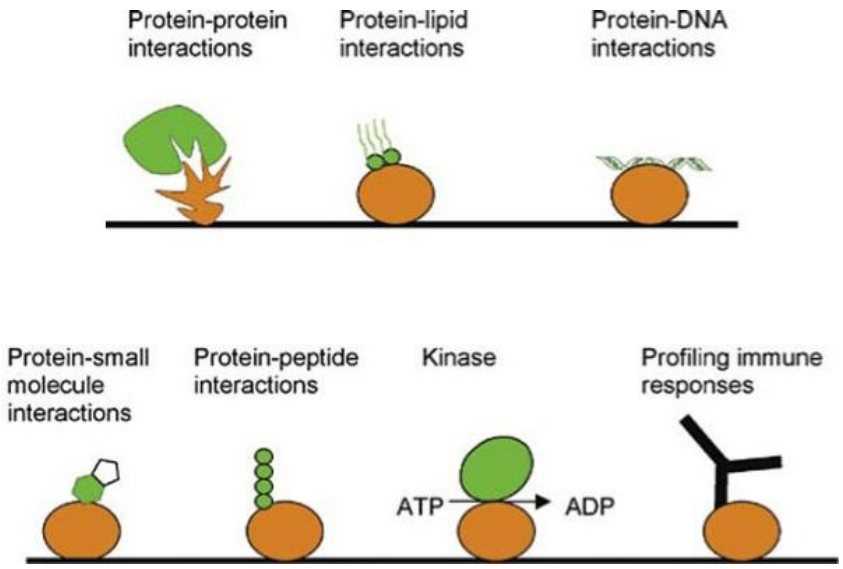

Fig. 5 Applications of functional protein microarrays [38]

1.3 Biomarkers

A protein biomarker is a protein or peptide that serves as a measurable indicator of a specific biological state, especially one relevant to the risk of contraction, the presence or the stage of a disease [39]. Biomarkers may be wild-type proteins that are differentially or specifically expressed, proteins that feature aberrant posttranslational modifications or unique proteins that only exist in diseased cells and that result from genetic lesions such as mutations, tranlocations or fusion events [40].

Biological fluids including serum, plasma and saliva serve as specimen for biomarker determination. Protein biomarkers can be used to clinically screen for, diagnose or monitor disease activity, to guide therapy, to assess prognosis and to predict or evaluate therapeutic response. Panels of protein biomarkers increasingly gain importance in the diagnosis of diseases, especially if conventional clinical criteria focusing on physical trait or physiological metric fail to describe disease state and prognosis accurately. Expression studies of whole marker panels have significant advantages in comparison to monitoring any single protein which may lack sufficient specificity and sensitivity to be of clinical use. In this work chips for the measurement of protein biomarkers involved in melanoma and sepsis are presented.

Melanoma is a malign form of skin cancer and a leading cause of cancer death, particularly in young adults [41]. Accurate staging of progression is of utmost importance as even small melanomas can readily metastasize. Diagnosis is typically based on histopathologic criteria such as tumour thickness, invasion and the presence of metastases. However these criteria alone cannot diagnose all melanomas and they do not account for the notoriously variable clinical course of the disease. The detection of biomarkers reflecting disease stage and likelihood of progression can thus give raise to new, more effective and less toxic therapies on an individual patient basis.

The incidence of sepsis, a severe whole-body inflammatory state, and sepsis-related deaths are on the increase. Successful therapy requires early and accurate diagnosis, appropriate antibiotic therapy and eradication of the source of infection [42]. In the acute phase of sepsis clinical manifestations include fever and changes in the level biomarkers of biomarkers such as cytokines, leucocytes, C-reactive protein (CRP) and procalcitonin (PCT). In response to an inflammatory stimulus most of the acute phase proteins increase in serum and plasma [43]. In a bacterial infection the cascade of inflammatory events is initiated by the activation of macrophages which release inflammatory cytokines and growth factors within minutes (Fig.

6). Major inflammatory cytokines are interleukin 6 (IL-6), interleukin 10 (IL-10) and tumour necrosis factor alpha (TNF-α). PCT rises within two hours. For the leucocytes indices and CRP it takes several hours to change significantly after the onset of reaction.

Microarrays for the detection of molecular biomarker signatures can thus help guide disease diagnosis, therapy selection and establishment of prognosis. Some of the systems described in literature are discussed in chapter 1.2. Also first commercial products are on the market which analyze protein biomarkers specific to fertility, cardiac disease, tumours, autoimmune diseases and infectious diseases (reviewed in [44]).

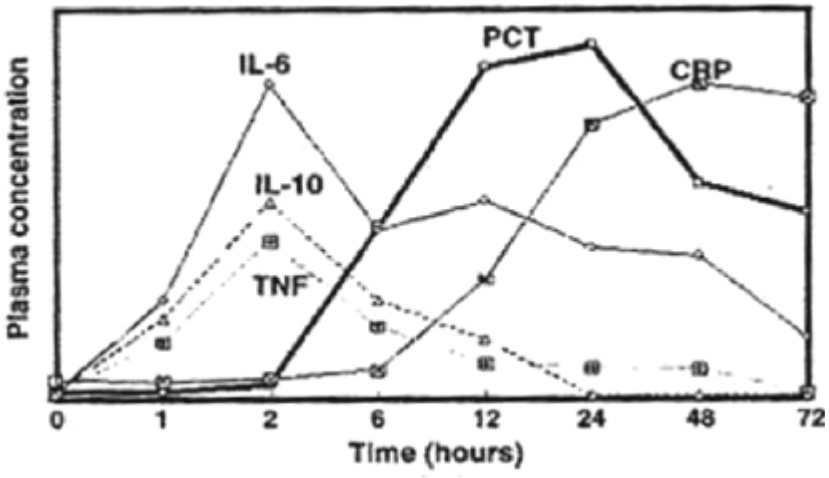

Fig. 6 Kinetics of various markers of the inflammatory host response after endotoxin challenge in human volunteers [43]

2 Chip fabrication

Protein chip technology has emerged from DNA chips, which is reflected by a similar overall chip fabrication route and the common use of devices for spot printing and slide processing. However protein chip fabrication has to consider the major differences in the physical properties and stability of proteins compared to DNA:

- DNA is generally more stable than proteins
- ssDNA and RNA are homogeneously negatively charged and hydrated and can thus be immobilized on cationic substrates
- the polarity as well as the isoelectric point vary from protein to protein
- in contrast to DNA proteins feature strong non-specific adsorption
- proteins have different sizes, charges and stability, which renders protein-protein interactions extremely difficult to control; conversely DNA sequences generally have similar chemical properties and predictable affinities

Due to these properties protein chips require special probe preparation, choice of adequate chip substrates, binding buffers, sample handling and chip processing. The basic tasks for each microarray experiment are summarized in Fig. 7. First the biological question and the aim of the experiment are formulated and further experimental details can be planned. In the next step the sample is prepared, which involves sample handling and modification. The probe for microarray printing is formulated in a spotting buffer which allows immobilisation and preserves the activity of the capture element. The third step in the cycle deals with the biochemical reaction between the on-chip probes and the analyte in the sample. Here incubation time and temperature, washing steps, buffer compositions, concentrations of reagents and coupling chemistry are optimized. Conditions strongly depend on the applied assay format (see section 1.2). In a subsequent detection step the assay signal is read with optical scanners (fluorescence, colorimetric, chemiluminescence) or alternative detector devices. The imaging mode, detector sensitivity, resolution and other parameters have to be tuned. Finally the acquired images have to be processed with algorithms for spot finding and background subtraction, individual spot intensities and quality parameters are calculated. Statistical methods for data normalization, outlier identification and data quality assurance have to be applied. Appropriate quantitative models can be fitted to the data and results can be calculated. For data analysis several commercial and public domain kits have been developed. In this work the statistical language R was used, which is especially apt in handling huge data

with several ten thousand elements. Furthermore several libraries for microarray data processing and model fitting are available for R.

All five steps require thorough optimization to ensure a high-quality microarray experiment. The main components in the process of chip fabrication are elucidated in the next chapters.

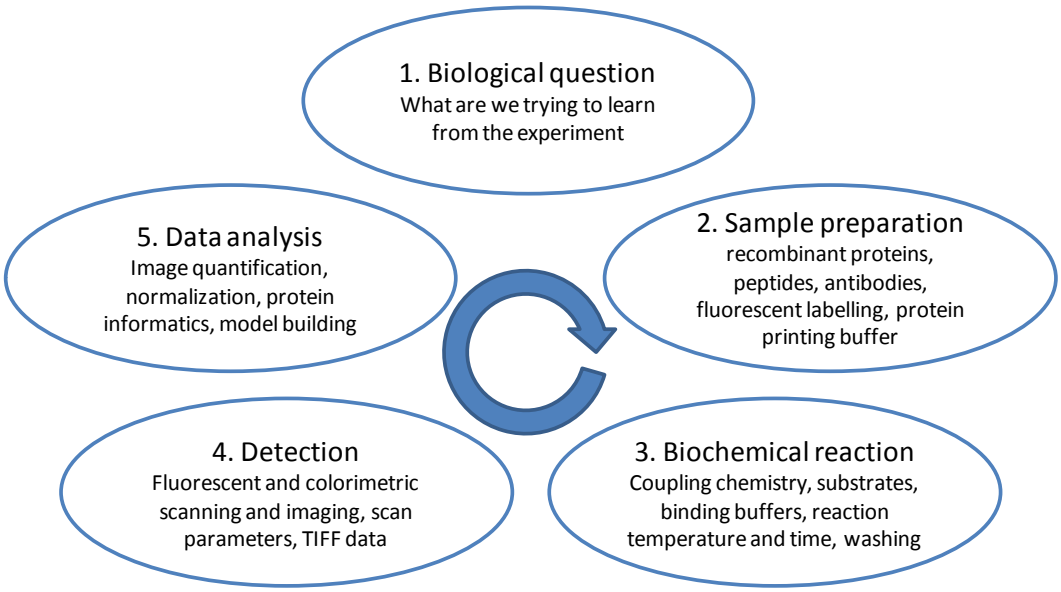

Fig. 7 Basic steps in a microarray experiment [45]

2.1 Microarray substrates

Protein microarrays demand an improvement in the efficiency of protein immobilisation. An ideal procedure must both maximize the amount of immobilized protein and conserve its function. To remain active, the protein must retain a native conformation. Loss of activity can be caused by denaturation, dehydration or oxidation. Thus the microarray substrate has to provide a protein-friendly environment that helps to minimize hazardous influences. Also proteins are ideally attached to the substrates in such a way, that the bioactive moiety is not masked.

Since the early 1970 protein immobilisation studies on solid materials have been reported, e.g. for macrosize biosensors, and results have proven applicable in microarrays as well. As proteins are constituted of a sequence of amino acids, immobilisation can harness their interaction with the substrate surface. As summarized in Table 1 the possible interactions

depend on the nature of the exposed amino acid moieties and their chemical functionalities. Hence there is no optimal substrate or immobilisation strategy applicable to all possible proteins. Advantages and disadvantages of the available approaches are outlined in the next sections.

Table 1 Protein immobilization methods [46]

Functional group of peptide		Available surface derivatization	Type of binding
Natural	**-COOH in Asp**	Amino	Electrostatic, covalent amide after carboxy activation
	-NH_2 in Lys, Gln, Arg	carboxilic acid active ester, epoxy, aldehyde	Electrostatic covalent amide
	-SH in Cys	Malemide	covalent thioether
	-OH in Ser, Thr	Epoxy	covalent ether
Synthetic	**His-tag**	Ni-NTA complex	coordination complex
	Biotin	Streptavidin	supramolecular complex

2.1.1 Binding principles

Although a vast range of microarray substrates is described in literature (see Table 2) immobilisation mechanisms of the proteins to the surface can be traced back to three basic principles [47]:

- Adsorption
- Covalent binding
- Affinity binding (biorecognition)

Table 2 Substrates for protein immobilisation and reported use. Adapted from [45]

Surface chemistry	Binding mechanism	Type of assay
Hydrazide-activated polyacrylamide gel	antibody carbohydrates oxidized with sodium periodate ($NaIO_4$)	Antibody [48]
Hydrogel	Adsorption/molecular sieving	Antibody & sera [49], antibody & antigen [50]
Agarose gel activated with $NaIO_4$	Amino groups	Sandwich assay [51]
Aminosilane	Electrostatic adsorption	Antigen & antibody [52], membrane proteins & lipids with ligands [53]
Poly-L-Lysine	Adsorption	Cell and tissue [54], antibody & antigen [55]
Poly(phenylalanine lysine)	Adsorption	antibody & cytokines in ELISA [56]
Nitrocellulose	Adsorption	bacterial antibody array [57], antibody & antigen [58-59]
Polyelectrolyte multilayers	Adsorption	direct and sandwich assay [60]
Aminosilane with oxidised dextran	Schiff base via protein amines	microarray ELISA for IgG & IgE[61]
Cyanosilane	Adsorption via antibody carbohydrates	Cytokine arrray [62]
Aldehyde silane	Schiff base via primary amines	Antibody & cell line lysates [63], antibody [58]
BSA with a bifunctional crosslinker	Amino groups	Antibody [64]
Poly-L-Lysine with photoreactive crosslinker	Amino groups	Antibody & sera [49]
Aminosilane with bifunctional N-hydroxysuccinimide	Amino groups	Antibody & sera [49]
Epoxy silane	Amine, thiol, and hydroxyl groups	Antibody & antigen [54], peptide assay [65], small protein [66]
Nickel coating	Histidine Tag	antibody antigen [64]
Dendrimers	Amino groups	Streptavidin & biotin [67]
Avidin	Biotinylated antibodies	peptide array [68], antibody & secondary antibody [64]

2.1.1.1 Adsorption

Passive physical adsorption is a simple method to immobilize proteins on a surface. It results in random orientation of the proteins and has proven particularly useful in the immobilisation of large proteins. Adsorption acts either via electrostatic or via hydrophobic interactions. Typical electrostatic substrates which originate from DNA microarray technology are poly-L-lysine [54-55] and aminosilane [52-53]. Also cyanosilane [62] and poly(phenylalanine lysine) surfaces [56] were employed. Polystyrene and nitrocellulose [57] are other adsorptive supports. Both act via hydrophobic interactions. Nitrocellulose as a three-dimensional support exhibits increased immobilization capacities but is plagued by a high background signal when using fluorescence detection. To address this issue, recently a black nitrocellulose surface with decreased autofluorescence was reported [69]. Hydrogels constitute a different class of three-dimensional adsorptive substrates [49-50]. They help to preserve the three-dimensional

structure (and thus stability and functionality) of proteins by providing a hydrating and hydrophilic environment and were reported to feature low non-specific adsorption. Hydrogel slides are commercialized by Perkin-Elmer (acrylamide coating) and Schott (Nexterion Slide H). Gel matrices have also been prepared from polyelectrolytes using a layer-by-layer assembly technique [60, 70]. Though universally applicably adsorption of proteins features no control over probe packing density and protein immobilisation capacity is generally low due to the low strength of the interactions and the reversibility of the process. Furthermore protein can possibly leach from the solid support [71]. Also adsorption of proteins may lead to conformational changes and hence to denaturation.

2.1.1.2 Covalent binding

The formation of covalent bonds provides a more robust linkage between protein and surface. Several chemical reactions between the protein's accessible amino acid residues and the surface functionalities are frequently applied (see Table 1, Fig. 8 and Fig. 9) and lead to a "statistical orientation" of the protein. The amino group of lysines is readily coupled to a surface bearing active esters, for instance N-hydroxysuccinimide (NHS) esters (Fig. 8 a). In this reaction a stable amide bond is formed between the protein and the support. However active NHS esters are prone to hydrolysis in aqueous solution which leads to poor immobilisation yields. Similarly the reaction of lysine residues with isocyanates (Fig. 8 b) is competing with the hydrolysis of isocyanates to carbon dioxide and amines. Alternatively coupling to surface aldehyde groups (Fig. 8 e) has been shown [58]. Here an additional reduction step (with e.g. sodium cyanoborohydride) is required to transform the imine into the stable secondary amine. Epoxide surfaces have the advantage to be very stable at ambient conditions. Also they are not prone to hydrolysis at neutral pH. Lysine but also the nucleophilic residue of cysteine can be coupled to epoxy groups (Fig. 8 d) [58]. Cysteines also form stable thioether bonds by adding to α,β-unsaturated carbonyls, such as maleimides (Fig. 8 c). Glutamate and aspartate residues can be coupled to amine-modified surfaces via in situ generated active NHS esters (Fig. 9). Yet this reaction requires the addition of the coupling reagents 1-ethyl-3-(3-dimethylaminopropyl)carbodiimide (EDC) and NHS [71].

To sum it up covalent immobilization is often favoured because it leads to stable protein attachment in high densities. The high immobilisation yield can translate into increased sensitivities and higher signal strengths. However too high a density of reactive surface groups may result in multi-point attachment and protein unfolding. Also one has to consider

that the covalent linkage possibly promotes undesired protein orientation and blocking of the active moiety.

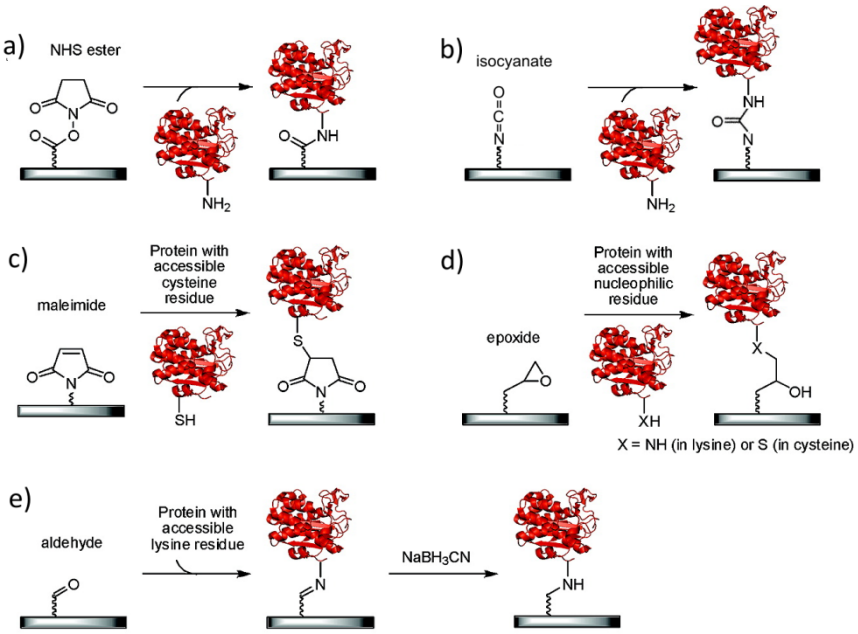

Fig. 8 Covalent protein immobilization methods using surface NHS esters (a), isocyantes (b), maleimides (c), epoxy groups (d) and aldehydes (e). Adapted from [71]

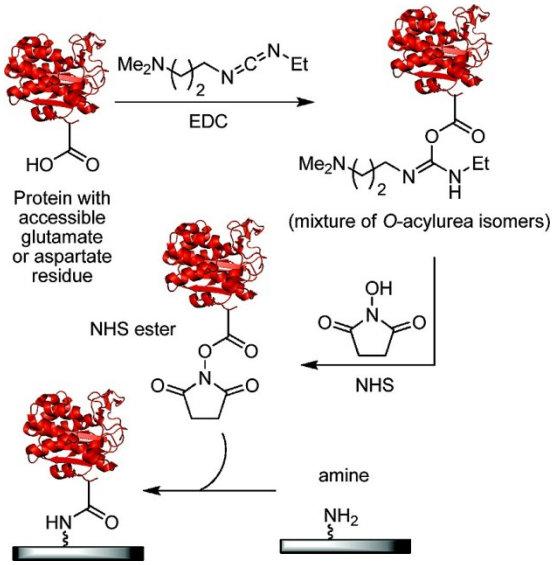

Fig. 9 Carbodiimide-mediated coupling of glutamate or aspartate residues to amine-modified surfaces [71]

2.1.1.3 Affinity binding

Affinity binding is a mode of protein attachment that overcomes possible disadvantages of covalent binding such as non-specific attachment and poorly defined orientation. The approach is based on biological reactions and features

- mild immobilization conditions and thus a reduced risk of protein degradation
- defined protein orientation as attachment occurs at a specific location
- attachment tags on the protein that can often be engineered into proteins at defined positions via standard molecular biology techniques

Polyhistidine tags are prominent examples for affinity tags [72]. It consists of a consecutive series of six histidine amino acids and can be fused with the amino- or carboxy-terminus of proteins or can be engineered into exposed loops [73]. This tag binds to transition metal ions via chelation (Fig. 10 b). Ni(II) is most frequently used, but also Cu(II), Zn(II) and Co(II) have been applied. The metal ion is bound to the surface via chelating ligands such as nitrilotriacetic acid (Fig. 10 a) and iminodiacetic acid. The his-tag is very small and usually does not alter the protein structure. As no specific structure is required for this affinity interaction, the tag even works in denatured proteins. Additionally many commercial proteins feature this tag. A disadvantage of the strategy is that the interaction is not very selective: Firstly many endogenous proteins have been shown to bind to nickel, thus purified protein probes have to be used instead of crude mixtures. For instance carboxylic amino acids as well as tyrosine and phosphorylated side chains of threonine, tyrosine and serine [74] have been identified to bind nickel. Secondly the strength of the interaction is relatively weak (Kd ≈ 1-10 μM).

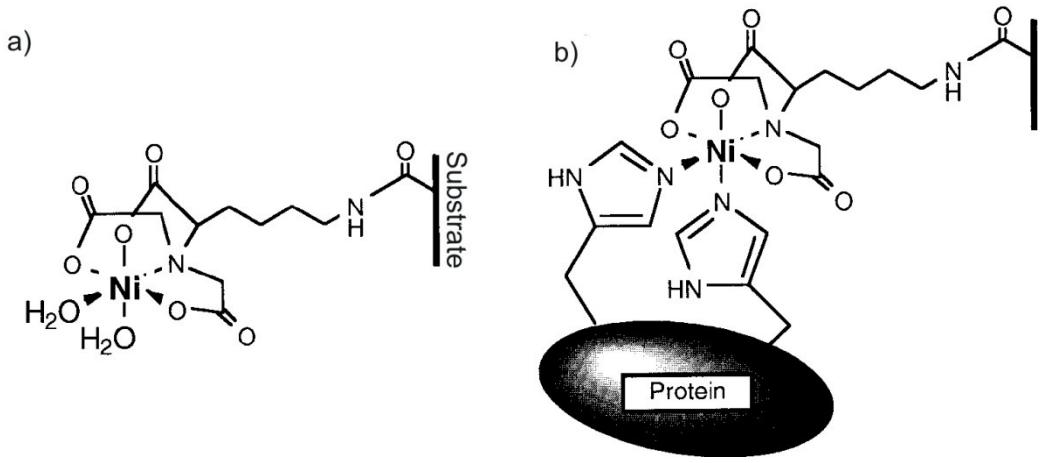

Fig. 10 His-tagged is chelated by substrate-bound Ni-NTA complex. a) The tetradendate NTA ligand occupies four coordination sites of nickel. b) The his-tagged protein binds to the two vacant coordination sides. Adapted from [72]

NTA is a widely applied chelator for the preparation of Ni-affinity microarray surfaces. Back in 1996 Sigal et al. [75] reported gold chips with self-assembled monolayers (SAMs) of a mixture of two alkanethiols: one terminated with a nitrilotriacetic acid (NTA) group, the other carried a protein resistant tri(ethylene glycol) group. The surface is subsequently loaded with Ni^{2+} and interacts with hexahistidine tagged proteins. Schmid et al. [76]bind NTA to a quartz chip via silane chemistry. In the same year, Nieba et al. [77] used a surface plasmon resonance system for binding studies of various recombinant proteins to a Ni^{2+}-NTA sensor chip. This gold chip is coated with carboxymethylated dextran pre-immobilized with NTA. Kröger et al. [78] developed a synthetic chelator thioalkane which was self-assembled on a gold surface for the oriented and reversible immobilization of proteins via hexahistidine tags. Kang et al. [79] presented silica surfaces modified with NTA-polyethyleneglycole derivatives for immobilizing hexahistidine-tagged proteins. It has been shown that the affinity of his-tagged proteins can be improved by employing multivalent chelator groups. Such chelator heads contain two [80-81] or three NTA moties [82] and offer stable protein immobilization.

In contrast to microarray surfaces which rely on NTA as the nickel chelating group, in this work iminodiacetic acid and amino acid-derivates are employed as alternative chelators. The preparation of the affinity substrates relies on simple chemical modification of polymeric coatings and thus avoids expensive SAM chemistry as well as the use of chemicals that have to be obtained via multistep organic synthesis. Notwithstanding the easy preparation the substrates show excellent binding sensitivities which are enhanced by optimized spotting buffers.

In alternative approaches to simplify the fabrication of nickel affinity slides, a solution of $NiCl_2$ was spin-coated onto a glass surface [83] or his-tagged proteins were patterned onto metallic nickel substrates [84-85] or onto surfaces coated with nickel-alloys [86].

Streptavidin and biotin are the partners in another popular affinity interaction [64, 68]. Chip surfaces are coated with streptavidin that features four biotin binding sites. The interaction between (strept)avidin and biotin is exceptionally strong ($K_d \approx$ 10-15 M) and essentially irreversible as it resists denaturants, heat and proteolysis. A drawback of the method is that protein probes have to be labelled with biotin prior to immobilisation. The final protein orientation therefore also depends on the biotin labelling strategy.

Antibodies can also be used to selectively immobilize other proteins on surfaces. Furthermore proteins A, G and L have been applied to capture antibodies.

2.1.2 Coating techniques

The biomolecule-reactive microarray coating can be deposited on the carrier substrates (often glass or plastic) using a wide range of techniques. If the coating is a polymer or resin the most frequently applied methods are:

- dip coating
- spin coating
- coating via a film applicator

Dip coating forms thin films of coating material on substrates. First the substrate is immersed into a solution of the coating material at defined speed. It remains immersed in the solution for a while and is then withdrawn at constant speed. During withdrawal a thin film is formed. Excess liquid drains from the substrate. Finally the solvent evaporates and a film of coating material is formed.

In the layer-by-layer (LbL) deposition of polyelectrolytes applied in this work (Fig. 11), the solvent evaporation step is replaced by a washing step to removes excess polymer that is not retained by electrostatic forces. The dipping cycle is subsequently repeated with solutions of oppositely charged polymer until a film of desired thickness is obtained.

Spin coating is another method for producing homogeneous films (Fig. 12). An excess amount of dissolved coating material is placed onto the substrate. The substrate is rotated at

high speed and centrifugal force spreads the fluid. Film thickness depends on rotation time, rotation speed and the concentration of the solution. The method is both fast and cheap.

Coatings of defined thickness can also be fabricated with a film applicator (Fig. 13). The applicator is loaded with the coating solution and drawn across the substrate by hand or electric motor drive. The thickness of the resulting film is influenced by the height of the applicator blade, the drawing speed and the flow properties of the coating material.

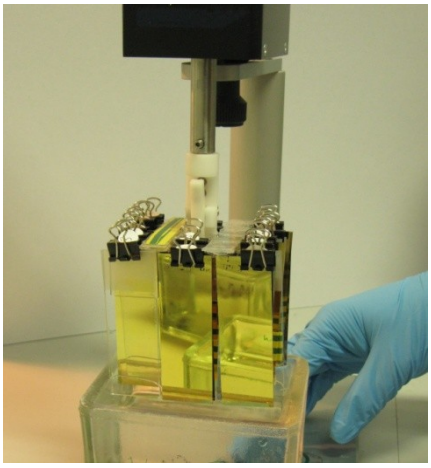

Fig. 11 Dip coating. A computer-controlled stepping motor is used to move a robotic arm up and down. Several slide substrates can be clipped to the arm and are immersed and withdrawn from the coating solution simultaneously. The shown assembly was used for LbL deposition of polyelectrolytes in this work.

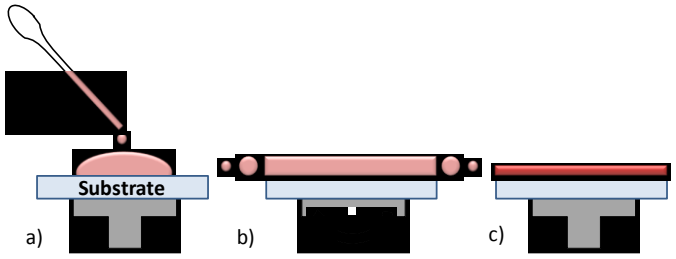

Fig. 12 Spin coating. (a) Application of the solution of coating material. (b) Rotation of the disk and film formation. (c) Solvent evaporation.

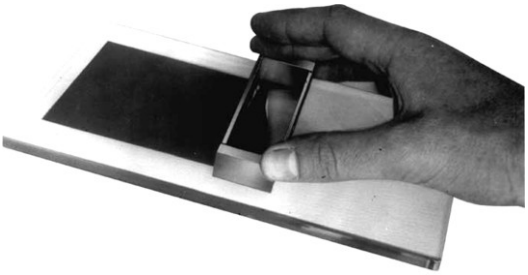

Fig. 13 Coating of a substrate using a film applicator (www.erichsen.de)

2.1.3 Surface characterisation

Surface chemistry plays a significant role in protein microarray fabrication (2.1.1) which demands for its efficient characterization prior to the use of such surfaces in biomolecular interaction studies. Many of the problems associated with microarray experiments such as denaturation of proteins, spot heterogeneity, smearing and non-specific interaction can be efficiently addressed by an appropriately prepared surface. Characterization tools can give guidance in surface optimization and help to grasp the underlying principles of biomolecule-substrate interactions. Furthermore they provide a means for monitoring the quality and reproducibility of the fabrication process.

A range of methods is available depending on the desired analytical information. Available techniques encompass – but are not limited to – infrared spectroscopy, Raman spectroscopy, auger electron spectroscopy, visible and ultraviolet spectroscopy, solid state nuclear magnetic resonance spectroscopy, small and wide angle X-ray scattering and electron microscopy. Atomic force microscopy, X-ray photoelectron spectroscopy and secondary ion mass spectroscopy are considered particularly surface sensitive, as they only collect information from the substrate's top molecular layers. Furthermore ellipsometry and contact angle measurements are frequently applied to characterize microarray chips.

Methods applied in this work are described in more detail in the following paragraphs.

2.1.3.1 AFM

Atomic force microscopy (AFM), a scanning probe microscopy technique, enables the investigation of surfaces down to the submolecular level. The advantage of AFM in comparison to other high-resolution techniques is that biological samples can be imaged in physiological conditions without complex sample preparation.

An AFM instrument is schematically depicted in Fig. 14. A sharp tip attached to a flexible cantilever (Fig. 15) is approached to the sample surface. The cantilever is moved relative to the surface with a piezoelectric actuator. Attractive and repulsive forces between tip and surface lead to bending of the cantilever as the tip scans the surface. This deformation, which is characteristic of the sample topology, is quantified by the deflection of a laser beam directed to the cantilever's top surface. The beam deflection is recorded by a split photodetector and used to create a topology image of the substrate. A feedback circuit monitors the deflection signal and keeps the tip-sample interaction at a fixed value which depends on the operation mode [87].

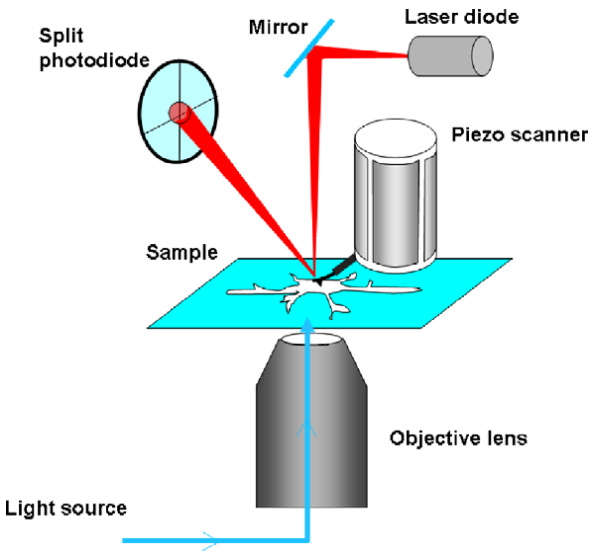

Fig. 14 Scheme of an AFM mounted on an inverted optical microscope. [87]

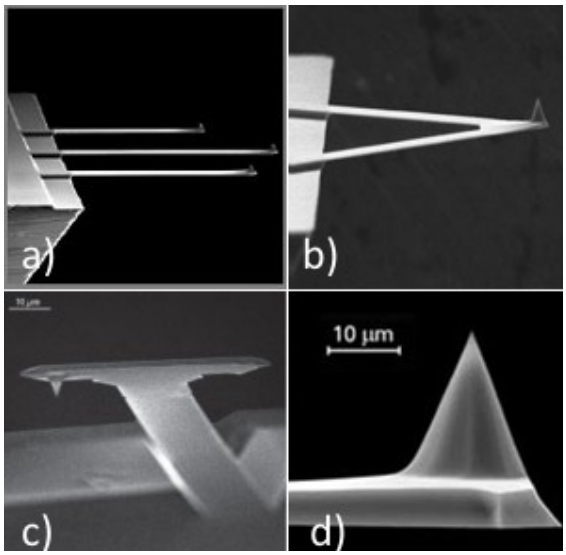

Fig. 15 AFM cantilevers and tips. (a) Chip with three silicon-etched cantilevers (b) Triangular cantilever (c) Torsional T-shaped cantilever for mapping of local adhesion and elastic modulus (d) Magnified probe tip (www.spmtips.com)

Depending on the distance between probe and sample surface, the tip experiences repulsive short range forces (<1 nm) and/or attractive long range forces (van der Waals-type, <100nm). According to the force regimen three imaging modes are differentiated:

- contact mode
- intermittent-contact mode
- true non-contact mode

The associated force regimen, the feedback system and the uses of the imaging modes are sampled in

Table 3.

AFM can be used to monitor the fabrication and modification steps of microarray substrates, to study structure and surface topology and to control the distribution of spotted probes. In this work AFM has been applied to measure the thickness of polyelectrolyte coatings on gold substrates developed for fluorescence signal enhancement (Fig. 16).

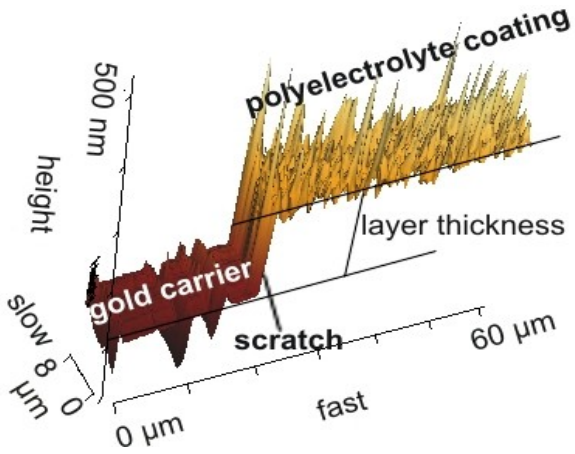

Fig. 16 AFM image of a scratch in a polyelectrolyte coating on a gold substrate

Table 3 AFM imaging modes [87-88]

Imaging mode	Force regimen	Feedback system	Measure-ment in	Samples	Comments
contact mode	repulsive, tip in constant contact	constant height mode: no feedback control constant force mode	air, solution	flat, rigid	(+) high resolution (+) high scan speeds (-) dragging forces, lateral movement of loosely bound particles (-) tip or sample damage
Intermittent-contact Mode	repulsive and attractive	cantilever oscillated near free resonance frequency; feedback signal to keep amplitude constant	air, solution	biological samples	(+) reduction of dragging forces
true-non-contact mode	attractive, tip never touches surface	external force applies frequency near free resonance frequency; monitoring of frequency shifts	vacuum, ultra-high-vacuum	often crystals, semi-conductors, metals	(+) highest resolution of all modes

2.1.3.2 X-ray photoelectron spectroscopy

X-ray photoelectron spectroscopy (XPS) or ESCA (electron spectroscopy for chemical analysis) is a surface sensitive analytical technique that provides information about the elemental composition and the chemical and electronic states of the elements in a material [89].

The basic components of a XPS system are depicted in Fig. 18. As measurements are performed under ultra high vacuum a mounting chamber to lock in the sample is available.

Additionally an X-ray source, a lens system to collect and focus the emitted photoelectrons, as well as an energy analyzer and a detector are required.

Basically the system measures the kinetic energy and the number of emitted electrons obtained by irradiating the sample with a beam of X-rays. The method causes relatively little damage to the analyzed material. Obtained information originates from the top 1 to 10 nm of the sample and is used to plot the number of detected electrons versus their calculated binding energy. For instance

Fig. 17 shows an XPS survey scan of a metal affinity surface, an epoxy chip surface modified with iminodiacetic acid and loaded with Ni^{2+} ions. All elements on the sample surface heavier than hydrogen produce a characteristic set of XPS peaks at characteristic binding energies. The peaks for each element correspond to the respective electron configurations (e.g. 1s, 2s, 2p, 3s, 3p, etc.). The area under the peaks is related to the amount of elements within the analyzed area (typically between 1 mm^2 and 1 cm^2). To generate atomic percentage values, the signals have to be corrected by a "relative sensitivity factor" [90].

Apart from the elemental composition of a material surface XPS can provide information about

- the chemical state of the elements via determining the chemical shift (difference between observed peak and peak of the pure element)
- surface contaminations
- elemental distribution as a function of depth by tilting the sample

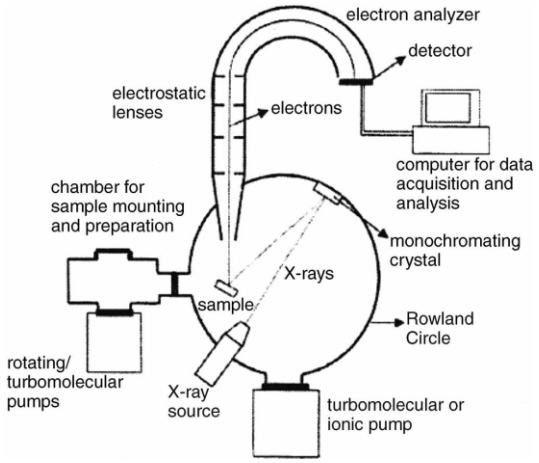

Fig. 18 Basic components of a XPS system [89]

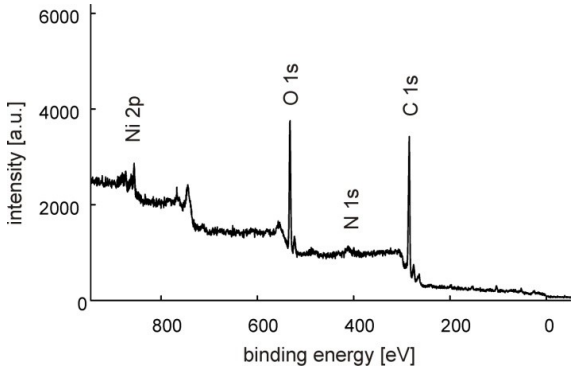

Fig. 17 XPS survey scan of epoxy chip surface modified with iminodiacetic acid and loaded with Ni^{2+}

2.1.3.3 Contact angle

The contact angle is commonly used to characterize the hydrophobicity of a solid substrate and it is an important parameter in understanding the interactions between solids and liquids. These interactions play a fundamental role when assessing adhesion as well as surface biocompatibility and surface wettability.

On an ideally smooth, homogenous and solid surface the contact angle of a drop of liquid is determined by the balance of forces at the gas-solid-vapour borderline as described by Young's equation [91]:

(1)

where Θ_Y is the Young contact angle and γ_{lv}, γ_{sv} and γ_{sl} are the interfacial (surface) tensions of the liquid–vapour, solid–vapour and solid–liquid interfaces, respectively (see also Fig. 19a). As shown in Fig. 19b a low Θ_Y indicates that the liquid wets well and spreads, while high contact angles indicate poor wetting. A value of 0° means complete wetting, at $\Theta_Y < 90°$ the liquid wets the solid and at $\Theta_Y > 90°$ the liquid is non-wetting.

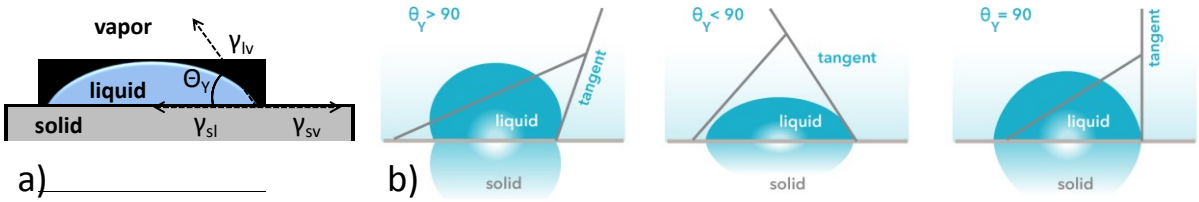

Fig. 19 Contact angle a) Scheme of the gas-solid-vapour borderline as described by Young b) Contact angles for systems with non-wetting, wetting and borderline liquids (www.attension.com)

However for real solid-liquid-vapour systems there is not a single but a range of contact angles. The smallest and the largest among them are called receding and advancing contact angle. The difference between them is the contact angle hysteresis, an effect caused by surface roughness and heterogeneity.

Hence several conclusions can be drawn from contact angle measurements:

- If water is used as the test liquid small contact angles indicate hydrophilic surfaces, while large contact angles indicate hydrophobic surfaces.
- The surface energy of the solid can be calculated using different test liquids.
- The hysteresis between advancing and receding contact angle indicates surface roughness, heterogeneity or contamination.

While contact angle measurement is a very inexpensive technique, it is one of the most surface-sensitive methods and thus highly valuable in characterizing microarray coatings and monitoring surface modifications. In the development of signal enhancement substrates in this work contact angle measurements were used to characterize the adhesion of xanthan and chitosan to gold substrates.

2.2 Microarray printing

Microarray printing is the process of depositing the probes on the chip substrates. The diameter of the microspots is typically between 50 µm and 500 µm depending on substrate surface chemistry, the print buffer composition, humidity during array fabrication and the spotting equipment.

Regarding the surface chemistry, spots on hydrophobic substrates are usually small and inhomogeneous, whereas hydrophilic substrates produce more homogeneous spots which are often irregularly shaped [92]. Similarly printing buffers and additives such as detergents and polyhydric alcohols (e.g. glycerol, sucrose, trehalose) have shown to influence spot size and morphology [93]. The concentration of the spotted protein, which can vary between several hundred µg/mL and many mg/mL not only influences signal intensity, but also spot homogeneity and reproducibility [94].

The process of spotting is carried out by dedicated microspot arrayers. Generally there are non-contact and contact devices. Currently there are two types of non-contact ink-jet technology, syringe-solenoid and piezoelectric pumps. Solenoid type spotters feature tips built from high quality ceramics available in different sizes for a range of probe volumes and spot diameters. The syringe-solenoid system is adequate to array high numbers of replicate spots.

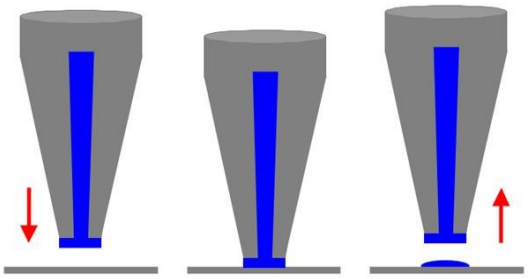

Fig. 20 Principle of contact printing. The sample-loaded pin contacts the printing surface during down-stroke, producing a droplet between substrate and pin. As the pin travels upward the droplet is pulled off the end of the pin. (www.arryit.com)

The piezoelectric spotter uses the vibration of a piezo crystal to dispense a probe droplet. The system is currently limited to 4-8 pins. Higher printing speeds are attainable with contact spotters. Their print heads can be equipped with dozen of pins that simultaneously dip into the protein probe solutions and deposit the probe when contacting the microarray surface (Fig.

20). For instance the OmniGrid Arrayer (GeneMachines) has a print head for 48 pins and allows high throughput manufacture of high-density arrays. It also features a washing, sonification and drying station to clean the pins and to avoid carry over between different probes (Fig. 21). Contact spotting pins are available as solid and split pins. Solid pins (Fig. 22a) are cheaper, more robust and exhibit no risk of clogging. On the other hand split pins (Fig. 22b-d) feature a sample reservoir that is loaded with the probe liquid by capillary force. Therefore these pins require less redipping cycles for the same number of printed spots.

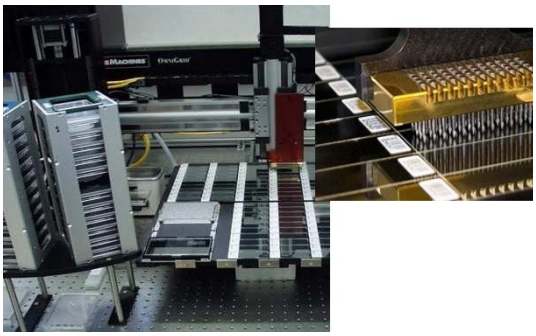

Fig. 21 Robotic microarray station with printhead for 48 pins.

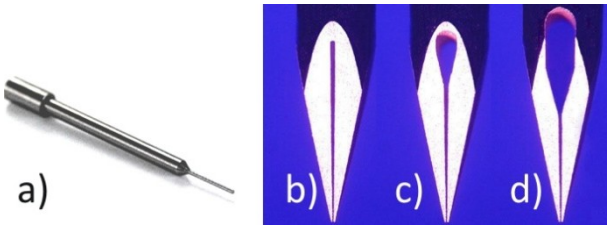

Fig. 22 Different contact pins. a) Solid pin b) – d) Split pins with 0.25, 0.60 and 1.25 µL sample loading volume. (www.arrayit.com)

2.3 Probes

2.3.1 Antibodies

Antibodies are the most frequently used type of probe in protein microarrays. These gamma globulin proteins are abundant in the bodily fluids of vertebrates and are secreted by the immune system's B cells. Different classes of antibodies, called isotypes, are known. In mammals immunoglobulins IgA, IgD, IgE, IgG and IgM are found, each of which has a distinct role in the immune system. The isotypes again can be subdivided. For instance IgG, which is almost exclusively used in immunoassays, has four subclasses in human (IgG1, IgG2, IgG3, IgG4). This isotype is so popular, because it binds to its epitope (recognition site on the antigen) with highest affinity, it is produced in animals in high amounts and it is very stable during purification [95].

In regard to their structure antibodies are glycoproteins and exist as mono- or multimers depending on the isotype. Ig monomers are "Y"-shaped molecules that consist of four polypeptide chains – two identical light and two identical heavy ones – that are connected by disulfide bonds (Fig. 23). Each chain is built up of several structural domains. Light chains

consist of one variable and one constant domain, whereas heavy chains are composed of one variable domain, followed by a constant one, a hinge region and two more constant domains. One variable and one constant domain from each heavy and light chain form the antibody's so called Fab region (fragment, antigen binding). It contains the binding site for the antigen, against which the antibody is specifically directed. The Fc region (fragment, crystallisable) is made up of the remaining constant domains of the heavy chains and mediates different physiological effects. Specific strategies to immobilize antibodies to the chip surface include attachment via their thiol groups, binding by way of their carbohydrate residues or coupling with protein A, L or G [92].

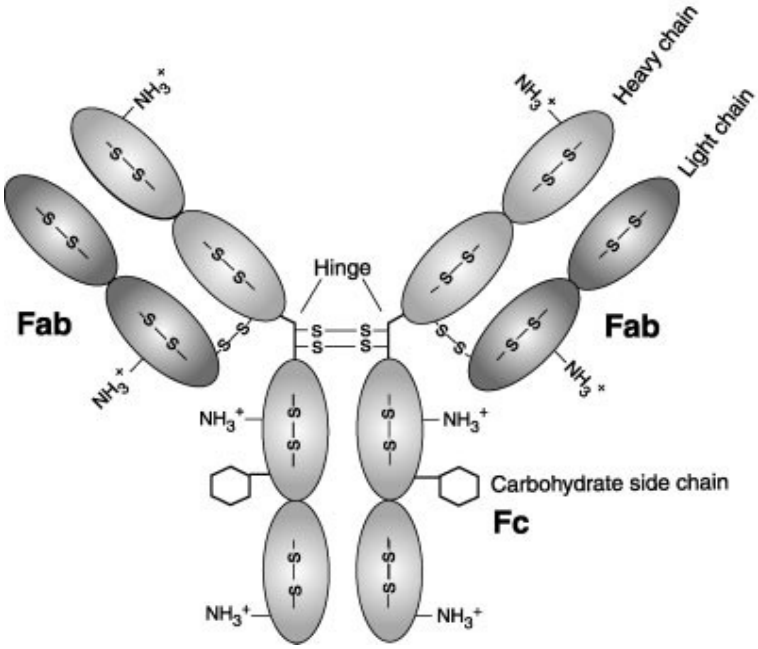

Fig. 23 Scheme of an antibody structure [92]

Moreover the Fab region can be cleaved off with a specific protease and, as its terminal loops constitute the antigen recognition site, can serve as a capture element in its own right.

The majority of antibodies are obtained via active immunization of a laboratory animal with an immunogen. The immunogen can be a protein, polysaccharide, lipid, nucleic acid or synthetic polypeptide that elicits an immune response when injected into the animal. After repeated immunization the animal has high serum titers of antibodies directed against the immunogen [95]. These antibodies are a mixture of different isotypes with varying binding affinities. They are termed "polyclonal antibodies" as the immunoglobulins are derived from different cells or cell lines. Also polyclonal antibodies feature different specificities,

recognizing both epitopes on the antigen and on co-injected impurities. The animal (anti)serum can be either used directly or further purified via

- salting out, dialysis/gel filtration
- ion-exchange chromatography
- protein A / G affinity columns
- immunoaffinity chromatography

In contrast to polyclonal antibodies, monoclonal antibodies are identical featuring the same affinity and specificity [95]. However their production is more laborious and expensive (Fig. 24): Antibody producing spleen cells are removed from an immunized mouse. These cells are fused with immortal myeloma cells (cancerous B cells), that do not produce antibodies and cannot build HGPRT (hypoxanthineguanine phosphoribosyltransferase), an enzyme that enables cells to grow on medium containing HAT (hydroxanthine, aminopterin and thymidine). The resulting hybridomas (hybrid cells) are immortal, produce high quantities of the antibody and can grow on HAT. A subsequent selection step on HAT medium eliminates both the short-lived spleen cells and the unfused myeloma cells. Only hybridoma cells are retained and screened for production of antibodies against the desired target. A selected hybridoma cell is allowed to multiply and its offspring only produces identical antibody molecules against the antigen.

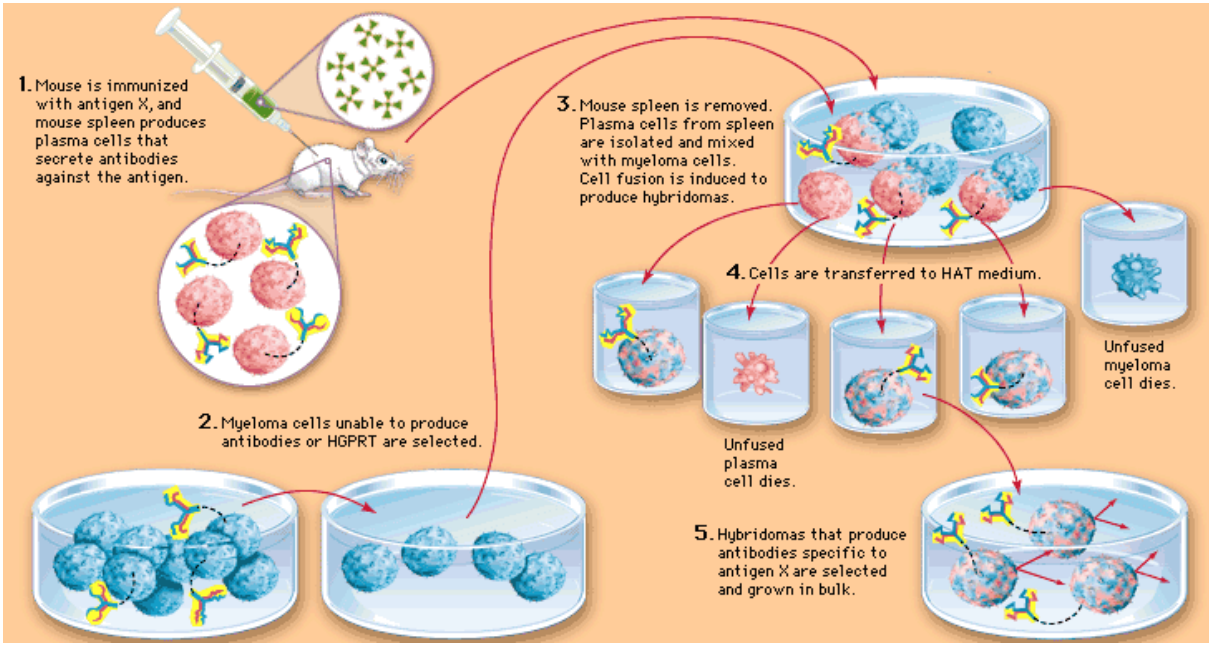

Fig. 24 Production of monoclonal antibodies (www.britannica.com)

Phage display is a method to produce antibodies in vitro without the need for a laboratory animal [96]. The genes coding for the variable antibody moieties are cloned from a large pool of B donor cells and are used to construct a library of FAB genes. They are inserted into viruses called phages, which infect Escherichia coli bacteria. The phages reproduce in the bacterial cells and finally leave the rupturing cells. Each phage exposes the antibody fragment on its surface for which it carries the coding gene. From the mixture of phages with antibody fragments of varying specificity those are selected that bind to the desired antigen. The isolated "monoclonal" antibody phages and the corresponding genes can be isolated and sequenced and thus the antibody fragments can be produced as soluble proteins.

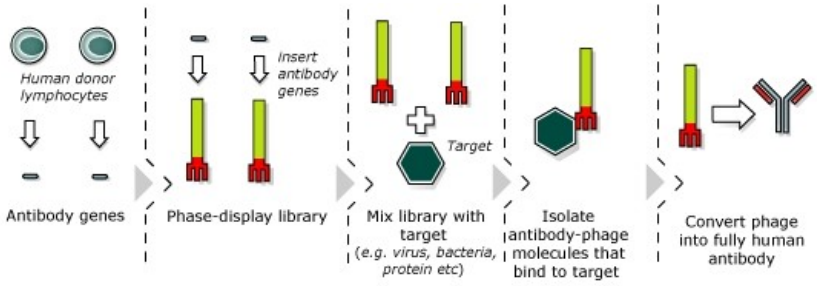

Fig. 25 Production of monoclonal antibodies via phage display (www.crucell.com)

When selecting the appropriate antibody production method it is important to consider the requirements of the intended application. Those include the level of antibody purity, specificity and affinity. To sum it up, the production of polyclonal antibodies is cheapest, quick and easy. However this type of antibody is limit by its degree of specificity, purity and yield. Also antibodies from different immunizations will vary in their properties. Conversely monoclonal antibodies feature invariable specificity. However one has to keep in mind that monoclonal antibodies are directed against a particular epitope on the antigen and not against the whole molecule. Phage display can be carried out in a few weeks but strongly depends on the quality of the gene library.

2.3.2 Aptamers

In 1990 it was discovered that subpopulations of RNA molecules bind specifically to a variety of ligands [97]. The term aptamer was introduced for single-stranded oligonuleotides – both RNA and DNA – which fold into unique 3-D structures, allowing them to bind to target molecules. Several aptamers have been identified to bind various ligands, including zinc ions, substance P, organic dye molecules, ribosomes, the enzyme DNA polymerase, viruses and human red blood cell membranes [98-100]. Aptamers' affinities and selectivities can rival

those of antibodies. Also this class of molecules provides orders of magnitude more sequence diversity than the phage display technique.

Aptamers are selected in a process known as systematic evolution of ligands by exponential enrichment (SELEX). A DNA or RNA library generated by chemical synthesis serves as the starting point of the production cycle (Fig. 26). In an appropriate selection step specific target-binding aptamer molecules are separated from nonbinding oligomers. Molecules with the desired binding activity are amplified by (reverse transcriptase) polymerase chain reaction. The enriched library is again exposed to the target. The cycle is repeated until the target-interacting sequences dominate the population [101].

Owing to their synthetic origin aptamers offer a range of interesting properties that render them attractive capture and detection elements in biochip applications (Table 4): Aptamers are very stable, their affinity can be tuned, they are amenable to straightforward modifications and their synthesis is extremely reproducible [102]. Thus aptamers can ideally complement antibodies as biorecognition elements.

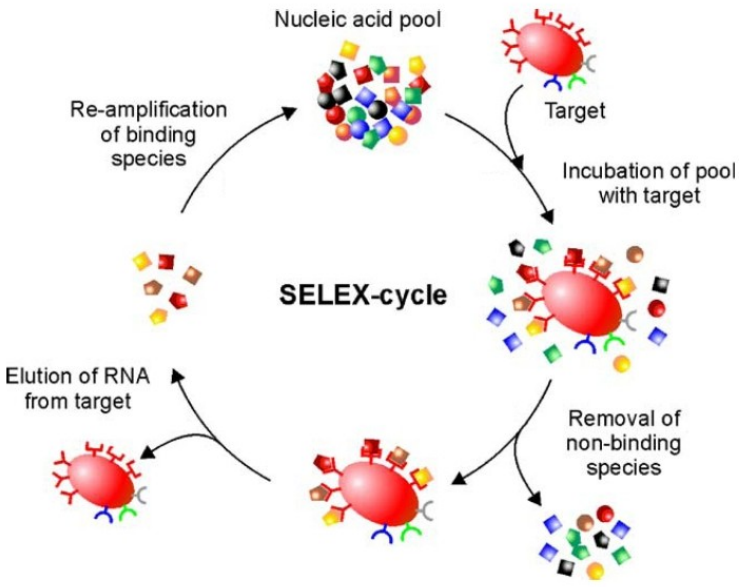

Fig. 26 Scheme of the SELEX process [101]

Table 4 Comparison of aptamers and antibodies [102]

	Aptamers	Antibodies
Affinity	low nM – pM	low nM – pM
Specificity	High	High
Production	in vitro chemical process	in vivo chemical process
Target range	wide: ions, small organic molecules, proteins, whole cells, etc.	narrow: only immunogenic compounds
Batch to batch variations	little or no	may be significant
Chemical modification	easy and straightforward	Limited
Thermal denaturation	Reversible	Irreversible
Shelf-life	Unlimited	Limited

The RNA aptamer directed against CRP, which is used in this study, was obtained by SELEX from an oligonucleotide library of random regions flanked by constant regions. The constant regions featured binding sites for PCR primers, cloning sites and a T7 promoter. The aptamer sequence obtained after 10 rounds of SELEX was a 44-mer with a dissociation constant (K_D) of 125 nM [103]. The secondary structure of the aptamer is important as it enables binding to the target protein CRP. Two possible structures are depicted in Fig. 27 [104]. In this work the aptamer was equipped with an aminohexaethylene glycol spacer at the 5'-end. The spacer confers certain flexibility to the molecule and the terminal amino group allows for immobilization.

Only recently a 72-mer single stranded DNA aptamer for CRP with a K_D of 3.51 nM was selected after 5 rounds of SELEX in an automatic, magnetic bead-based microfluidic chip system [105].

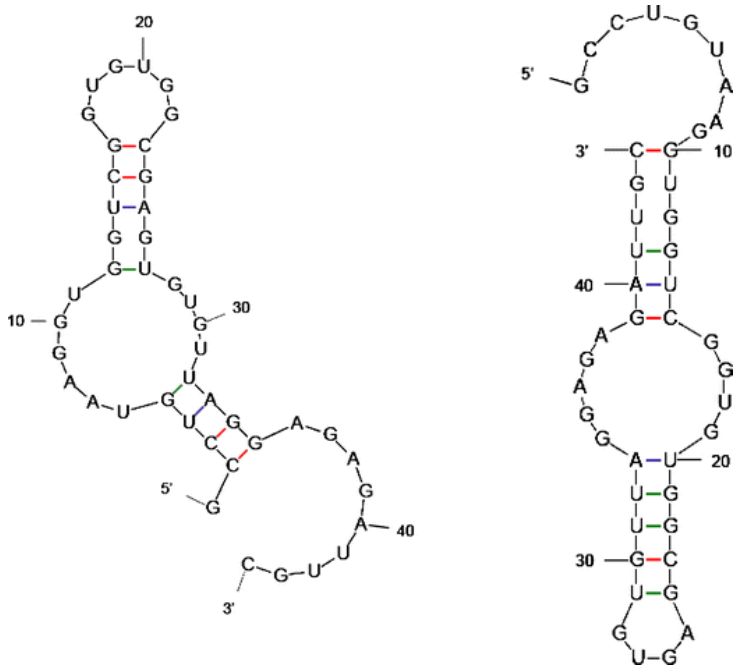

Fig. 27 Two of the possible secondary structures of the CRP RNA aptamer used in this study. The structures have a comparable energy [104].

2.3.3 Other binding elements

Apart from antibodies, which are the most frequently described protein binding elements, and aptamers, other capture elements are found in literature such as molecularly imprinted polymers, peptides and scaffolds.

Molecularly imprinted polymers (MIP) are formed in the presence of a target molecule that is extracted after synthesis, thus leaving a complementary cavity behind. These cavities act as binding pockets and show affinity for the analyte.

Proteins and peptides have been used as on chip binding elements. They either serve as the target of antibodies or exhibit other affinity interactions with the assay compounds. Furthermore low molecular ligands and substances have been employed as capture molecules. For instance Zuo and co-workers have generated a "hapten microarray" from immobilized synthetic compounds [106] that act as β-adrenergic agonists. Similarly immobilized phosphocholine serves as a natural ligand for C-reactive protein (CRP) [107].

Protein scaffolds represent another important group of protein binders. Protein scaffolds are domains that possess regions suitable for engineering. In these regions targeted mutations can be used to create ligand binders with antibody-like specificity and affinity [108]. Examples are "Anticalins" modelled on lipocalin structures, "Trinectins" based on a firbronectin III domain and "Affibody" molecules derived from Staphylococcus aureus protein A [109]. While synthesis and selection [110-111] of these molecules were already described in proof-of-concept studies the utility of these new affinity reagents in diagnostic applications still remains to be demonstrated.

3 Microarray processing

Protein microarray processing involves all the handling steps needed for carrying out the immunoassay (see chapters 1.2 and 1.2.2). Typically the first step in microarray processing is blocking, i.e. masking the reactive sites of the printed microarray surface in order to prevent unspecific adsorption of assay components. Blocking provides the added value of washing away unbound printed protein.

In the next steps samples, standards and detection molecules are added to the microarrays. To promote the biological interactions and to preserve the proteins' activity optimized buffers are used which are supplemented with all necessary ions and set to ideal values of pH and ionic strength. Furthermore additives suppress unspecific interactions and aid in homogeneous wetting of surfaces.

Additives can be polymers and proteins as well as surfactants. They may serve as blocking agents, facilitate surface wetting, act as solubilizers or even promote biological interactions. Some of the additives tested in this work during the optimization of assay protocols are sampled in Table 5.

Table 5. Buffer additives and their uses

Substance class		Name	Use
detergents	non-ionic	Polyoxyethylene (20) sorbitan monolaurate (Tween-20)	wetting of hydrophobic surfaces, blocking of vacant sites on the substrate
		Octylphenyl-polyethylene glycol (IGEPAL)	potential assay enhancer
		Decanoyl-N-methylglucamide (MEGA 10)	potential assay enhancer
	zwitter-ionic	3-[(3-Cholamidopropyl)dimethylammonio]-1-propanesulfonate (CHAPS)	potential assay enhancer
	Anionic	sodium deoxycholate	potential assay enhancer
	Cationic	dodecyl-trimethylammonium bromide (DTAB)	potential assay enhancer
other polymers		Xanthan	blocking of positively charged surfaces
		polyacrylic acid	reduction of non-specific binding and spot comet formation [70]
	Proteins	bovine serum albumine	blocking, protein stabilization
Natural		fat-free milk powder	Blocking
		quillaja bark extract (contains saponins)	potential assay enhancer

To develop both sensitive and quick tests incubation steps are optimized in respect to time and temperature. Shaking during incubation decreases necessary incubation time and increases assay reproducibility.

In order to individually address replicate probe arrays on the microarray slides, 16 well array incubation chambers can be used on each slide (Fig. 28). Thus up to 16 different samples or standards can be incubated on one chip (see also Fig. 1). The incubation chambers simplify liquid handling and high throughput processing of the microarray is enabled by pipetting and withdrawing target and washing solutions with a multi-pipette.

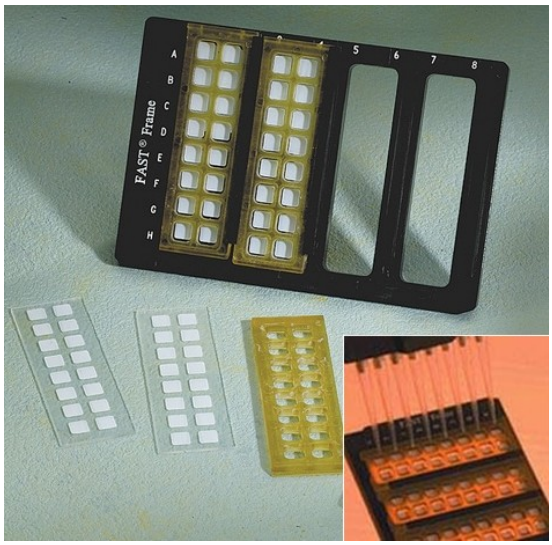

Fig. 28 Incubation chambers for microarray processing (www.whatman.com)

4 Detection

Detection techniques which have been implemented for protein microarrays are based on optics, radioactivity, electrochemistry, as well as on piezoelectric principles.

Optical detection methods can be subdivided into label-free and label-based methods. Both approaches have their merits and disadvantages. The label-based approach requires labelling of the detection molecules with dyes, which can alter the proteins natural activity. Additionally labelling procedures are lengthy and laborious and limit the number and types of molecules that can be studied. Yet the label-based approach is popular as reagents are widely available and the required instruments are simple.

In contrast optical label-free techniques avoid interference due to tagging of the molecules as they monitor changes in refractive index or layer thickness due to biomolecule interactions. Label-free methods enable the determination of reaction kinetics in real-time. However the label-free approach is more prone to sensitivity and specificity issues.

4.1 Optical label-free techniques

4.1.1 Surface plasmon resonance

Surface plasmon resonance (SPR) is a surface sensitive spectroscopic technique that measures the change in refractive index or thickness of biomaterials at the interface between metal surfaces and ambient medium. The probe proteins are usually bound to a 50-100 nm thick gold film and interact with binding partners in a flow cell [112] (Fig. 29). When the gold surface is illuminated with light surface plasmons are excited. Surface plasmons are surface electromagnetic waves that propagate perpendicular to the metal surface. When surface plasmons are excited in a resonant manner at a given wavelength and angle of incidence, a minimum in the intensity of the reflected light is observed. The angle of minimum intensity is very sensitive to the dielectric constant of the medium just a few tens of nanometers across the gold-solution interface and thus responds to binding events in the receptor layer. Direct immunoassays are not suitable for SPR detection of low molecular weight analytes as the increase in refractive index is too small. Therefore often binding inhibition [113] and sandwich immunoassay formats [114] have been adopted.

SPR has advanced to a high throughput technique in SPR imaging, where multiple biomolecular interactions are analyzed simultaneously.

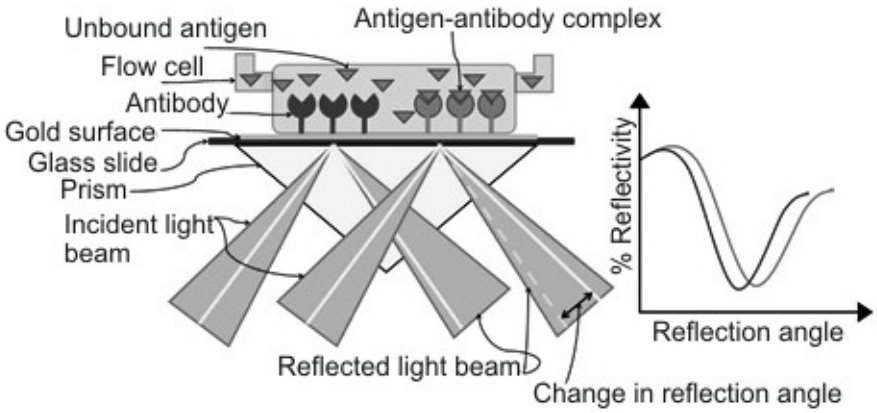

Fig. 29 Principle of SPR [112]

4.1.2 Reflectometric interference spectroscopy

Reflectometric interference spectroscopy is a time-resolved label-free technique to monitor molecular interactions between immobilized proteins and analytes in solution [115]. A typical RIfS set-up is shown in Fig. 30. A light source illuminates the RIfS substrate with immobilized proteins from beneath. The light passes the bulk carrier glass slide and is reflected partially at the bottom and the top of the thin interference layer which typically consists of functionalized silicon dioxide. The reflected light beams (I1 + I2) result in a wavelength-dependent interference pattern. If an analyte binds to the immobilized receptors the optical thickness of the biomolecule layer increases and the interference spectrum of the reflected light changes.

RIfS is temperature-independent (in contrast to SPR) and features a higher depth of penetration into the solution. RIfS has been used to monitor both protein-protein and DNA-protein interactions.

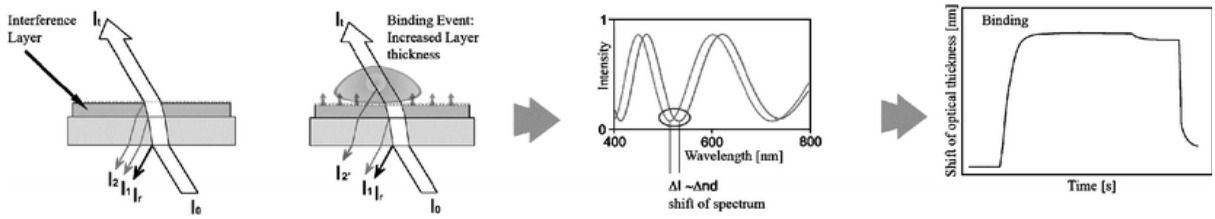

Fig. 30 Principle of RIfS. The technique is based on the interference of reflected beams which is influenced by analyte binding. The shift in the resulting characteristic interference spectrum can be transformed into a binding curve [115].

4.2 Optical label-based techniques

Optical label-based detection techniques can be divided into fluorescence, chemiluminescence and colorimetric methods. Fluorescence is widely employed because it is sensitive, simple, and provides high resolution [7]. In this approach a fluorophore is either covalently linked to the detection antibody or the biotinylated antibody binds a fluorophore streptavidin conjugate. Fluorophores are often dyes either derived from coumarin, rhodamine, xanthene or cyanine. Popular excitation wavelengths are 532 and 635 nm and a whole range of corresponding dye molecules from several companies are on the market (e.g. Cy3 and Cy5 from GE Healthcare, Dy547 and Dy647 from Dyomics, Alexa Fluor 555 and 647 from Invitrogen).

Chemiluminescence is an alternative scheme for sensitive analyte detection. It is currently implemented in many assay types including ELISA. In this approach detection antibodies are conjugated to alkaline phosphatase or horseradish peroxidise (HRP). The enzymatic oxidation of a substrate, such as luminol, produces a prolonged emission of light, which is captured with a phosphor imager or a CCD camera [116].

In colorimetric detection HRP or alkaline phosphatase generate a coloured insoluble reaction product [117] or gold nanoparticle labels catalyze the deposition of elemental silver [118].

4.2.1 Fluorescence scanners

The read-out of fluorescence microarrays is usually performed with fluorescence scanners. These devices work like fluorescence microscopes and acquiring images from chips in standard microscopy slide format (25 mm x 76 mm x 1 mm). This format is supported by >90% of all currently used detection instruments [45]. Most commercial scanners feature two helium-neon lasers for excitation at λ=635 nm and λ=532 nm. New models already offer slots for four lasers with different emission wavelengths which can be adapted to many different fluorescence modes with filters. Scanner performance such as sensitivity, dynamic range, resolution, field uniformity and reproducibility are of paramount importance for high-quality scans.

Laser scanners are available as confocal and non-confocal devices. Optics of a non-confocal scanner, such as used throughout this work, are depicted in Fig. 31a. A light beam emitted from a laser source is focused by a lens and reflected at a beamsplitter. It further passes through another focusing lens and irradiates the biochip surface. The fluorescence dye on the microarray is excited and emits fluorescence which passes through the focusing lens, the beam splitter and a filter which eliminates light of the wavelength of the light source. The

fluorescence is focused by another lens and detected by a photomultiplier tube (PMT), which converts the optic signal into an electrical signal, which is processed by a computer [119]. Non-confocal scanners detect all light emitted from the microarray substrate.

Conversely confocal scanners reduce out of focus light by introducing a pinhole into the light path (Fig. 31b). Fluorescence is detected only in a single plane. However the very narrow depth of focus makes this system particularly sensitive to slight variations in the flatness of the slide or slide holder.

In contrast to scanners which rely on steady-state measurements of the emitted fluorescence, emerging detection technologies feature time-resolved data acquisition and alternative approaches for fluorophore excitation and signal detection. Besides fluorescence intensity these technologies allow monitoring fluorescence lifetime [120].

As an alternative to direct laser excitation evanescent wave excitation has been applied in the construction of very detection sensitive systems. Coherent light is trapped in a thin surface layer and creates evanescent fields with large field strengths (Fig. 32). The evanescent field provides an enhanced excitation efficiency of surface-bound fluorophores [121].

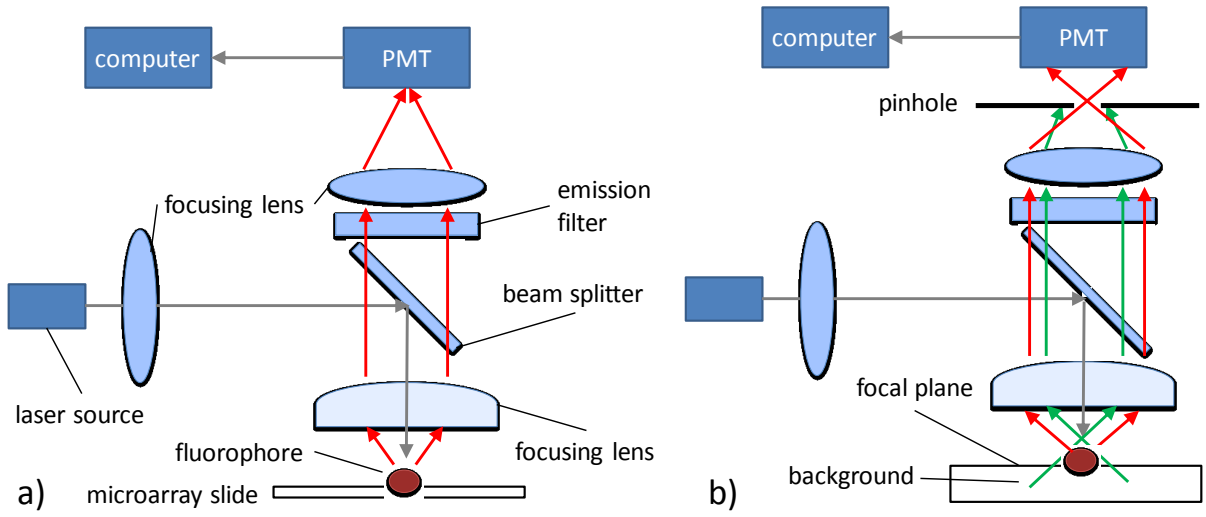

Fig. 31 Scheme of laser scanner with PMT detection and a) non-confocal and b) confocal optics.

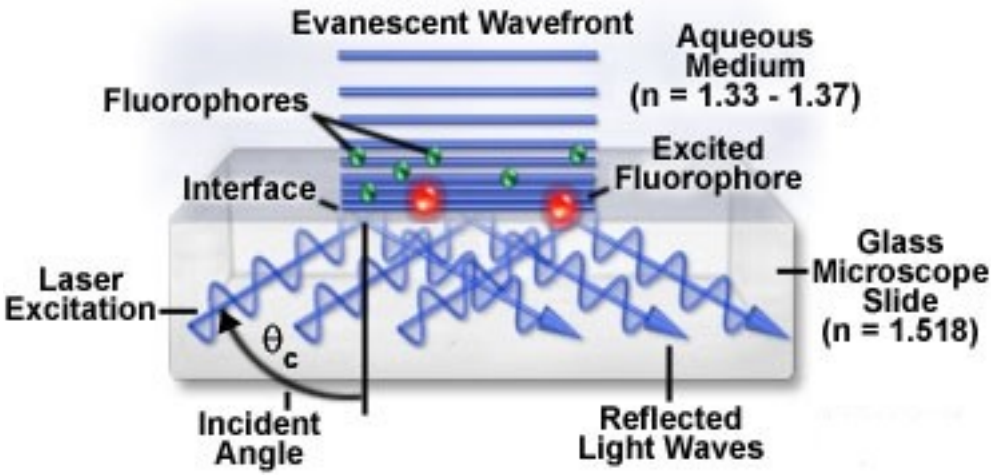

Fig. 32 Evanescent wave excitation of surface-bound fluorophores (www.microscopyu.com)

4.2.2 Fluorescence signal amplification techniques

Owing to its good resolution, high sensitivity and dynamic range optical fluorescence detection of microarray spots has become an established laboratory technique. Striving for even higher sensitivity researchers have developed substrates with increased loading capacity [122] and techniques to maximize the target concentration on the surface [123]. Also alternative fluorescence labels and approaches to increase the optical efficiency of the fluorescence measurement have been introduced.

Alternative labels include dendrimers, fluorescent nanoparticles, quantum dots, and biological molecules which initiate the accumulation of dye molecules – e.g. in the tyramide precipitation reaction or the rolling circle amplification.

- ***Dendrimers*** are repeatedly branched, roughly spherical large molecules which can be conjugated to a large number of fluorescence dye molecules as well as to detection molecules (e.g. antibodies) [124].
- ***Fluorescent nanoparticles*** labels are also based on the concept of attaching a large number of dye molecules to a reporter protein. The dye molecules are confined in a matrix, e.g. silica [125].
- ***Quantum dots*** are inorganic semiconductor nanocrystals with a typical diameter between 2 and 8 nm. Generally they are composed of group II and VI elements (e.g. CdSe and CdTe) or groups III and V elements (e.g. InP and InAs). Their physical dimensions are smaller than the exciton Bohr radius. This leads to a quantum confinement effect, which is responsible for the quantum dots' unique optical and electronic properties. The wavelength of the fluorescence light emitted

by quantum dots can be tuned by varying their size [126]. As quantum dots are not soluble usually an additional coating which renders them water-compatible is applied. The most frequently used system is CdSe coated with an outer shell of ZnS. The ZnS shell aids to chemically and optically stabilize the CdSe core. In comparison to conventional dye molecules this class of luminescent labels is twenty times brighter, and one hundred times more stable against photobleaching [127]. Thus the detection limit of protein assay can be significantly decreased.

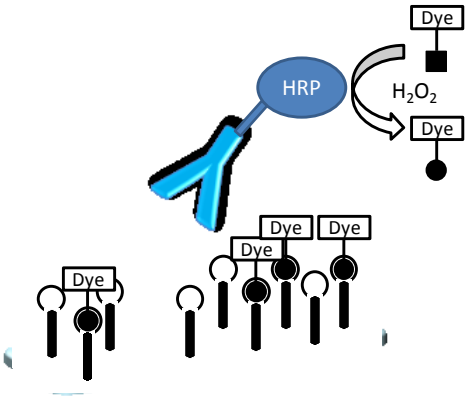

Fig. 33 Principle of tyramide precipitation in a sandwich immunoassay set-up. HRP – horseradish peroxidase coupled to detection antibody, ■ – inactive tyramide, ● – active tyramide radical, ○ – nucleophilic residue

- ***Tyramide precipitation*** uses the catalytic activity of HRP to generate high-density labelling at the site of the detection molecule [128] . The detection molecule is coupled to HRP either directly or via a biotin-streptavidin linkage (Fig. 33). HRP activates multiple copies of a fluorescent dye tyramide derivate. The generated highly reactive, short-lived tyramide radicals couple to nucleophilic residues (often the phenol moiety of protein tyrosine residues) in the vicinity of the HRP-site. The turnover of multiple tyramide substrates per peroxidise label leads to a strong increase in signal intensity. However the process only results in minimal diffusion-related loss of signal localization.
- ***Rolling circle amplification*** generates increased signals by accumulating dye molecules in a long strand of DNA attached to the detector molecules [129]. The detailed process is depicted in Fig. 34: The assay detection antibody is conjugated to an oligonucleotide primer. The primer hybridizes with a complementary synthetic DNA circle. In the presence of nucleotides the enzyme DNA polymerase extends the primers in a reaction called rolling-circle replication. A long single stranded DNA molecule is generated. It is a concatamer of complements of the circle DNA sequence and remains attached to the antibody. This product is subsequently detected by hybridization with multiple fluorescent, complementary oligonucleotide probes [16].

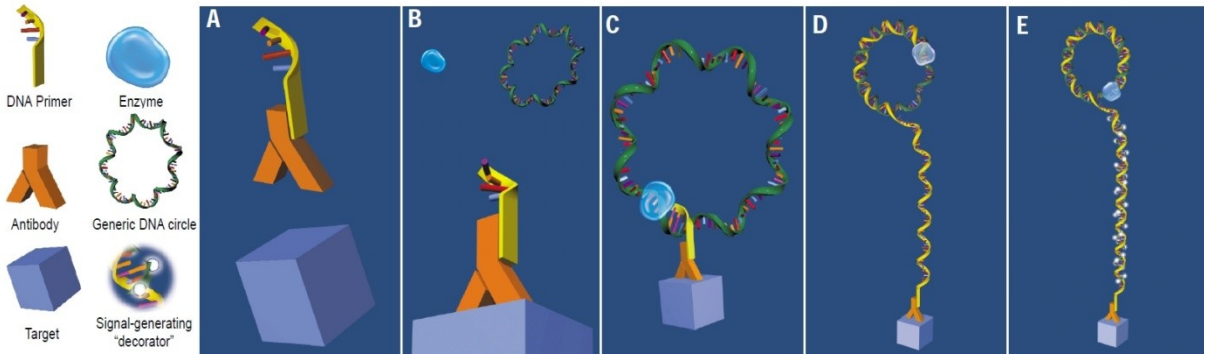

Fig. 34 Principle of rolling circle amplification [16]. An oligonucleotide primer label (A) hybridizes to a complementary DNA circle (B). DNA-polymerase dependent DNA replication generates a single-stranded concatamer (C-D) that is detected by hybridization with labelled oligonucleotides (E).

Other approaches for improving the detection sensitivity aim at increasing the optical efficiency of the fluorescence measurement.

Metallic surfaces and particles have also been applied to increase fluorescence intensities [130]. This phenomenon is termed "metal enhanced fluorescence". Metallic surfaces and particles can increase the radiative decay rates of fluorophores. This phenomenon is caused by metal surface plasmon electrons which interact with the excited-state fluorophores. Another effect is the spatial concentration of the incident light field.

The following equations illustrate the effect of the radiative rate, Γ on the fluorophore. The quantum yield (Q_0) and the lifetime of the fluorophore (τ_0) in free-space conditions are given by [131]:

(2)

(3)

where k_{nr} is the non-radiative rate. A nearby metal surface (m) increases the radiative rate by a new rate Γ_m. Consequently the quantum yield (Q_m) and the lifetime of the fluorophore (τ_m) in the proximity of the metal surface are

(4)

(5)

It can be seen from equations (2)-(5) that an increase in Γ_m leads to an increase in the fluorescence dye's quantum yield and a decrease in lifetime. Thus fluorophore bleaching is reduced and fluorescence intensity is increased due to increased fluorophore excitation and emission stimulated by the concentrated electromagnetic field.

Metallic particles and nanostructures, predominantly silver colloids and silver island films, have been applied to harness this amplification effect. The fluorescence enhancement was shown to depend on the particle size, the interparticle distance, and the metallic particle-dye interdistance [132]. In metallic nanostructures these optical properties were linked to the concept of localized surface plasmon resonance (LSPR). LSPR is generated by collective oscillations of the electron gas in metal nanostructures surrounded by a dielectric. Both absorption and scattering of incident light are greatly enhanced when the LSPR is excited [133].

Apart from metallic nanostructures fluorescence signal amplification was also observed in front of metal mirrors. The phenomenon was first described by Drexhage in 1974 [134]. It was demonstrated that the decay time (lifetime of a fluorophore) oscillates with distance from the mirror. This observation was explained by the changes in phase of the mirror-reflected field which interacts with the fluorophore. When the reflected field is in phase with the fluorophore's oscillating dipole (i.e. equation (5)) a decrease in lifetime is found, whereas an increase is seen when the reflected field is out of phase with the fluorophore's dipole.

A simple configuration which uses this fluorescence enhancement principle consists of a silicon planar reflector coated with a thin film of silicon dioxide (e.g. [135-136]). Optimal signal enhancement is obtained when the fluorophore on the silicon dioxide layer is spaced by an odd number of quarter-wavelengths from the reflective silicon substrate.

5 References

1. Martin, D.B. and P.S. Nelson, *From genomics to proteomics: techniques and applications in cancer research.* Trends in Cell Biology, 2001. **11**(11): p. S60.
2. Lockhart, D.J. and E.A. Winzeler, *Genomics, gene expression and DNA arrays.* Nature, 2000. **405**(6788): p. 827-36.
3. Sharma, H., et al., *DNA microarray analysis for human congenital heart disease.* Cell Biochemistry and Biophysics, 2006. **44**(1): p. 1.
4. Glanzer, J., P. Haydon, and J. Eberwine, *Expression Profile Analysis of Neurodegenerative Disease: Advances in Specificity and Resolution.* Neurochemical Research, 2004. **29**(6): p. 1161.
5. Csillag, C., et al., *Clinical phenotype and gene expression profile in Crohn's disease.* Am J Physiol Gastrointest Liver Physiol, 2007. **292**(1): p. G298-304.
6. Cutler, P., *Protein arrays: the current state-of-the-art.* Proteomics, 2003. **3**(1): p. 3-18.
7. Zhu, H. and M. Snyder, *Protein chip technology.* Curr Opin Chem Biol, 2003. **7**(1): p. 55-63.
8. Knezevic, V., et al., *Proteomic profiling of the cancer microenvironment by antibody arrays.* Proteomics, 2001. **1**: p. 1271 - 1278.
9. Haab, B.B. and P.M. Lizardi, *RCA-Enhanced Protein Detection Arrays*. 2006. p. 15-29.
10. Ivanov Iu, D., et al., *[Detection of hepatitis B virus surface antigen with the use of an optical biosensor]*. Zh Mikrobiol Epidemiol Immunobiol, 2003(2): p. 58-62.
11. Huff, J.L., et al., *Label-Free Protein and Pathogen Detection Using the Atomic Force Microscope.* J Biomol Screen, 2004. **9**(6): p. 491-497.
12. Huang, R.-P., et al., *Simultaneous Detection of Multiple Cytokines from Conditioned Media and Patient's Sera by an Antibody-Based Protein Array System.* Analytical Biochemistry, 2001. **294**(1): p. 55.
13. Lin, Y., et al., *Detection of Multiple Cytokines by Protein Arrays from Cell Lysate and Tissue Lysate.* Clinical Chemistry and Laboratory Medicine, 2003. **41**(2): p. 139.
14. Wiese, R., et al., *Simultaneous multianalyte ELISA performed on a microarray platform.* Clin Chem, 2001. **47**(8): p. 1451-7.
15. Whicher, J.T. and S.W. Evans, *Cytokines in disease.* Clin Chem, 1990. **36**(7): p. 1269-81.
16. Schweitzer, B., et al., *Multiplexed protein profiling on microarrays by rolling-circle amplification.* Nat Biotech, 2002. **20**(4): p. 359-365.
17. Matsunaga, K., et al., *Airway cytokine expression measured by means of protein array in exhaled breath condensate: Correlation with physiologic properties in asthmatic patients.* Journal of Allergy and Clinical Immunology, 2006. **118**(1): p. 84.
18. Du, H., et al., *Development of Miniaturized Competitive Immunoassays on a Protein Chip as a Screening Tool for Drugs.* Clin Chem, 2005. **51**(2): p. 368-375.
19. Charboneau, L., et al., *Utility of reverse phase protein arrays: Applications to signalling pathways and human body arrays.* Briefings in Functional Genomics and Proteomics, 2002. **1**(3): p. 305-315.
20. Nishizuka, S., et al., *Proteomic profiling of the NCI-60 cancer cell lines using new high-density reverse-phase lysate microarrays.* Proceedings of the National Academy of Sciences of the United States of America, 2003. **100**(24): p. 14229-14234.
21. Tibes, R., et al., *Reverse phase protein array: validation of a novel proteomic technology and utility for analysis of primary leukemia specimens and hematopoietic stem cells.* Molecular Cancer Therapeutics, 2006. **5**(10): p. 2512-2521.

22. Paweletz, C.P., et al., *Reverse phase protein microarrays which capture disease progression show activation of pro-survival pathways at the cancer invasion front.* Oncogene, 2001. **20**(16): p. 1981-9.
23. Fung, E.T., et al., *Protein biochips for differential profiling.* Current Opinion in Biotechnology, 2001. **12**(1): p. 65.
24. Seliger, B., R. Lichtenfels, and R. Kellner, *Detection of renal cell carcinoma-associated markers via proteome- and other 'ome'-based analyses.* Brief Funct Genomic Proteomic, 2003. **2**(3): p. 194-212.
25. Paweletz, C.P., et al., *Loss of annexin 1 correlates with early onset of tumorigenesis in esophageal and prostate carcinoma.* Cancer Res, 2000. **60**(22): p. 6293-7.
26. Petricoin Iii, E.F., et al., *Use of proteomic patterns in serum to identify ovarian cancer.* The Lancet, 2002. **359**(9306): p. 572.
27. Xiao, Z., et al., *Quantitation of Serum Prostate-specific Membrane Antigen by a Novel Protein Biochip Immunoassay Discriminates Benign from Malignant Prostate Disease.* Cancer Res, 2001. **61**(16): p. 6029-6033.
28. Luo, X., et al., *Macrophage proteomic fingerprinting predicts HIV-1-associated cognitive impairment.* Neurology, 2003. **60**(12): p. 1931-1937.
29. Lewczuk, P., et al., *Amyloid [beta] peptides in cerebrospinal fluid as profiled with surface enhanced laser desorption/ionization time-of-flight mass spectrometry: evidence of novel biomarkers in Alzheimer's disease.* Biological Psychiatry, 2004. **55**(5): p. 524.
30. Merkel, J.S., et al., *Functional protein microarrays: just how functional are they?* Current Opinion in Biotechnology, 2005. **16**(4): p. 447.
31. Kim, T.E., et al., *Quantitative measurement of serum allergen-specific IgE on protein chip.* Exp Mol Med, 2002. **34**(2): p. 152-8.
32. Lueking, A., et al., *Profiling of Alopecia Areata Autoantigens Based on Protein Microarray Technology.* Mol Cell Proteomics, 2005. **4**(9): p. 1382-1390.
33. Joos, T.O., et al., *A microarray enzyme-linked immunosorbent assay for autoimmune diagnostics.* Electrophoresis, 2000. **21**(13): p. 2641-2650.
34. Robinson, W.H., et al., *Autoantigen microarrays for multiplex characterization of autoantibody responses.* Nat Med, 2002. **8**(3): p. 295.
35. Lu, D.-D., et al., *Screening of specific antigens for SARS clinical diagnosis using a protein microarray.* The Analyst, 2005. **130**(4): p. 474-482.
36. Mezzasoma, L., et al., *Antigen Microarrays for Serodiagnosis of Infectious Diseases.* Clin Chem, 2002. **48**(1): p. 121-130.
37. Zhang, W., et al., *Protein chip for detection of different HCV antibodies: preparation, quality control, and clinical evaluation.* Mol Diagn, 2005. **9**(2): p. 81-7.
38. Chen, C.S. and H. Zhu, *Protein microarrays.* Biotechniques, 2006. **40**(4): p. 423-+.
39. Rifai, N., M.A. Gillette, and S.A. Carr, *Protein biomarker discovery and validation: the long and uncertain path to clinical utility.* Nat Biotech, 2006. **24**(8): p. 971-983.
40. Mayeux, R., *Biomarkers: Potential Uses and Limitations.* NeuroRx, 2004. **1**(2): p. 182-188.
41. Haass, N.K. and K.S.M. Smalley, *Melanoma Biomarkers Current Status and Utility in Diagnosis, Prognosis, and Response to Therapy.* Molecular Diagnosis & Therapy, 2009. **13**(5): p. 283-296.
42. Hotchkiss, R.S. and I.E. Karl, *The Pathophysiology and Treatment of Sepsis.* New England Journal of Medicine, 2003. **348**(2): p. 138-150.
43. Reinhart, K., M. Meisner, and F.M. Brunkhorst, *Markers for Sepsis Diagnosis: What is Useful?* Critical Care Clinics, 2006. **22**(3): p. 503-519.

44. Yu, X., N. Schneiderhan-Marra, and T.O. Joos, *Protein Microarrays for Personalized Medicine.* Clin Chem, 2010. **56**(3): p. 376-387.
45. Schena, M., *Protein microarrays*. 2005, Sudbury, Mass.: Jones and Bartlett.
46. Schäferling, M. and D. Kambhampati, *Protein Microarray Surface Chemistry and Coupling*
Schemes, in *Protein microarray technology*, D. Kambhampati, Editor. 2004, Wiley-VCH: Weinheim.
47. Seong, S.y. and C.y. Choi, *Current status of protein chip development in terms of fabrication and application.* Proteomics, 2003. **3**(11): p. 2176-2189.
48. Arenkov, P., et al., *Protein Microchips: Use for Immunoassay and Enzymatic Reactions.* Analytical Biochemistry, 2000. **278**(2): p. 123-131.
49. Miller, J.C., et al., *Antibody microarray profiling of human prostate cancer sera: Antibody screening and identification of potential biomarkers.* Proteomics, 2003. **3**(1): p. 56-63.
50. Angenendt, P., et al., *Toward optimized antibody microarrays: a comparison of current microarray support materials.* Analytical Biochemistry, 2002. **309**(2): p. 253-260.
51. Lv, L.L., et al., *Construction of an antibody microarray based on agarose-coated slides.* Electrophoresis, 2007. **28**(3): p. 406-413.
52. Seurynck-Servoss, S.L., et al., *Evaluation of surface chemistries for antibody microarrays.* Analytical Biochemistry, 2007. **371**(1): p. 105-115.
53. Fang, Y., A.G. Frutos, and J. Lahiri, *Membrane Protein Microarrays.* Journal of the American Chemical Society, 2002. **124**(11): p. 2394-2395.
54. Jiang, H.-y., S.-q. Zhang, and T. Zhao, *A New Method to Make Nuclei or Cell Microarrays.* Diagnostic Molecular Pathology, 2006. **15**(2): p. 109-114.
55. Urbanowska, T., et al., *Development of protein microarray technology to monitor biomarkers of rheumatoid arthritis disease.* Cell Biology and Toxicology, 2003. **19**(3): p. 189-202.
56. Jenison, R., et al., *Silicon-based Biosensors for Rapid Detection of Protein or Nucleic Acid Targets.* Clin Chem, 2001. **47**(10): p. 1894-1900.
57. Thirumalapura, N.R., et al., *Bacterial cell microarrays for the detection and characterization of antibodies against surface antigens.* Journal of Immunological Methods, 2006. **309**(1-2): p. 48-54.
58. Olle, E.W., et al., *Comparison of antibody array substrates and the use of glycerol to normalize spot morphology.* Experimental and Molecular Pathology, 2005. **79**(3): p. 206-209.
59. Steinhauer, C., et al., *Biocompatibility of surfaces for antibody microarrays: design of macroporous silicon substrates.* Analytical Biochemistry, 2005. **341**(2): p. 204-213.
60. Zhou, X. and J. Zhou, *Protein microarrays on hybrid polymeric thin films prepared by self-assembly of polyelectrolytes for multiple-protein immunoassays.* Proteomics, 2006. **6**(5): p. 1415-1426.
61. Avseenko, N.V., et al., *Immunoassay with Multicomponent Protein Microarrays Fabricated by Electrospray Deposition.* Analytical Chemistry, 2002. **74**(5): p. 927-933.
62. Shao, W.P., et al., *Optimization of rolling-circle amplified protein microarrays for multiplexed protein profiling.* Journal of Biomedicine and Biotechnology, 2003(5): p. 299-307.
63. Sreekumar, A., et al., *Profiling of Cancer Cells Using Protein Microarrays.* Cancer Research, 2001. **61**(20): p. 7585-7593.

64. Lue, R.Y., et al., *Site-Specific Immobilization of Biotinylated Proteins for Protein Microarray Analysis*. 2004. p. 85-100.
65. Shreffler, W.G., et al., *IgE and IgG4 epitope mapping by microarray immunoassay reveals the diversity of immune response to the peanut allergen, Ara h 2.* Journal of Allergy and Clinical Immunology, 2005. **116**(4): p. 893-899.
66. Hackler, L., et al., *Development of chemically modified glass surfaces for nucleic acid, protein and small molecule microarrays.* Molecular Diversity, 2003. **7**(1): p. 25-36.
67. Pathak, S., et al., *Dendrimer-Activated Surfaces for High Density and High Activity Protein Chip Applications.* Langmuir, 2004. **20**(15): p. 6075-6079.
68. Lesaicherre, M.-L., et al., *Developing site-Specific immobilization strategies of peptides in a microarray.* Bioorganic & Medicinal Chemistry Letters, 2002. **12**(16): p. 2079-2083.
69. Walter, J.G., et al., *Protein microarrays: Reduced autofluorescence and improved LOD.* Engineering in Life Sciences, 2010. **10**(2): p. 103-108.
70. Spillman, S.D., H.M. McEvoy, and B.D. MacCraith, *Fabrication of Substrate-Independent Protein Microarrays Using Polyelectrolyte Scaffolding.* Langmuir, 2008. **25**(3): p. 1403-1411.
71. Wong, L.S., F. Khan, and J. Micklefield, *Selective Covalent Protein Immobilization: Strategies and Applications.* Chemical Reviews, 2009. **109**(9): p. 4025-4053.
72. Paborsky, L.R., et al., *A Nickel Chelate Microtiter Plate Assay for Six Histidine-Containing Proteins.* Analytical Biochemistry, 1996. **234**(1): p. 60-65.
73. Paramban, R.I., R.C. Bugos, and W. Wen Su, *Engineering green fluorescent protein as a dual functional tag.* Biotechnology and Bioengineering, 2004. **86**(6): p. 687-697.
74. Zoroddu, M.A., et al., *Molecular mechanisms in nickel carcinogenesis: Modeling Ni(II) binding site in histone H4.* Environmental Health Perspectives, 2002. **110**: p. 719-723.
75. Sigal, G.B., et al., *A Self-Assembled Monolayer for the Binding and Study of Histidine-Tagged Proteins by Surface Plasmon Resonance.* Analytical Chemistry, 1996. **68**(3): p. 490-497.
76. Schmid, E.L., et al., *Reversible Oriented Surface Immobilization of Functional Proteins on Oxide Surfaces.* Analytical Chemistry, 1997. **69**(11): p. 1979-1985.
77. Nieba, L., et al., *BIACORE Analysis of Histidine-Tagged Proteins Using a Chelating NTA Sensor Chip.* Analytical Biochemistry, 1997. **252**(2): p. 217-228.
78. Kroger, D., et al., *Immobilization of histidine-tagged proteins on gold surfaces using chelator thioalkanes.* Biosensors & Bioelectronics, 1999. **14**(2): p. 155-161.
79. Kang, E., et al., *Specific Adsorption of Histidine-Tagged Proteins on Silica Surfaces Modified with Ni2+/NTA-Derivatized Poly(ethylene glycol).* Langmuir, 2007. **23**(11): p. 6281-6288.
80. Tinazli, A., et al., *High-Affinity Chelator Thiols for Switchable and Oriented Immobilization of Histidine-Tagged Proteins: A Generic Platform for Protein Chip Technologies.* Chemistry – A European Journal, 2005. **11**(18): p. 5249-5259.
81. Klenkar, G., et al., *Piezo dispensed microarray of multivalent chelating thiols for dissecting complex protein-protein interactions.* Analytical Chemistry, 2006. **78**(11): p. 3643-3650.
82. Lata, S. and J. Piehler, *Stable and functional immobilization of histidine-tagged proteins via multivalent chelator headgroups on a molecular poly(ethylene glycol) brush.* Analytical Chemistry, 2005. **77**(4): p. 1096-1105.
83. Hyun, J.W., et al., *Protein adsorption on the nickel-coated glass slide for protein chips.* Bulletin of the Korean Chemical Society, 2002. **23**(12): p. 1724-1728.

84. Agarwal, G., R.R. Naik, and M.O. Stone, *Immobilization of Histidine-Tagged Proteins on Nickel by Electrochemical Dip Pen Nanolithography.* Journal of the American Chemical Society, 2003. **125**(24): p. 7408-7412.
85. Zhu, H., et al., *Global analysis of protein activities using proteome chips.* Science, 2001. **293**(5537): p. 2101-2105.
86. Chang, Y.-J. and C.-H. Chang, *Protein microarray chip with Ni-Co alloy coated surface.* Biosensors and Bioelectronics, 2010. **25**(7): p. 1748-1754.
87. Alessandrini, A. and P. Facci, *AFM: a versatile tool in biophysics.* Measurement Science and Technology, 2005. **16**: p. R65-R92.
88. Lauritsen, J.V. and M. Reichling, *Atomic resolution non-contact atomic force microscopy of clean metal oxide surfaces.* Journal of Physics: Condensed Matter, 2010. **22**(26): p. 263001.
89. Ha, C.-S. and J.A. Gardella, *X-ray Photoelectron Spectroscopy Studies on the Surface Segregation in Poly(dimethylsiloxane) Containing Block Copolymers.* 2005. **45**(1): p. 1 - 18.
90. Briggs, D. and J.T. Grant, *Surface analysis by Auger and x-ray photoelectron spectroscopy*. 2003, Chichester, West Sussex, U.K.: IM Publications. xi, 899 p.
91. Long, J., et al., *Thermodynamic modeling of contact angles on rough, heterogeneous surfaces.* Advances in Colloid and Interface Science, 2005. **118**(1-3): p. 173-190.
92. Kusnezow, W. and J.D. Hoheisel, *Solid supports for microarray immunoassays.* Journal of Molecular Recognition, 2003. **16**(4): p. 165-176.
93. Lee, C.-S. and B.-G. Kim, *Improvement of protein stability in protein microarrays.* Biotechnology Letters, 2002. **24**(10): p. 839-844.
94. Guilleaume, B., et al., *Systematic comparison of surface coatings for protein microarrays.* Proteomics, 2005. **5**(18): p. 4705-4712.
95. Liddell, E., *Antibodies*, in *The Immunoassay handbook*, D. Wild, Editor. 2001, Nature Pub. Group: London.
96. Vaughan, T.J., et al., *Human Antibodies with Sub-nanomolar Affinities Isolated from a Large Non-immunized Phage Display Library.* Nat Biotech, 1996. **14**(3): p. 309-314.
97. Ellington, A.D. and J.W. Szostak, *In vitro selection of RNA molecules that bind specific ligands.* Nature, 1990. **346**(6287): p. 818-822.
98. Tuerk, C. and L. Gold, *Systematic evolution of ligands by exponential enrichment: RNA ligands to bacteriophage T4 DNA polymerase.* Science, 1990. **249**(4968): p. 505-510.
99. Pan, W., et al., *Isolation of virus-neutralizing RNAs from a large pool of random sequences.* Proceedings of the National Academy of Sciences of the United States of America, 1995. **92**(25): p. 11509-11513.
100. Morris, K.N., et al., *High affinity ligands from in vitro selection: Complex targets.* Proceedings of the National Academy of Sciences of the United States of America, 1998. **95**(6): p. 2902-2907.
101. Proske, D., et al., *Aptamers—basic research, drug development, and clinical applications.* Applied Microbiology and Biotechnology, 2005. **69**(4): p. 367-374.
102. Nimjee, S.M., C.P. Rusconi, and B.A. Sullenger, *Aptamers: An Emerging Class of Therapeutics.* Annual Review of Medicine, 2005. **56**(1): p. 555-583.
103. Kim, S.D., et al., *Construction of C-reactive protein-binding aptamer as a module of the DNA computing system for diagnosing cardiovascular diseases.* Proceedings of the 10th International Meeting on DNA Based Computers, 2004: p. 334–343.
104. Bini, A., et al., *Development of an optical RNA-based aptasensor for C-reactive protein.* Analytical and Bioanalytical Chemistry, 2008. **390**(4): p. 1077-1086.

105. Huang, C.-J., et al., *Integrated microfluidic system for rapid screening of CRP aptamers utilizing systematic evolution of ligands by exponential enrichment (SELEX).* Biosensors and Bioelectronics, 2010. **25**(7): p. 1761-1766.
106. Zuo, P., et al., *Determination of [beta]-adrenergic agonists by hapten microarray.* Talanta, 2010. **82**(1): p. 61-66.
107. Roper, M.G., et al., *Extraction of C-reactive protein from serum on a microfluidic chip.* Analytica Chimica Acta, 2006. **569**(1-2): p. 195-202.
108. Ladner, R.C. and A.C. Ley, *Novel frameworks as a source of high-affinity ligands.* Current Opinion in Biotechnology, 2001. **12**(4): p. 406.
109. Taussig, M.J. and U. Landegren, *Progress in antibody arrays.* TARGETS, 2003. **2**(4): p. 169.
110. Renberg, B., et al., *Affibody protein capture microarrays: Synthesis and evaluation of random and directed immobilization of affibody molecules.* Analytical Biochemistry, 2005. **341**(2): p. 334.
111. Schlehuber, S., G. Beste, and A. Skerra, *A novel type of receptor protein, based on the lipocalin scaffold, with specificity for digoxigenin.* Journal of Molecular Biology, 2000. **297**(5): p. 1105.
112. Ray, S., G. Mehta, and S. Srivastava, *Label-free detection techniques for protein microarrays: Prospects, merits and challenges.* Proteomics, 2010. **10**(4): p. 731-748.
113. Mauriz, E., et al., *Determination of carbaryl in natural water samples by a surface plasmon resonance flow-through immunosensor.* Biosensors and Bioelectronics, 2006. **21**(11): p. 2129-2136.
114. Li, Y., et al., *Flow sandwich immunoassay for specific anti-OVA IgG antibody by use of surface plasmon resonance sensor.* Talanta, 2008. **77**(2): p. 473-478.
115. Möhrle, B., et al., *Label-free characterization of cell adhesion using reflectometric interference spectroscopy (RIfS).* Analytical and Bioanalytical Chemistry, 2006. **384**(2): p. 407-413.
116. Heyries, K.A., et al., *Microfluidic biochip for chemiluminescent detection of allergen-specific antibodies.* Biosensors and Bioelectronics, 2008. **23**(12): p. 1812-1818.
117. Lebrun, S.J., et al., *Development of a sensitive, colorometric microarray assay for allergen-responsive human IgE.* Journal of Immunological Methods, 2005. **300**(1-2): p. 24-31.
118. Liang, R.-Q., C.-Y. Tan, and K.-C. Ruan, *Colorimetric detection of protein microarrays based on nanogold probe coupled with silver enhancement.* Journal of Immunological Methods, 2004. **285**(2): p. 157-163.
119. Wang, J.-h., et al., *Fluorescent microarray analyzer*. 2005: United States.
120. Bohmer, M., et al., *Time-resolved confocal scanning device for ultrasensitive fluorescence detection.* Review of Scientific Instruments, 2001. **72**(11): p. 4145-4152.
121. Taitt, C.R., G.P. Anderson, and F.S. Ligler, *Evanescent wave fluorescence biosensors.* Biosensors and Bioelectronics, 2005. **20**(12): p. 2470-2487.
122. Bessueille, F., et al., *Assessment of porous silicon substrate for well-characterised sensitive DNA chip implement.* Biosensors and Bioelectronics, 2005. **21**(6): p. 908-916.
123. Morozov, V.N., et al., *Three Minutes-Long Electrophoretically Assisted Zeptomolar Microfluidic Immunoassay with Magnetic-Beads Detection.* Journal of the American Chemical Society, 2007. **129**(42): p. 12628-12629.
124. Mora, J.R., et al., *Protein detection enhanced by 3DNA dendrimer signal amplification.* Biotechniques, 2008. **44**(6): p. 815-818.

125. Järås, K., et al., *ENSAM: Europium Nanoparticles for Signal Enhancement of Antibody Microarrays on Nanoporous Silicon.* Journal of Proteome Research, 2008. **7**(3): p. 1308-1314.
126. Vashist, S.K., et al. (2006) *Review of Quantum Dot Technologies for Cancer Detection and Treatment*. AZojono **2**, DOI: 10.2240/azojono0113.
127. Chan, W.C., et al., *Quantum Dot Bioconjugates for Ultrasensitive Nonisotopic Detection.* Science, 1998. **281**(5385): p. 2016-2018.
128. Bobrow, M.N., et al., *The use of catalyzed reporter deposition as a means of signal amplification in a variety of formats.* Journal of Immunological Methods, 1992. **150**(1-2): p. 145-149.
129. Schweitzer, B., et al., *Immunoassays with rolling circle DNA amplification: A versatile platform for ultrasensitive antigen detection.* Proceedings of the National Academy of Sciences of the United States of America, 2000. **97**(18): p. 10113-10119.
130. Schuller, J.A., et al., *Plasmonics for extreme light concentration and manipulation.* Nat Mater, 2010. **9**(3): p. 193-204.
131. Lakowicz, J.R., et al., *Plasmon-controlled fluorescence: a new paradigm in fluorescence spectroscopy.* Analyst, 2008. **133**(10): p. 1308-1346.
132. Aslan, K., et al., *Metal-enhanced fluorescence: an emerging tool in biotechnology.* Current Opinion in Biotechnology, 2005. **16**(1): p. 55-62.
133. Sepúlveda, B., et al., *LSPR-based nanobiosensors.* Nano Today, 2009. **4**(3): p. 244-251.
134. Drexhage, K.H., *IV Interaction of Light with Monomolecular Dye Layers*, in *Progress in Optics*, E. Wolf, Editor. 1974, Elsevier. p. 163-192, 192a, 193-232.
135. Volle, J.N., et al., *Enhanced sensitivity detection of protein immobilization by fluorescent interference on oxidized silicon.* Biosensors and Bioelectronics, 2003. **19**(5): p. 457-464.
136. Cretich, M., et al., *High Sensitivity Protein Assays on Microarray Silicon Slides.* Analytical Chemistry, 2009. **81**(13): p. 5197-5203.

CHAPTER 1

Protein microarray for the analysis of human melanoma biomarkers

Sensors and Actuators B: Chemical 139(1): 2-8

Patrick Domnanich, Ursula Sauer, Johanna Pultar and Claudia Preininger

"Protein microarray for the analysis of human melanoma biomarkers"

CHAPTER 2

Aptamer-antibody on-chip sandwich immunoassay for detection of CRP in spiked serum

Biosensors and Bioelectronics 24(5): 1456-1461

Johanna Pultar, Ursula Sauer, Patrick Domnanich and Claudia Preininger

"Aptamer-antibody on-chip sandwich immunoassay for detection of CRP in spiked serum"

CHAPTER 3

Xanthan/chitosan gold chip for metal enhanced protein biomarker detection

submitted to

Biosensors and Bioelectronics

Patrick Domnanich, Dacimoneida Brito Peña, Claudia Preininger

"Xanthan/chitosan gold chip for metal enhanced protein biomarker detection"

Xanthan/chitosan gold chip for metal enhanced protein biomarker detection

Patrick Domnanich, Dacimoneida Brito Peña, Claudia Preininger*

AIT Austrian Institute of Technology GmbH, Health & Environment / Bioresources, 2444 Seibersdorf, Austria

*corresponding author: Claudia.Preininger@ait.ac.at, fax: +43 (0) 50 550-3666

Abstract

Protein microarrays for disease diagnostics are required to accurately quantify analytes in the low pg/mL range. This task is hampered by weak signal strengths and too low detector sensitivity. Herein we present reflective gold chips coated with polyelectrolyte multilayers (PEMs) for signal enhancement in immunoassays for melanoma-relevant biomarkers. Among tested (semi)natural polysaccharides (xanthan, chitosan, carboxymethylcellulose, hyaluronic acid) PEMs composed of xanthan and chitosan performed best in terms of assay sensitivity, spot morphology, fluorescence background and variability (< 10%). Fluorescence signals on gold slides with a 75 nm coating of seven crosslinked polyelectrolyte double layers were up to 50 times higher than on bare glass slides. In comparison to commercial substrates the signal to noise ratio is enhanced by up to factor 11. Furthermore sandwich assays for interleukins 6, 8, 10, tumour necrosis factor alpha (TNFα), vascular endothelial growth factor A (VEGF-A) and S100B show working ranges which cover significantly lower concentrations (up to 38 fold).

Not limited to above assays the presented substrates, which combine a biocompatible interface with metal-based signal amplification, are a valuable tool in a variety of biosensor applications.

Keywords: metal enhanced protein chip, melanoma biomarkers, polyelectrolyte multilayers, xanthan, chitosan

1 Introduction

Protein microarrays are an emerging technology in clinical applications with diagnostic potential in many diseases such as melanoma (Domnanich et al. 2009). Though extremely promising accurate quantification of low abundance proteins in highly complex biological fluids like serum and plasma is still a major challenge in assay development. For instance cytokines, like interleukins 6, 8, 10 and TNFα, which are involved in many immunomodulatory processes and play a significant role in the development of melanoma, already act in pg/mL concentrations. These low analyte levels translate into small concentrations of labelled molecules and thus weak signals. If the collected signal intensity is comparable with the background intensity and the detector noise, it is difficult to extract reproducible information from the array.

This issue becomes even more acute if the assay is to be integrated into a portable diagnostic device. There high sensitive laser scanners with tuneable photomultiplier tube (PMT) cannot be used due to high costs, low scanning speeds and weight. Charge-coupled device (CCD) cameras offer a robust alternative for signal detection, yet in practical terms, their limit of detection is significantly higher than in PMT based scanners.

Low physical signal levels and poor detector sensitivity both hamper accurate quantification. Thus normal and moderately elevated levels of the biomarkers cannot be differentiated. To overcome this problem, samples may be preconcentrated and the incubation time may be prolonged. Unfortunately both strategies can also increase background fluorescence (Rifai et al. 2006). Moreover the available sample volume is often limited, and tedious, time-consuming tests have a low chance to find their way into clinical practice.

Alternatively signal amplification strategies and the use of surface enhancing matrices, that increase biomolecule immobilization capacity and promote protein stability, can help to attain the required assay sensitivities.

Amplification of the optical signal has been achieved with advanced labels including quantum dots, fluorescent nanoparticles and fluorescent proteins or by applying enzymatic and chemical reactions. Furthermore, metallic surfaces and nanometallic objects such as noble metal nanoparticles and colloids, silver nanostructures and metal island films were exploited for signal enhancement. These techniques are based on a concept termed metal-enhanced

fluorescence and make use of reflective and surface plasmonic effects thereby changing the light emission properties of the nearby fluorophores (Ray et al. 2010; Schuller et al. 2010).

By contrast, improved assay performance as a result of superior surface materials used for protein immobilization was obtained by applying porous supports and surface enlarging nanostructures, dendrimers, hydrogels and polyelectrolyte multilayers (PEMs) (Lee et al. 2007). PEMs are thin films constructed by alternate adsorption of oppositely charged polyelectrolytes from their aqueous solutions using a layer-by-layer (LbL) technique. Due to multiple charge neutralisation interactions, PEMs are highly stable. Moreover the method is capable of varying film composition and provides enormous design flexibility. Thus it is not surprising that PEMs receive increasing attention in medical as well as in biotechnological applications.

In this study, we combine both physical signal amplification and a biocompatible PEM hydrogel for protein immobilisation. We build up an assembly of PEMs on gold substrates and optimize conditions for metal enhanced fluorescence. Slides are printed with arrays of antibodies against several cytokines and melanoma biomarkers: IL6, IL8, IL10, TNFα, S100B and VEGF. We evaluate the respective assays in 10% human serum and demonstrate the superior performance of the gold PEM substrates in comparison to commercial slides.

2 Materials and Methods

2.1 Materials and reagents

ARChips Epoxy are proprietary slides developed at AIT. BioGold coated substrates and Poly-L-Lysine slides were from Erie Scientific Company. Histobond Slides, positively charged glass slides, were from Marienfeld. Nexterion HiSens Slides E (reflective slides) for high-sensitive detection are from Schott. Phosphate buffered saline (PBS) was purchased from Gibco. Polyoxyethylene-sorbitan monolaurate (Tween-20), bovine serum albumin (BSA), sodium chloride, sodium deoxycholate, N-(3-Dimethylaminopropyl)-N′-ethylcarbodiimide (EDC), N-Hydroxysuccinimide (NHS), medium molecular weight chitosan (> 75% deacetylation, viscosity 200 - 800 cps at 1%), xanthan gum from Xanthomonas capestris (Brookfield Viscosity 800 - 1200 cps at 1%) and sodium carboxymethyl cellulose (average Mw ~250,000) were purchased from Sigma. Sodium hyaluronate from Streptococcus pyrogenes (MW $5.0*10^5$-$1.2*10^6$) was from Merck.

Anti-S100 protein (MAb 8B10), biotinylated anti-S100 protein (MAb 6G1), human S100 protein, biotinylated anti-human TNFα (F6C5) and CRP-free serum were purchased from HyTest (Finland). Monoclonal anti-VEGF (Clone 26503) and biotinylated anti-VEGF antibody (BAF293) were from R&D Systems. Anti-procalcitonine antibody was kindly provided by Dr. Petra M. Krämer (Helmholtz Center Munich) and conjugated with Dy547 by Exbio Praha. Anti-human TNFα (B-F7) and recombinant human TNFα were from Exbio Praha. Anti-IL8 antibody (H8A5), recombinant human IL8 and biotinylated anti-IL8 antibody (E8N1) were from Biolegend.

Recombinant human VEGF-A was from Invitrogen Corporation. Recombinant human IL6, IL10, biotin-conjugated anti-human IL6 (MQ2-39C3) and anti-IL10 (JES3-12G8) proteins as well as anti-human IL6 (MQ2-13A5) and anti-human IL10 (JES3-9D7) antibodies were from Bioscience. Fluorolink Cy5 labelled streptavidin was from Amersham Biosciences UK Limited.

2.2 Substrate Preparation

Substrates for PEM microarray fabrication were positively charged glass slides and gold slides. PEMs were deposited using a KSV dip coater model D: First slides were incubated in 1 mg/mL negatively charged polyelectrolyte in 150 mM NaCl (adjusted to pH 5 with acetic acid) for 900 s. The negatively charged polyelectrolyte was xanthan, carboxymethylcellulose or hyaluronic acid. Afterwards substrates were washed three times in 150 mM NaCl for 360 s. Next, slides were incubated alternating in 1 mg/mL chitosan, 150 mM NaCl (pH 5) and 1 mg/mL of the negatively charged polyelectrolyte, 150 mM NaCl (pH 5) for 360s each. Each polyelectrolyte incubation step was followed by three washing steps in 150 mM NaCl for 360 s. The process was repeated until the desired number of polyelectrolyte bilayers was deposited (Fig. 1a). For crosslinking slides were treated in NHS (20 mM) / EDC (10 mM) for 2 h and subsequently washed in water.

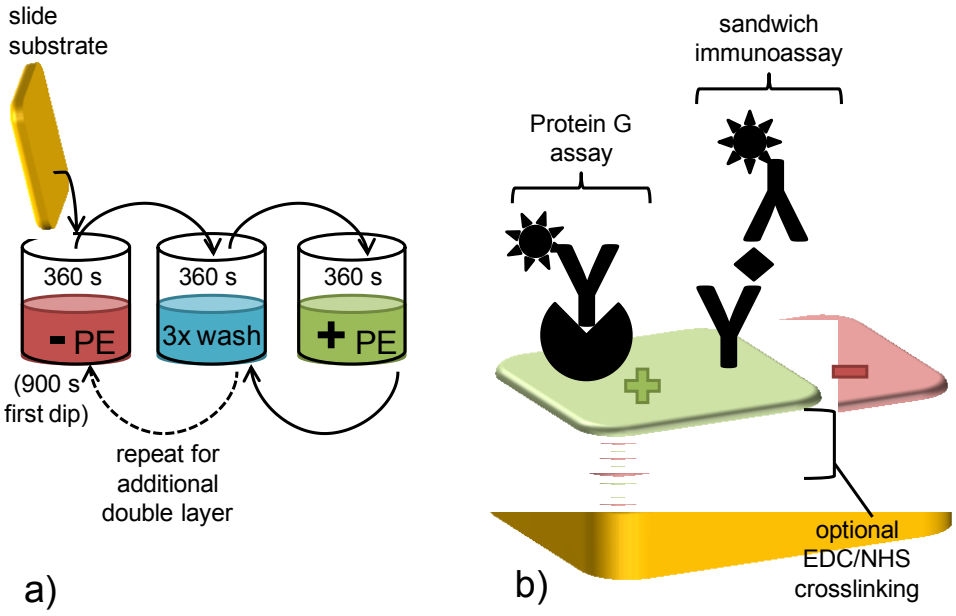

Fig. 1 Fabrication and use of polyelectrolyte multilayer slides. a) PEM are assembled on substrates by sequential incubations in negatively (- PE) and positively charged polyelectrolytes (+ PE). b) PEM substrates can be crosslinked and serve as platforms for electrostatic protein immobilization.

2.3 Probe arraying and blocking

0.4 mg/mL anti-IL6, 0.4 mg/mL anti-IL10, 0.4 mg/mL anti-IL8, 1 mg/mL anti-TNFα, 0.5 mg/mL anti-VEGF-A, 1 mg/mL anti-S100B and 1 mg/mL Protein G in print buffer (1x PBS, pH 7.2, 0.01% sodium deoxycholate) were arrayed on PEM modified substrates (Fig. 1b), Epoxy slides, poly-L-lysine slides and reflective slides at 70% relative humidity using the contact spotter OmniGrid from GeneMachines (2 pins SMP3). Spot-to-spot distance was 400 µm and array-to-array distance was 8950 µm. All probes were immobilized in triplicate and 10 identical arrays were spotted per slide.

After spotting slides were kept in a humid chamber at 4°C for a minimum of three days to ensure complete probe immobilization.

Before the experiment EDC/NHS activated substrates were treated in 1 M ethanolamine (pH 9) for 10 min to inactivate residual NHS esters. Epoxy slides were blocked for 30 minutes in 1x PBS (pH 7.2)/ 0.1% Tween to remove any unbound receptors. Blocking of the other substrates was performed in 1x PBS (pH 7.2)/1% BSA /0.1% Tween-20 for 30 minutes at room temperature (RT). Afterwards slides were washed twice in 1x PBS (pH 7.2) and dry-centrifuged for 4 minutes (900 rpm).

2.4 Chip processing

All incubation steps were done at RT on The Belly Dancer (Stovall, Greensboro, NC, USA). Slides were processed applying the Fast Frame system (Whatman) with 16 well incubation chambers.

For the Protein G assay substrates were incubated in 1 µg/mL Dy647-conjugated anti-procalcitonine antibody in assay buffer (0.1 M Tris, pH 7.4, 10 mM $CaCl_2$, 100 mM NaCl) for 45 min. Slides were washed 2 times in 1x PBS (pH 7.2)/0.1% Tween 20, 2 times in 1xPBS (pH 7.2) and dry-centrifuged for 4 minutes (900 rpm).

For the sandwich immunoassays antigen standards were prepared by serial dilution of an antigen mix (IL6, IL8, IL10, VEGF-A, S100B, TNFα) in a matrix of CRP-free HyTest serum diluted 1:10 with assay buffer.

Bound monoclonal capture antibodies were incubated with antigen standards for 120 min. Next, wells were washed three times with 1x PBS (pH 7.2)/0.1% Tween 20 and incubated with 1 µg/mL of each of the biotin-labelled antibodies anti-IL6, anti-IL10, anti-IL8, anti-TNFα, anti-VEGF-A and anti-S100B in assay buffer for 45 min.

After washing 3 times with PBS (pH 7.2)/0.1% Tween 20 wells were treated with 2 µg/mL Cy5 labelled streptavidin in assay buffer for 45 min. Finally slides were washed 2 times in 1x PBS (pH 7.2)/0.1% Tween 20, 2 times in 1xPBS (pH 7.2) and dry-centrifuged for 4 minutes (900 rpm).

2.5 Fluorescence detection and data analysis

Slides were stored in the dark till scanning. Fluorescence measurements (λ_{ex}=635nm, λ_{em}=670nm) were taken using a Genepix 4000B non-confocal scanner (Axon Instruments). For data comparison, the scanner photomultiplier tube gain was kept constant throughout scans. Reported fluorescence signals are background corrected and calculated as mean values from at least 6 replicate spots. Calibration curves were set up using the five parameter logistic model (stats package of the statistic program R). EDx value is the estimated effective analyte concentration for the signal response level of x%. Moreover the slope k at the ED50 was calculated. The coefficient of variation (CV% = SD / mean * 100%) was a measure for data reproducibility. Signal-to-noise ratios were computed for each data point by dividing the mean fluorescence intensity of the spot after background subtraction with the mean fluorescence intensity of the same spots in assays without added analyte.

2.6 Contact angle measurements

Contact angle measurements were performed with a CAM101 (KSV Instruments). Reported values were calculated from at least 6 replicate measurements.

2.7 Measurement of polyelectrolyte coating thickness

PEM thickness measurements were carried out at scratches with a Nanowizard II (JPK Instruments) atomic force microscope (AFM) with cantilever CSC38/AIBS (MikroMasch) in contact mode. Reported values were calculated from at least five measurements taken at different positions.

3 Results and Discussion

3.1 Evaluation of polysaccharide PEM systems for protein immobilisation

PEMs have proven to be favourable matrices in protein and enzyme technology as many immobilized proteins were reported to retain their activity for prolonged times. This effect was frequently attributed to the gel-like environment which keeps proteins hydrated and in a native conformation.

Typical polyelectrolytes reported for protein microarray fabrication are poly(vinylsulfonate), poly(styrenesulfonate) (PSS), poly(acrylate), poly(allylamine) and poly(ethyleneimine) (Dai et al. 2005; Shim et al. 2007; Spillman et al. 2008; Sung et al. 2009; Zhou and Zhou 2006). Unlike those macromolecules we employ (semi)natural polysaccharides for on-chip multilayer assembly: chitosan (CS) as positively charged building block, and either hyaluronic acid (HA), carboxymethylcellulose (CMC) or xanthan (XA) as anionic PEM component.

A PEM architecture of five double layers was built up on positively charged glass substrates and evaluated as platform for protein arrays (Fig. 1b). Criteria were low autofluorescence at the excitation wavelength (λ_{ex}=635 nm), high assay sensitivity for protein G in a direct fluorescence assay, uniform spot morphology, low fluorescence background and good reproducibility.

The autofluorescence of HA/CS, CMC/CS and XA/CS assemblies was comparable and similar to that of a bare glass slide. Thus the PE layers do not significantly contribute to the

chip's autofluorescence. In order to evaluate assay performance we spotted protein G and incubated with fluorescently labelled antibody (Table 1). While signals were similar for both $[HA/CS]_5$ and $[XA/CS]_5$, signals obtained on the $[CMC/CS]_5$ assembly were dramatically reduced (by about 85%). In contrast to spots on $[CMC/CS]_5$ which feature a doughnut morphology, spots on both $[HA/CS]_5$ and $[XA/CS]_5$ are homogeneous and regular without comet effects. Yet the interspot-variability on $[XA/CS]_5$ only amounts to 4% in comparison to 13% on $[HA/CS]_5$ (Table 1). The highest variability is found for $[CMC/CS]_5$.

Termination of the assemblies by a layer of chitosan, instead of the anionic polysaccharide, contributes to a lower unspecific background as can be seen clearly from the comparison between the chitosan and the hyaluronic acid terminated systems $[HA/CS]_5$ and $[HA/CS]_4HA$ (Table 1). This phenomenon may be explained by a more efficient blocking step on the chitosan surface. At physiological pH, the negatively charged blocking agent BSA (pI≈5.5) (Chang et al. 2005) will adsorb on polycationic chitosan, whereas adsorption on the polyanion is impeded by electrostatic repulsion.

Changes in the background level also occur among chitosan terminated PEMs (Table 1). The lowest background is found for $[CMC/CS]_5$, whereas background fluorescence of $[XA/CS]_5$ is slightly decreased in comparison to $[HA/CS]_5$.

Thus owing to the low background, excellent spot morphology and reproducibility, as well as the high signal strengths, the $[XA/CS]_5$ system was chosen as PEM support.

Table 1 Performance characteristics of different PEMs on glass slides. CV calculated from 30 replicate spots.

Coating	signal [a.u.]	CV [%]	background [a.u.]	spot morphology
$[CMC/CS]_5$	5489	23	68	
$[XA/CS]_5$	35251	4	82	
$[HA/CS]_5$	35628	13	97	
$[HA/CS]_4HA$	29784	18	129	

3.2 The xanthan/chitosan system

To create stable PEMs we investigated the effect of matrix crosslinking and studied the assembly of the system on gold substrates as characterized by contact angle and layer thickness.

3.2.1 Crosslinking

In this study the PEM film serves as a spacer between the gold surface and the fluorophores. Controlled PEM thickness and uniformity are important as signal amplification strongly depends on the distance between the labelled antibodies and the gold layer. However the assay procedure, which involves both incubation steps at different ionic strength and mechanical strains, stresses the PEM.

Unlike other polyelectrolyte systems XA/CS multilayers are insensitive to changes in ionic strength and do not swell due to the high chain stiffness of xanthan (Maurstad et al. 2005). In order to further strengthen the film the layer was stabilized by EDC/NHS crosslinking which couples the activated carboxylate groups of xanthan to the amino groups of chitosan. We found that the crosslinked XA/CS PEM exhibits a dramatically smoother and more homogeneous surface than the native one: AFM thickness measurements for crosslinked films did not vary by more than 20%. In contrast, thickness measurements for native XA/CS PEMs varied by about 700%, reflecting a very rugged surface. In fact this correlates well with the finding that on-chip immunoassays for IL10 in 10% human serum exhibit a 30% higher reproducibility on crosslinked than on native XA/CS slides.

3.2.2 PEM assembly on gold chips

To achieve signal amplification in an assay set-up, the XA/CS PEM was assembled on a reflective metal substrate. Gold substrates were chosen, as gold is both stable at physiological conditions and insensitive to humidity and prolonged storage.

PEMs can be either deposited directly onto gold substrates (Spillman et al. 2008) or onto a priming monolayer of self-assembled carboxythiol (Caruso et al. 1997). The first scenario is very attractive as the gold surface can be used without any special pre-treatment. However to ensure stable initiation of multilayer growth, this approach demands good adherence of the PEM components to the uncharged bare gold substrates. To test for adsorption of XA and CS to gold, substrates were immersed in either solution of the polyelectrolyte and rinsed in wash solution. The water contact angle, a very sensitive indicator for surface modifications, was recorded. Clearly, both hydrophilic polymers CS and XA adsorb to the gold surface. This is

reflected by a significant decrease in the contact angle of CS on gold (51.8±4.6°) and XA on gold (74.8±2.1°) as compared to bare gold slides (83.3±1.9°). Therefore both polyelectrolytes can contribute to tether the PEM assembly to the gold surface and no mediating layer is needed for adhesion.

3.2.3 Thickness of the PEM assembly

Thickness of the XA/CS system increases strongly with the number of deposited bilayers (Table 2). After a short lag-phase of about 3 polyelectrolyte bilayers, a stable growth regimen dominated by the multilayer charge density is reached. These growth characteristics apply to both PEM assemblies on Au and glass slides.

While 3 bilayers build up to an about 5 nm thick hydrogel layer, 12 bilayers amount to a 250 nm thick assembly. Such a growth regimen is typical for so-called exponentially growing PEMs. In contrast to linearly growing films, which feature heights between 50 and 100 nm after the deposition of 20 bilayers, exponentially growing films show thicknesses between 0.1 and 10µm. This behaviour facilitates the built-up of films of substantial thickness after only several polyelectrolyte deposition cycles.

Table 2 PEM thickness and figures of merit of IL10 assay standard curves on gold slides with 1, 3, 5, 7, 9 and 12 [XA/CS] double layers.

PEM	thickness [nm]	ED10 [pg/mL]	ED90 [pg/mL]	ED50 [pg/mL]	Slope	mean CV [%]
$[XA/CS]_1$	< 2	167	46718	2790	0.40	9
$[XA/CS]_3$	2 ± 2	251	120342	5491	0.70	9
$[XA/CS]_5$	31 ± 1	18	29002	726	0.64	28
$[XA/CS]_7$	74 ± 3	5	1201	166	0.83	5
$[XA/CS]_9$	141 ± 11	100	30600	1746	0.83	12
$[XA/CS]_{12}$	247 ± 21	24	7588	431	0.73	11

3.3 Effect of metal enhanced fluorescence

AFM thickness measurements reveal spacer layers on gold slides ranging from several nm (1 bilayer of [XA/CS]) up to 250 nm (12 bilayers). Using these slides signal amplification was studied in a sandwich immunoassay for IL10 at an antigen concentration of 780 pg/mL, which is within the linear assay range. Control experiments with the same polyelectrolyte assemblies on glass slides were carried out (Fig. 2). While the control experiments showed a very weak dependence of signal strengths on PEM thickness (number of deposited bilayers), a significant difference is seen for gold carrier substrates: Signal on gold substrates is

significantly smaller than on glass supports for 1 and 3 polyelectrolyte bilayers. This phenomenon can be explained by quenching of the dye molecules in the vicinity of the gold surface, as the distance amounts only to several nm. However the situation changes dramatically as the PEM assembly continues to grow. At 5 double layers (31 nm thickness) signal intensity on gold is about 6 times higher than on the glass control. On a 7 double layer PEM (74 nm) the amplification factor raises to 13. Then, at 9 double layers (141 nm), amplification dramatically breaks down and increases again at 12 bilayers. Thus a fluorescence signal maximum is found at 7 XA/CS bilayers. The amplification factor amounts to about 50 and 13, as compared to the untreated glass slide and glass slides coated with 7 bilayers of XA/CS respectively. This illustrates that both the protein-friendly gel environment of the polyelectrolyte as well as the gold substrate contribute to fluorescence enhancement.

The metal substrate associated amplification phenomenon can grossly be explained by the fact that emitted fluorescence light, which is normally scattered and lost through the glass substrate, is reflected back to the detector by the gold mirror. However, as can be seen from the data, the amplification factor is not constant but varies periodically with the thickness of the transparent layer between the fluorophore and the underlying reflecting surface. The observed oscillating trend was confirmed with different batches of polyelectrolyte slides which were spotted and processed on different days. Additionally the phenomenon was previously reported on reflective silicon wavers coated with SiO_2 layers of defined thickness (Cretich et al. 2009; Lambacher and Fromherz 1996; Moiseev et al. 2004). The oscillating signal amplification is thought to arise from interference phenomena: Both incident and emitted light independently interfere with their reflection from the mirror. Depending on the distance between dye and metal surface either constructive wave interference leads to amplification maxima or destructive interference results in attenuation of the signal. Thereby enhanced signal intensities are associated with shortened excitation lifetimes and increased quantum yields of the fluorophores (Ray et al. 2010).

Qualitatively the observed oscillating trend with strongest amplification at a coating thickness of about 75 nm perfectly corresponds to the theoretical calculations by Bras and co-workers (Bras et al. 2004). They investigate a dye layer on a Si/SiO_2 system and predict the first and strongest amplification maximum for Cy5 at a SiO_2 thickness of about 100 nm. A further maximum is at 320 nm, whereas attenuation is maximal at 0 and 210 nm. The quantitative divergence between the SiO_2 system and the polyelectrolyte system in this study has two reasons: Firstly, the distance between amplification maxima in the XA/CS system is smaller.

This is, because the phase-shift leading to interference is caused by the length of the optical light path through the transparent spacer layer. Therefore spacer layers with higher refractive index result in amplification patterns with apparent lower periodicity. This is reasonable, as many natural polysaccharide films have refractive indices higher than that of fused silica, SiO_2 (n=1,46 at 650nm (Malitson 1965)), e.g. chitosan (n=1.53 (Nosal et al. 2005)) . Secondly, in our approach, the dye molecule is not directly situated at the air-PEM interface but located on top of the IL10 immunosandwich. This results in an additional distance of several nm.

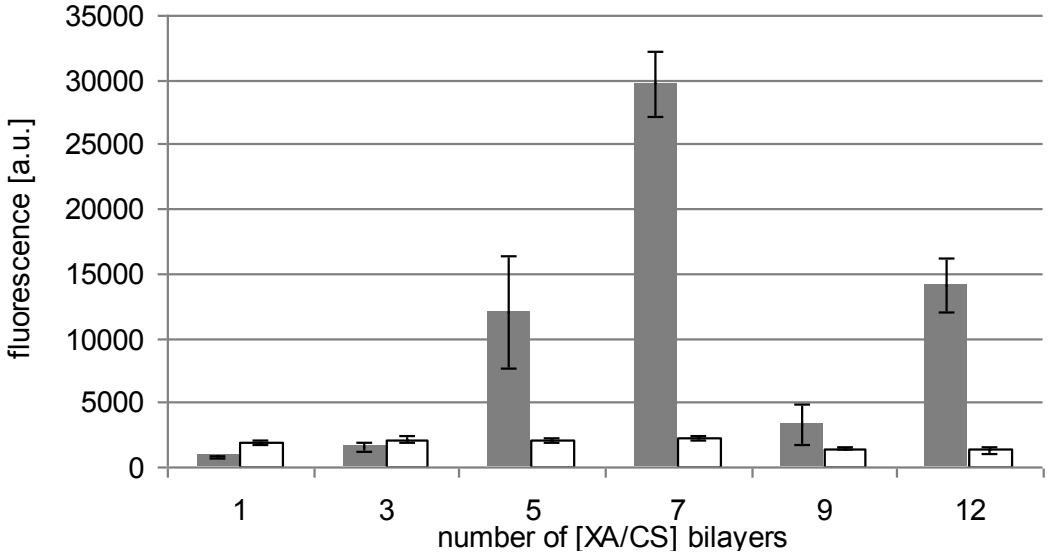

Fig. 2 The number of deposited [XA/CS] polyelectrolyte bilayers affects IL10 sandwich immunoassay signal strengths. PEM coated substrates were gold (grey) and glass (white).

3.4 Gold enhanced assays for melanoma-relevant protein biomarkers

Having observed increasing signal strengths on gold substrates with up to 7 double layers of XA/CS, we studied the amplification effect on whole calibration curves. Investigated parameters were the working range defined as 10–90% of the dynamic signal range (ED10 and ED90), ED50, the slope of the curves and the variability (mean CV). The effect of a growing number of XA/CS layers on IL10 calibration curves is shown in Fig. 3. Figures of merits are sampled in Table 2. When increasing the number of deposited PEM double layers from 1 to 3, the working range broadens significantly due to the strong rise of the upper limit of the dynamic range (ED90). When the number of double layers further grows to 5 and 7, the dynamic range successively downshifts to ranges at lower concentration. The downshift of the

ED50 from 5491 pg/mL for 3 double layers to 166 pg/mL for 7 double layers clearly illustrates that quantifications at lower concentrations become possible. Opposed to this trend, at 9 double layers the working range strongly shifts up to higher concentrations. Finally at 12 double layers the working range again covers an interval at lower concentrations. This oscillating behaviour is in complete agreement with the signal intensities obtained in section 3.3. In summary slides coated with 7 double layers of XA/CS show the strongest left shift. Similarly the standard curves' slope rises with increasing coating thickness and reaches a maximum at 7 and 9 double layers, which indicates best sensitivity. Reproducibility, expressed by a low mean CV, is optimal at 7 double layers. Owing to the excellent performance in all four investigated parameters gold slides coated with 7 double layers of XA/CS were used for further comparisons.

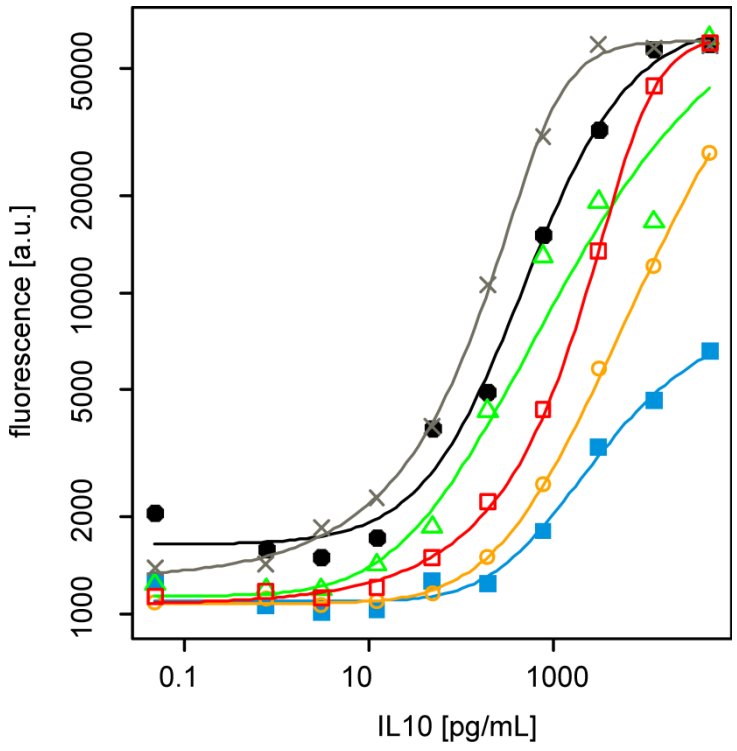

Fig. 3 Amplification affects working range of calibration curves. IL10 sandwich immunoassay was performed on gold slides coated with increasing number of [XA/CS] bilayers: 1 bilayer (■), 3 (○), 5 (△), 7 (×), 9 (□), and 12 (●) bilayers. Mean CVs are given in Table 2.

3.4.1 Commercial slides

Gold $[XA/CS]_7$ substrates were compared with commercial epoxy and poly-L-lysine slides as well as with commercial reflective slides. Fluorescence images shown in Fig. 4a illustrate that the substrates exhibit largely different signal strengths: For example at 195 pg/mL IL10 signals on the polyelectrolyte slides are about 6 times as high as on epoxy and poly-lysine surfaces and about twice the strength as on the reflective slides. Consequently signal saturation (white spots) occurs for gold $[XA/CS]_7$ already at 3125 pg/mL IL10, whereas reflective and poly-lysine slides are fully saturated at only 12500 pg/mL and 50000 pg/mL respectively. While commercial reflective slides exhibit excessive smearing at high analyte concentrations, polyelectrolyte surfaces produce homogenous, consistent spots throughout all tested concentrations. Also slides have very different sensitivities: the PEM slides are the only tested substrates that show significant spot intensities at 12 pg/mL IL10.

In order to compare the assay performance of these very different chip surfaces we calculated the signal-to-noise ratios (SNRs) for each spot and plotted SNR as a function of the analyte concentration. Calibration curves for the markers IL10, IL8, IL6, TNFα, S100B and VEGF-A (Fig. 4b) reveal that SNRs for gold $[XA/CS]_7$ are excellent even at extremely low analyte concentrations. In comparison to the other slides the increases in SNR amounts up to factor 11 (between PEM slides and epoxy for analyte TNFα). Stagnation of the SNRs at very high concentrations is due to saturation effects.

Our primary aim is to use chips to quantify proteins at very low concentrations. One prerequisite for accurate quantifications is high reproducibility. Surprisingly, reproducibility is remarkably similar for all slide types, ranging from a CV of 6±2% for the poly-lysine slides to 8±4% for the epoxy slides. Likewise the slopes of the curves on the different substrates are comparable for many of the analytes. Yet clear differences in the working range are discernible: Epoxy and poly-lysine surfaces feature rather similar standard curves (Fig. 4b) and working ranges (Table 3). In comparison to poly-lysine slides standard curves of XA/CS and reflective slides experience a left-shift to lower concentrations. For the XA/CS slides this shift clearly depends on the analyte and varies between factor 3 for VEGF-A (determined as the ratio between respective ED50 values) and factor 23 for IL10. The lower limit of the working range even decreases between factor 3 for S100 and factor 38 for IL10.

Apart from the S100 immunoassay, where gold $[XA/CS]_7$ and reflective slides produce similar curves, XA/CS slides cover working ranges at lower analyte concentrations than the reflective slides: Curves are left-shifted between factor 1.4 (IL6) and 3 (IL8).

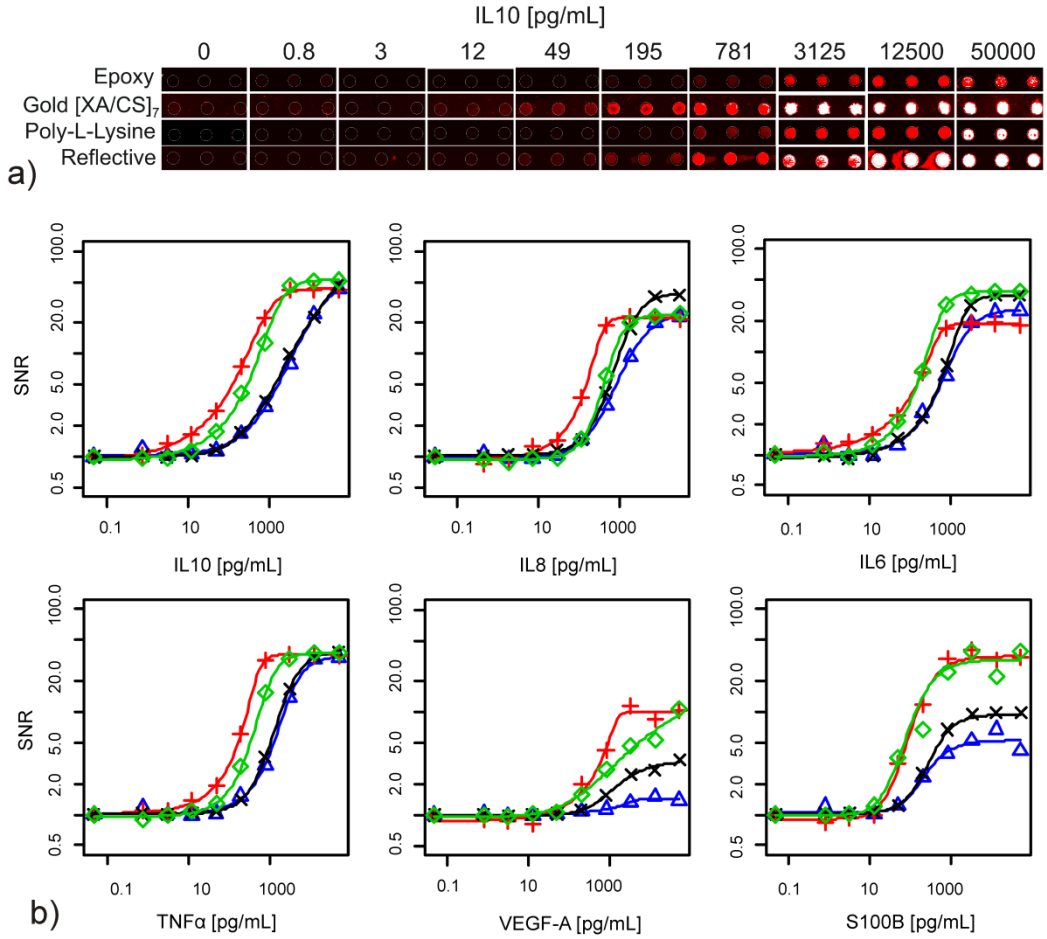

Fig. 4 Comparison of PEM substrates to commercial slides. a) Spots of IL10 sandwich immunoassay on different substrates. b) Standard curves for melanoma-relevant immunoassays expressed as SNR on gold [XA/CS]7 (+), commercial reflective high sensitivity (◊), epoxy (Δ) and poly-L-lysine slides (×).

Table 3 Working range and midpoint of the working range for melanoma-relevant immunoassays on gold [XA/CS]7 slides and commercial reflective slides, epoxy and poly-L-lysine slides scanned with the same settings.

Analyte	Slide	ED10 [pg/mL]	ED90 [pg/mL]	ED50 [pg/mL]
IL6	Gold $[XA/CS]_7$	6	507	129
	Reflective	20	691	180
	Poly-L-Lysine	50	2435	616
	Epoxy	63	3681	605
IL8	Gold $[XA/CS]_7$	17	381	141
	Reflective	94	1431	393
	Poly-L-Lysine	111	3478	686
	Epoxy	110	7777	845
IL10	Gold $[XA/CS]_7$	5	1201	166
	Reflective	19	2182	398
	Poly-L-Lysine	181	232342	3885
	Epoxy	186	55817	3105
TNFα	Gold $[XA/CS]_7$	22	544	196
	Reflective	59	1497	387
	Poly-L-Lysine	217	6481	1261
	Epoxy	203	6617	1481
VEGF-A	Gold $[XA/CS]_7$	44	1319	510
	Reflective	77	362584	2590
	Poly-L-Lysine	211	13435	1309
	Epoxy	76	4146	1353
S100B	Gold $[XA/CS]_7$	19	490	85
	Reflective	16	471	75
	Poly-L-Lysine	52	1229	262
	Epoxy	52	1206	211

4 Conclusion

Among three tested (semi)natural polysaccharide PEMs we chose the xanthan/chitosan system for the assembly of coatings on gold substrates. Thorough optimization of the layer thickness and homogeneity led to significant fluorescence signal enhancements over PEM coated glass substrates and to even larger gains, up to factor 50, in respect to bare glass slides. This finding illustrates that both the protein-friendly gel environment of the polyelectrolyte assembly as well as the metal enhancement of fluorescence via the gold substrates contribute to the amplification process.

Comparing the performance of melanoma-relevant sandwich immunoassays on gold PEM slides to commercial substrates in a matrix of 10% human serum we found

- up to 6 fold increased signal strengths
- superior signal to noise ratios (up to 11 fold)
- a left-shift of the working range enabling quantifications at significantly lower concentrations

Furthermore the PEM layer, which is deposited by a simple aqueous LbL dipping technique, has the potential to be applied to gold – and (possibly) other reflective metal surfaces – of virtually any geometry. Involving biocompatible materials this amplification technique is envisioned to be a valuable tool in a variety of biosensor applications.

5 Acknowledgements

The authors thank the Austrian Science Foundation FWF and the Spanish Ministry of Education for financial support through the Translational-Research (L415-N19) and the ARGO programme.

6 References

Bras, M., Dugas, V., Bessueille, F., Cloarec, J.P., Martin, J.R., Cabrera, M., Chauvet, J.P., Souteyrand, E., Garrigues, M., 2004. Optimisation of a silicon/silicon dioxide substrate for a fluorescence DNA microarray. Biosens Bioelectron 20(4), 797-806.

Caruso, F., Niikura, K., Furlong, D.N., Okahata, Y., 1997. 2. Assembly of Alternating Polyelectrolyte and Protein Multilayer Films for Immunosensing. Langmuir 13(13), 3427-3433.

Chang, W.W.P., Hobson, C., Bomberger, D.C., Schneider, L.V., 2005. Rapid separation of protein isoforms by capillary zone electrophoresis with new dynamic coatings. ELECTROPHORESIS 26(11), 2179-2186.

Cretich, M., di Carlo, G., Longhi, R., Gotti, C., Spinella, N., Coffa, S., Galati, C., Renna, L., Chiari, M., 2009. High Sensitivity Protein Assays on Microarray Silicon Slides. Analytical Chemistry 81(13), 5197-5203.

Dai, J., Baker, G.L., Bruening, M.L., 2005. Use of Porous Membranes Modified with Polyelectrolyte Multilayers as Substrates for Protein Arrays with Low Nonspecific Adsorption. Analytical Chemistry 78(1), 135-140.

Domnanich, P., Sauer, U., Pultar, J., Preininger, C., 2009. Protein microarray for the analysis of human melanoma biomarkers. Sensors and Actuators B: Chemical 139(1), 2-8.

Lambacher, A., Fromherz, P., 1996. Fluorescence interference-contrast microscopy on oxidized silicon using a monomolecular dye layer. Applied Physics A: Materials Science & Processing 63(3), 207-216.

Lee, J.-H., Shim, H.-W., Choi, H.-S., Son, Y.-A., Lee, C.-S., 2007. Protein patterning on self-assembled polyelectrolyte thin films. Journal of Physics and Chemistry of Solids 69(5-6), 1581-1584.

Malitson, I.H., 1965. Interspecimen Comparison of the Refractive Index of Fused Silica. J. Opt. Soc. Am. 55(10), 1205-1208.

Maurstad, G., Bausch, A.R., Sikorski, P., Stokke, B.T., 2005. Electrostatically Self-Assembled Multilayers of Chitosan and Xanthan Studied by Atomic Force Microscopy and Micro-Interferometry. Macromolecular Symposia 227(1), 161-172.

Moiseev, L., Cantor, C.R., Aksun, M.I., Dogan, M., Goldberg, B.B., Swan, A.K., Unlu, M.S., 2004. Spectral self-interference fluorescence microscopy. J Appl Phys 96(9), 5311-5315.

Nosal, W.H., Thompson, D.W., Yan, L., Sarkar, S., Subramanian, A., Woollam, J.A., 2005. UV-vis-infrared optical and AFM study of spin-cast chitosan films. Colloids and Surfaces B: Biointerfaces 43(3-4), 131-137.

Ray, K., Chowdhury, M., Zhang, J., Fu, Y., Szmacinski, H., Nowaczyk, K., Lakowicz, J., 2010. Plasmon-Controlled Fluorescence Towards High-Sensitivity Optical Sensing. In: Rao, G. (Ed.), Optical Sensor Systems in Biotechnology, pp. 29-72. Springer Berlin / Heidelberg.

Rifai, N., Gillette, M.A., Carr, S.A., 2006. Protein biomarker discovery and validation: the long and uncertain path to clinical utility. Nat Biotech 24(8), 971-983.

Schuller, J.A., Barnard, E.S., Cai, W., Jun, Y.C., White, J.S., Brongersma, M.L., 2010. Plasmonics for extreme light concentration and manipulation. Nat Mater 9(3), 193-204.

Shim, H.-W., Lee, J.-H., Hwang, T.-S., Rhee, Y.W., Bae, Y.M., Choi, J.S., Han, J., Lee, C.-S., 2007. Patterning of proteins and cells on functionalized surfaces prepared by polyelectrolyte multilayers and micromolding in capillaries. Biosensors and Bioelectronics 22(12), 3188-3195.

Spillman, S.D., McEvoy, H.M., MacCraith, B.D., 2008. Fabrication of Substrate-Independent Protein Microarrays Using Polyelectrolyte Scaffolding. Langmuir 25(3), 1403-1411.

Sung, W.-C., Chen, H.-H., Makamba, H., Chen, S.-H., 2009. Functionalized 3D-Hydrogel Plugs Covalently Patterned Inside Hydrophilic Poly(dimethylsiloxane) Microchannels for Flow-Through Immunoassays. Analytical Chemistry 81(19), 7967-7973.

Zhou, X., Zhou, J., 2006. Protein microarrays on hybrid polymeric thin films prepared by self-assembly of polyelectrolytes for multiple-protein immunoassays. PROTEOMICS 6(5), 1415-1426.

CHAPTER 4

Iminodiacetic acid and carboxymethyl amino acids as metal chelate affinity ligands in protein microarrays

to be submitted to

Anal. Biochem.

Patrick Domnanich, Robert Svagera, Maria F. Ebel, Claudia Preininger

"Iminodiacetic acid and carboxymethyl amino acids as metal chelate affinity ligands in protein microarrays"

Iminodiacetic acid and carboxymethyl amino acids as metal chelate affinity ligands in protein microarrays

Patrick Domnanich[1], Robert Svagera[2], Maria F. Ebel[2], Claudia Preininger[1*]

[1] AIT Austrian Institute of Technology GmbH, Health & Environment / Bioresources, 2444 Seibersdorf, Austria

[2] Institute of Solid State Physics, Vienna University of Technology, 1040 Vienna, Austria

[*]corresponding author: Claudia.Preininger@ait.ac.at, fax: +43 (0) 50 550-3666

Abstract

Emerging microarray applications require immobilisation of picogram amounts of protein per spot in a functionally and structurally intact form and possibly defined spatial orientation. We herein report on microarray metal affinity slides based on iminodiacetic acid (IDA) and carboxymethyl amino acid ligands that enable immobilisation of poly-histidine-tagged proteins via nickel-chelate complexes. Surfaces contain a protein-repellent inserted layer of hydroxyl groups and derivates of aminoacids like aspartate which are classified low-adsorbent. Substrates were analyzed via XPS and compared to commercial hydrogel and nitrilotriacetic acid (NTA) substrates. For surface characterisation a Protein G based fluorescence assay is performed under varying ionic strength (NaCl concentration 0.1-1.5M). Addition of glycerol to the print buffer leads to a significant decrease in non-specifically bound protein, high selectivities > 95% and signal strengths up to six times higher than on commercial products. Furthermore selectivities and signal strengths conferred by other metal ions like Cu(II), Zn(II), Fe(II) and Fe(III) are reported. The novel metal affinity ligand *N*-(carboxymethyl)methionine (CMM) is studied which shows signal strengths superior over IDA, *N*-(carboxymethyl)aspartate (CMA), hydrogel and NTA slides.

Keywords: his-tag mediated oriented immobilisation, metal affinity slides, nickel, protein microarray

1 Introduction

Solid-phase-based assays and protein microarrays are emerging techniques in functional proteomics, drug discovery and medical diagnostics. While combining reduced analysis time with low sample consumption those high throughput techniques allow for parallelization and assay miniaturization. However they require an immobilisation method that minimizes structural protein perturbation and maximizes activity. Moreover functional and structural studies often demand uniform orientation of immobilized proteins [1].

Metal ion affinity is commonly applied for separation and purification of proteins and has also proven useful in protein immobilisation [2]. This method uses the coordinative interaction between certain amino acids on the surface of proteins and metal ions that are immobilized on a solid support via chelating groups. The amino acid histidine plays the most prominent role in mediating the binding of proteins to transition metal ions such as Ni^{2+}. Therefore genetically engineered polyhistidine units which can be either inserted at the C or N-terminus of proteins have been applied as affinity tags (his-tag). Poly-his modifications usually do not compromise biological function [3] and allow for controlled and oriented protein immobilisation. Compared to other biospecific affinity techniques metal affinity features low cost and high stability of the chemical ligands. Formation of the histidine-Ni^{2+} complex is a fast process and results in high protein loading.

Conventional metal affinity chromatographic resins are largely based on silica supports and are prone to nonspecific and irreversible protein adsorption. For instance Ho and coworkers [4] who purified his-tagged proteins from bacterial cell lysates describe a Cu^{2+}-IDA silica resin that irreversibly binds more than 50% of adsorbed protein. This phenomenon neither impairs chromatographic yield nor separation performance as non-specifically bound protein only contains traces of his-tagged protein. However such properties are not acceptable in microarray applications which require highly defined and structurally homogeneous protein spots. Recently chelation-based immobilisation schemes were combined with high-density poly(ethylene glycol) surface layers [5, 6]. Obtained substrates exhibit decreased nonspecific protein adsorption while preserving the specific interaction with His-tagged proteins.

Most metal affinity immobilisation studies on planar surfaces use either monovalent NTA [7] or cumulated NTA clusters [8, 9] with multivalent interaction sites for histidines. [7-9].

In this study we use a polymer based chip platform grafted with Ni-chelating compounds such as IDA and amino acid derivates for binding of Protein G in microarray format. The issue of non-specific protein adsorption is tackled by the generation of substrate-bound hydroxyl-groups in high density during the grafting process and by using derivates of compounds like aspartate which were classified as protein repellent [10]. The printing buffer was supplemented with glycerol which suppresses non-specific protein adsorption and thus enhances surface binding specificity. Additionally the increased content of the hyperthermic protector glycerol [11] may help to stabilize delicate proteins and could thus prove useful in the storage of such microarrays.

In literature data concerning alternative chelators in this field of research is still very limited. Choice of the metal ligand and variation of the chelating compound's structure can significantly affect the performance of metal affinity based immoblisation. Thus this work examines selectivity and signal strengths attained by chelators iminodiacetic acid (IDA) and *N*-(carboxymethyl)aspartate (CMA) and elucidates the impact of the metal cation.

In a pursuit to design a ligand with enhanced immobilisation characteristics we modified CMA by replacing the aspartate building block with methionine affording *N*-(carboxymethyl)methionine. This leads to both an altered set of metal chelating atoms and a decrease in overall molecule charge. We present data on this novel metal affinity ligand which shows signal strengths superior over IDA, CMA and commercial hydrogel and NTA slides.

2 Materials and methods

2.1 Materials and reagents

ARChips Epoxy are proprietary slides developed at AIT. Phosphate buffered saline pH 7.2 (PBS) was purchased from Gibco. Untagged Protein G, L-aspartic acid, L-methionine, bromoacetic acid, iminodiacetic acid (IDA), glycerol, tris(hydroxymethyl)aminomethane (Tris), 4-(2-hydroxyethyl)piperazine-1-ethanesulfonic acid (HEPES), 3-[(3-Cholamidopropyl)dimethylammonio]-1-propanesulfonate (CHAPS), polyoxyethylene(20)-sorbitan monolaurate (Tween-20), bovine serum albumin (BSA), sodium deoxycholate, sodium hydroxide, sodium phosphate monobasic dehydrate, sodium chloride, copper(II)chloride hydrate, nickel(II)chloride hexahydrate, zinc chloride and iron(III)chloride hexahydrate were purchased from Sigma. Iron(II)chloride tetrahydrate was from Alfa Aesar. His-tagged Protein G (H6-Protein G) was from Abcam. Rat IgG2c anti procalcitonine

antibody was kindly provided by Dr. Petra M. Krämer (Helmholtz Center Munich) and conjugated with Dy547 by Exbio Praha. Ni-NTA HisSorb Plates (Ni-NTA ELISA plates) were obtained from Quiagen. NiHC slides were from Xantec and nickel chelate on glass slides were obtained from Xenopore. According to manufacturers' specification both commercial affinity slides are ready-to-use preloaded with nickel. Xantec's slides carry a three-dimensional matrix consisting of a polycarboxylate hydrogel (hydrogel slides) while Xenopore's glass slides have nitrilotriacetic acid covalently linked to the surface (NTA slides).

2.2 Ni-NTA ELISA based assay

All incubation steps were done at RT on The Belly Dancer (Stovall, Greensboro, NC, USA) at maximum speed. Different concentrations of H6-Protein G and untagged Protein G were prepared in PBS with 0.2% (w/v) BSA. Next 200 µL protein solution was added to each well of the Ni-NTA ELISA plate and incubated for 2 h. Wells were washed 4 times with HEPES buffered saline with Tween-20 (HBS-Tween: 20 mM HEPES, 150 mM NaCl, 0.1% Tween-20, pH 7.5). Next 200 µL of 1 µg/mL Dy547 labelled rat anti procalcitonine antibody (isotype IgG2c) in HBS-Tween was added and incubated for 1 h. Wells were again washed 4 times with HBS-Tween. Well fluorescence was read out using the IQ5 Multicolor Real-Time PCR detection system (Biorad).

2.3 Affinity slide fabrication

2.3.1 IDA slides

Synthesis of IDA slides was performed based on an adapted protocol from Yang and coworkers [12] (Fig. 1). Briefly ARChip Epoxy slides were incubated in 0.1 M NaOH, 2.0M iminodiacetic acid and 0.01% sodium deoxycholate (pH adjusted to 9) for 24 h at 70°C on a shaker. Slides were washed with an excess of distilled water and stored at 4°C.

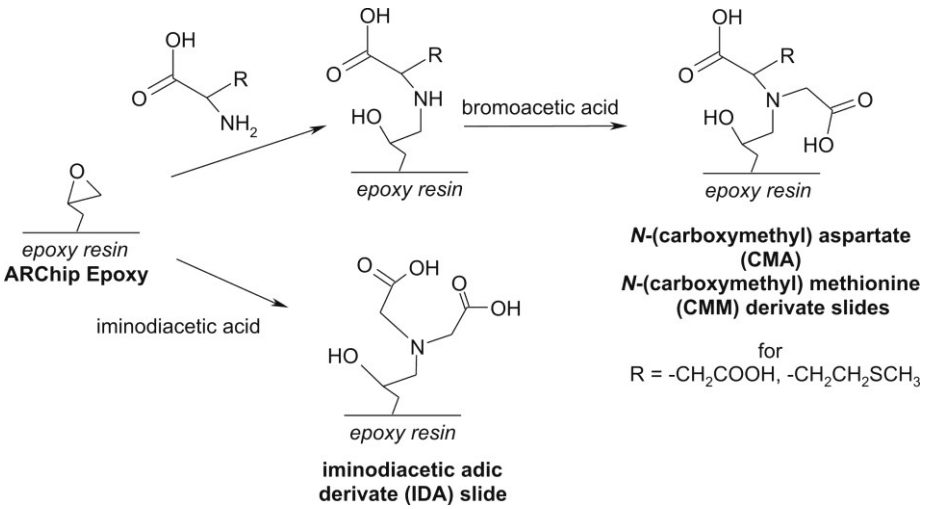

Fig. 1 Surface synthesis starts from the ARChip Epoxy platform and affords affinity slides with attached iminodiacetic acid and carboxymethyl amino acid ligands.

2.3.2 CMA and CMM slides

Synthesis protocol was adapted from Caga and coworkers [13] (Fig. 1). For CMA and CMM slides 1.2 M solutions of L-aspartic acid or L-methionine were prepared in 1 M sodium carbonate and the pH was adjusted to 11.5 with anhydrous pellets of NaOH. ARChip Epoxy slides were incubated in this solution on a shaker overnight. Slides were washed in deionized water, 10% acetic acid, deionized water and 0.2 M $NaHCO_3$ / Na_2CO_3 (pH 10). 12.6 g bromoacetic acid were dissolved in 30 ml of 4 M NaOH and the pH was adjusted to 10.5 with 4 M NaOH. 30 ml of 1 M $NaHCO_3$ / Na_2CO_3 (pH 10.0) were added to the bromoacetate solution and substrates were shaken in this mixture overnight. Slides were washed in deionized water, 10% acetic acid and deionized water.

2.3.3 Charging slides with metal cations

Slides were charged by incubation in the respective 100 mM metal chloride solutions for 2 h at RT and were washed with distilled water.

2.4 XPS

Ni(II)-charged affinity slides were investigated by XPS using a Kratos XSAM 800 spectrometer. For excitation Mg Kα radiation with an energy of 1253.6 eV was used. The angle between incident x-rays and sample surface was about 35° and photoelectrons leaving parallel to surface normal were detected. The electron energy analyser was operated in fixed analyser transmission mode with a hemispherical analyser transmission energy of 38 eV. After recording a survey spectrum of each specimen, where binding energy ranges from 0 eV to 1150 eV, we acquired higher resolution step-scans with energy steps of 0.1 eV of the photo

emission lines of interest. The counted photo electrons originate from a sample area of a few mm^2. Each series of spectra was acquired two or more times to find out if the exposure to x-rays induces any modifications on slide surfaces. As the reproducibility of spectra was good, no modifications are observable on time scales larger than a few minutes. The specimens can be considered as insulating and therefore charging has to be taken into account. The adjustment of binding energies was done by assuming the maximum of N1s line to be at 400.00 eV.

2.5 Chip fabrication and blocking

Several commercial metal affinity products (amongst them the Ni-NTA ELISA plates used in this study) are specified to be preblocked with BSA. Accordingly hydrogel slides were preblocked with HBS-Tween/1% BSA for 30 minutes at RT and washed one time in HBS-Tween and twice in HBS before printing.

Print buffers without or with 40% glycerol were prepared based on 50 mM NaH_2PO_4, 50 mM Tris, 0.01% BSA and 0.005% CHAPS. NaCl was added to stated concentrations and the pH was set to the respective value with NaOH/HCl. 83 µg/mL untagged protein G or H6-Protein G in print buffer were arrayed on ARChip Epoxy and affinity slides at a relative humidity of 70% using the contact spotter OmniGrid from GeneMachines (4 pins; pin SMP3, spotting volume: 0.7 nl/ spot). Spot to spot distance was 400 µm and the array to array distance was 8950 µm. All probes were immobilized in triplicate and 6 identical arrays were spotted per slide. After spotting slides were kept at 4°C for a minimum of three days. One hour before the experiment affinity surfaces were blocked in HBS-Tween/1% BSA for 30 minutes at RT to remove any unbound molecules and to deactivate reactive surface groups. Afterwards the slides were washed one time in HBS-Tween and twice in HBS. ARChip Epoxy slides were blocked in PBS-Tween for 30 minutes at RT and were washed three times in PBS. All slides were dry-centrifuged for 4 minutes (900 rpm).

2.6 Chip processing

After blocking, slides were processed using the Fast Frame system (Whatman). The 16 well array incubation chambers were applied on each slide. High throughput processing of the microarray was enabled by pipetting and withdrawing target and washing solutions with a multi-pipette. Bound probes were incubated with 1 µg/mL fluorescently labelled rat anti procalcitonine antibody (isotype IgG2c) in HBS-Tween for 2 h at RT. Finally, slides were washed 2 times in HBS-Tween, 2 times in HBS and dry-centrifuged for 4 minutes (900 rpm).

2.7 Fluorescence detection and data processing

Slides were stored in the dark till scanning. Fluorescence measurements (λ_{ex}=635nm, λ_{em}=670nm) were taken using a Genepix 4000B non-confocal scanner (Axon Instruments). Fluorescence signals processed with GenePix Pro 6.0 software are background corrected and calculated as mean values from 18 replicate spots. Selectivity for his-tagged protein in comparison to non-tagged protein is defined as $Selectivity = 100\% - F_{untagged}/F_{his\text{-}tagged} * 100\%$ with $F_{untagged}$ and $F_{his\text{-}tagged}$ as the fluorescence signals of his-tagged and non-tagged protein under the same spotting conditions.

3 Results and discussion

3.1 Development of a functional binding assay based on Protein G

Binding capacity and binding selectivity are key characteristics in affinity substrates for microarray experiments. To evaluate these properties for metal chelate slides a functional on-chip assay was developed. Truncated recombinant streptococcal Protein G [14] as well as its N-terminally his-tagged version (H6-Protein G) both of which bind to Fc fragments of IgG were used for probing the surface. The assay is based on the principle that a metal affinity surface retains H6-Protein G while untagged Protein G is washed off (Fig. 2). In a subsequent detection step bound Protein G captures fluorescently labelled antibodies via their Fc fragment.

This approach requires functional integrity of the immobilized proteins and therefore prevents signals from proteins denaturated by adsorption-induced unfolding. Furthermore as each Protein G can simultaneously bind to two antibodies [15] signal amplification and gain in sensitivity is achieved. In contrast to the native protein G recombinant Protein G does not contain albumin or cell-wall binding domains [14] which enhances antibody binding selectivity and permits the use of BSA as an assay blocking agent.

Signal strength and detection limit of the binding assay were optimized with regard to assay buffer and detection antibody isotype. Assay buffer HBS-Tween resulted in 2.4 times higher fluorescence signals than buffer PBS with 0.1% Tween-20 at an immobilisation concentration of H6-Protein G of 7.7 µg/mL. Since some discrepancies exist among literature reported affinity values of Protein G due to differences in binding buffer conditions and form of the proteins used [16, 17] we further tested several dye-labelled antibody subtypes as detection agent. A rat IgG2c detection antibody was used in subsequent assays as fluorescence signals

were 5 and 6.5 times higher than for antibody subtypes mouse IgG1 and mouse IgG2a respectively.

Selectivity and sensitivity of the assay carried out in buffer HPS with Dy647-labelled rat IgG2c as detection agent were checked on a Ni-NTA ELISA plate. On average fluorescence signals from H6-Protein G loaded wells were 15 fold higher than fluorescence response from corresponding wells incubated with untagged Protein G. Furthermore signals from untagged Protein G were in the order of magnitude of the blank. Overall results indicate a very broad assay working range covering the interval between 1.56 and 200 µg/mL (H6-)Protein G.

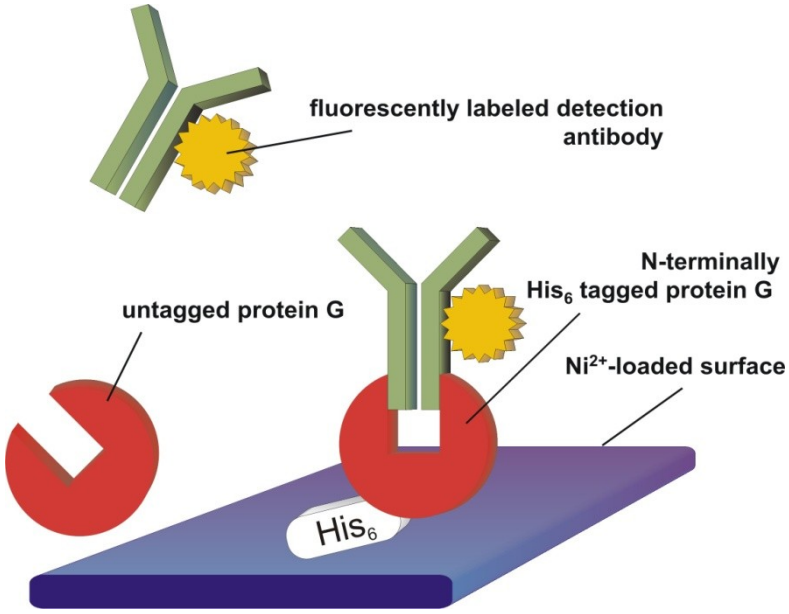

Fig. 2 Principle of the functional assay based on his-tagged Protein G and its untagged counterpart. A nickel loaded surface binds tagged protein G which is subsequently detected via a fluorescently labelled antibody. Conversely an untagged protein G cannot bind to the surface, is washed off and no signal is generated.

3.2 Synthesis of IDA and *N*-(carboxymethyl) aminoacid based surfaces

Iminodiacetic acid (IDA) and *N*-(carboxymethyl) aspartate (CMA) were attached to the surface of ARChip Epoxy via solid phase synthesis affording tridentate and tetradentate metal chelator surface groups. In an effort to enhance binding properties of CMA based nickel slides the aspartate building block of the surface moeity was replaced by the amino acid methione leading to the corresponding *N*-(carboxymethyl) aminoacid derivate CMM.

The slides' surface nickel concentration as well as signal intensities and selectivity obtained on the substrates were studied in comparison to commercial products.

3.2.1 XPS

Fabricated and commercial nickel-loaded surfaces were analyzed by XPS. The Ni2p high-resolution spectrum is shown in Fig. 3a. On the one hand side for hydrogel slides and surfaces IDA, CMA and CMM it features a Ni2p3/2 photopeak at ~856 eV and a Ni2p1/2 peak located at 17.6 eV higher binding energy. These spectra correspond well to those reported for Ni-chelates based on NTA derivates [18, 19]. On the other hand side no surface nickel could be detected on NTA slides. The amount of immobilized nickel on IDA and hydrogel slides is larger than on CMA and CMM slides. Nevertheless nickel concentration does not necessarily correlate with signal strength generated on slides. This is because stable immobilisation can be obtained already at a low surface concentration of metal-loaded chelator sites [9]. For instance Ho et al. prepared IDA based immobilised metal affinity sorbents with increasing amounts of ligand and chelated Cu^{2+}. Their obtained capacities for recombinant his-tagged protein did not correlate with ligand densities [4]. This is because too high a concentration of ligands can lead to undesired electrostatic phenomena, protein rearrangements and multisite attachment [20].

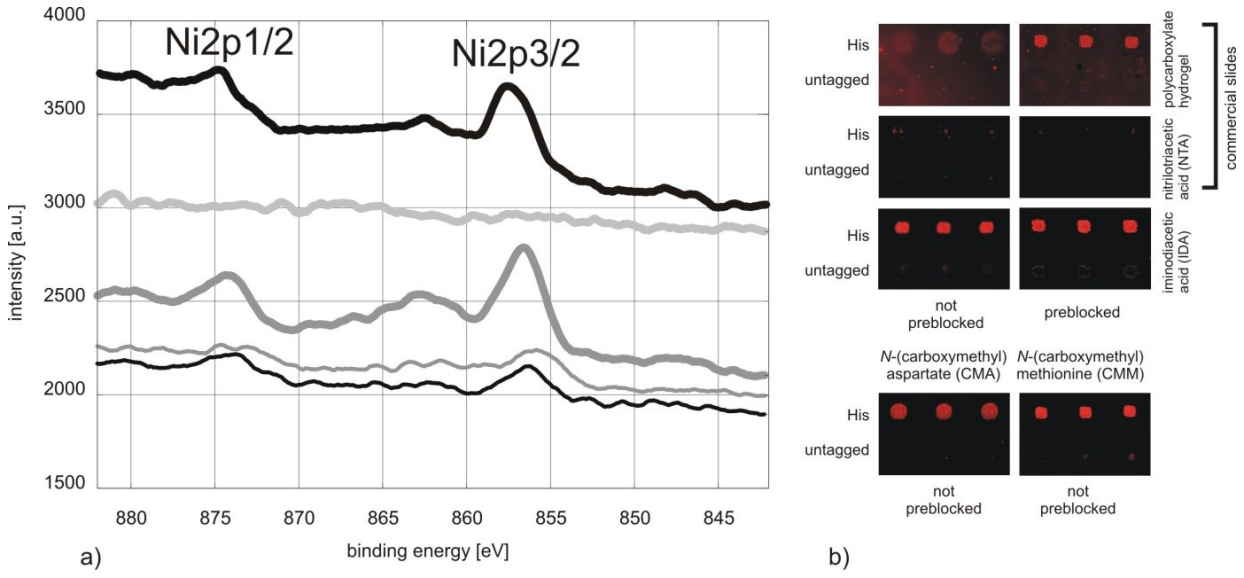

Fig. 3 (a) XPS Ni2p high-resolution spectra of Ni(II) loaded slides: commercial hydrogel (■) and commercial NTA slides (■), IDA (■), CMA (—) and CMM (—). (b) Comparison of nickel-loaded affinity slides surfaces with spots of H6-Protein G (His) and untagged Protein G (untagged) in print buffer PBS/Tris/CHAPS/BSA. Hydrogel, NTA and IDA slides were either blocked with BSA before spotting (preblocked) or were used without pre-treatment (not preblocked).

3.2.2 Slide pretreatment

H6-Protein G and untagged Protein G were spotted onto surfaces and detected with fluorescently labelled antibody. Several commercial metal affinity ELISA plates (amongst them those used in this study) are specified to be preblocked with BSA. Therefore a set of hydrogel, NTA and IDA slides was also preblocked with BSA before spotting. Obtained fluorescence images are presented in Fig. 3b. No major difference between BSA preblocked and untreated surfaces is observed for NTA and IDA slides. Contrarily on hydrogel slides preblocking results in lower background, more compact spots and a five-fold increase in fluorescence. In agreement with this finding Everhart et al. report superior results when preblocking metallized polymer surfaces before patterning. They theorize that the physisorbed unspecific blocker is replaced by the specifically interacting spotted material [21]. We argue that the increased signal strengths on preblocked hydrogel slides can be attributed to its 3d coating as we have obtained similar characteristics in a preliminary study on nickel-chitosan-gel slides (unpublished data). Due to the proximity and sterical constraints a specifically attached and gel-embedded protein may interact with chains of the network that would otherwise be low-adsorbent. Subsequent migration of the printed proteins into the gel matrix in the course of rebinding processes [9, 22, 23] may add to inaccessibility and adsorption mediated denaturation. Preblocking with BSA therefore reduces unspecific interactions with the polymer surface and restricts protein mobility by reducing the apparent pore size.

The selectivity of the surfaces in regard to the his-tag was evaluated on preblocked hydrogel and not pre-treated NTA, IDA, CMA and CMM slides. On surfaces CMA, IDA, CMM and gel slides signals generated by spotted H6-Protein G were 5 fold, 7 fold, 15 fold and 5 fold higher than those at untagged Protein G. On commercial NTA slides the signal of his-tagged protein does not differ significantly from the untagged control.

The background fluorescence level on commercial gel slides is three times higher than on CMA, IDA and CMM surfaces (Fig. 3b). The surface grafting process directly contributes to the low non-specific protein adsorption: The functional substrate ARChip Epoxy consists of SU8, a bisphenol A based resist that provides eight epoxy groups per molecule for amino acid binding [24]. As the epoxy ring is opened during the nucleophilic attack of the amino compound a hydroxyl group is generated. OH-functionalization of substrates was reported to reduce protein adsorption [25]. As the polymeric substrate carries a high density of epoxy groups (1.3 epoxy groups per monomeric unit) coupling of the chelating ligand introduces a protein-repellent layer between the grafted groups and the polymer.

Furthermore the modification of membranes with the amino acid aspartate was reported to infer a reduced ability to adsorb protein from either plasma solution or protein solutions [10]. An aspartate derivate is used on CMA slides as the nickel chelator. We speculate that similar protein repellent effects are also exerted by other amino acids than aspartate used in the fabrication of the CMM surfaces.

Fluorescence signals of H6-Protein G on hydrogel and CMA slides were three times higher than on NTA slides. Intensities on IDA and CMM slides were about twice as high as on hydrogel slides.

NTA substrates exhibit low signal intensities and selectivity and no surface nickel was detected. Therefore NTA substrates were not further characterized.

3.3 Functional characterisation

3.3.1 Print buffer

Choice of print buffer is a constant issue in microarray experiments because buffering agent, pH and additives affect spot morphology, signal strength and reproducibility [26]. As this study investigates affinity interactions between proteins and surfaces in microarray format the print buffer also has to establish conditions for specific immobilisation.

3.3.1.1 Glycerol as an additive enhances selectivity

A prerequisite for specificity is equilibrium between proteins and available binding sites. This requirement is not a primary issue in affinity column based applications as the metal chelating resin is always contacted by liquid phase enabling dissociation of nonspecifically bound proteins.

In microarray printing on the other hand small droplets are deposited which dry on the surface. Evaporation of solvent leads to constantly changing ionic strength and protein concentration. Additionally dried protein may irreversibly attach to the surface by unspecific interactions. In covalent and electrostatic immobilisation strategies non-specific adsorption is often not noticed as it adds to immobilisation yield [27]. However in affinity immobilisation this effect conflicts with the intended correct orientation of biomolecules.

Supplementing the print buffer with 40% glycerol avoids drying of the spots [28]. On Ni^{2+}-loaded IDA slides addition of glycerol results in a decrease in H6-Protein G generated signal by about 30%. At the same time non-specific binding of untagged Protein G is reduced by

more than 80% leading to > 95% selectivity. Similarly on the uncharged surface the amount of non-specifically bound H6-Protein G decreases by 86%. Those effects are mediated by glycerol which firstly preserves liquid phase conditions and secondly lowers non-specific hydrophobic interactions [29]. Decreased signal strengths are attributable to more selective buffer conditions and are not caused by mass transport limitations due to the high viscosity of glycerol. This was demonstrated by increased signal strengths using glycerol containing immobilisation buffer on substrates acting by covalent immobilisation (data not shown). Also signals of H6-His on Ni-loaded CMM slides show no alteration after addition of glycerol, while non-specific signals from untagged Protein G (-79%) as well as signals on uncharged slides drop significantly (-89% for untagged and -62% for his-tagged Protein G). Selectivities on CMM, CMA and hydrogel slides in glycerol buffer are all above 95%.

The coefficient of variation (CV) for signals of tagged protein spotted in glycerol is about 17% for surfaces Ni(II)-CMA, Ni(II)-IDA and Ni(II)-CMM. A CV of <20% is acceptable for protein microarrays and variabilities in this order of magnitude are common for commercial microarray slides [30, 31].

Due to the significant rise in selectivity all experiments were carried out in spotting buffer supplemented with 40% glycerol.

3.3.1.2 Ionic strength

Protein adsorption on metal affinity surfaces is envisioned to be a cumulative effect of ionic (or electrostatic), hydrophobic and coordination interactions [32]. In fact increasing ionic strength has a considerable impact on the characteristics of Ni(II)-loaded CMA (Fig. 4): At pH 8 increasing the NaCl concentration from 100 to 1500 mM leads to a drop of 58% in signal intensity of his-tagged protein. This effect was also reported on Ni(II)-TREN and ascribed to the lowering of ionic interactions by higher salt concentrations. We propose that the net charge of the nickel loaded CMA complex in which the negative charge of three carboxylic groups is not fully compensated by the divalent nickel plays a role in this effect. Consequently on IDA and CMM slides where the Ni(II)-charged ligands are electroneutral we did not observe pronounced effects of ionic strength. However on hydrogel slides fluorescence signal of H6-Protein G at pH 8 constantly decreases when augmenting the NaCl concentration from 100 mM to 3 M.

The ensemble of developed slides suggests optimal binding and best selectivity for 100 mM NaCl concentration (pH 8), thus those conditions were chosen as spot buffer parameters.

Higher ionic strengths were avoided because they encourage protein rearrangement processes at binding sites and counteract uniform protein orientation [20].

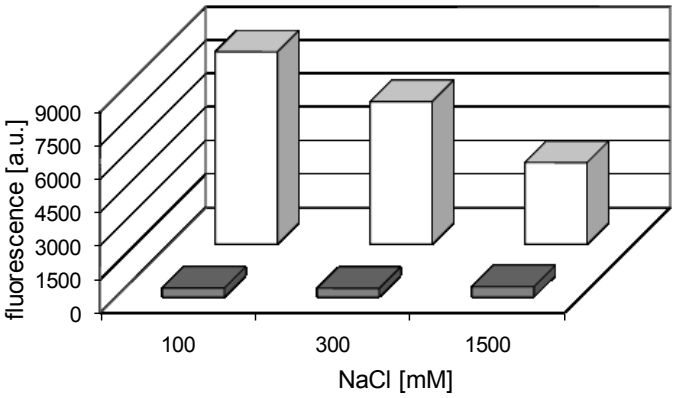

Fig. 4 Signal intensities of untagged Protein (■) and H6-Protein G (□) on CMA slides at different ionic strength. The printing buffer was supplemented with 40% glycerol.

3.3.2 Metal cation

To gain insight into the metal affinity slides' binding specificity and to test the hypothesis that selectivity is conferred by the chelated nickel ion and not mainly by electrostatic phenomena surfaces were charged with different metal cations. As representatives of tridendate and tetradentate ligands we studied slides IDA and CMA in detail (Fig. 5a and b). Both Ni(II)-loaded substrates show excellent selectivities for H6-Protein G, the signal strength on Ni(II)-CMA attaining half of the corresponding response on Ni(II)-IDA.

Cu(II)-loaded IDA and CMA slides feature binding characteristics similar to the uncharged surface. However this finding is in line with Porath et al. who report higher amounts of less specifically bound protein on Cu(II)-IDA as compared to Ni(II)-IDA [33]: Unlike conventional affinity chromatography microarray fabrication requires a blocking step to reduce unspecific binding. The present study uses BSA as a blocking agent which binds copper with extraordinarily high affinity (K_a=1.6×10 ^{16} M $^{-1}$) [34] and was reported to be retained by Cu(II)-IDA [35]. This affinity leads to both competition with his-tagged Protein G and sterical crowding at the copper-centre resulting in decreased fluorescence response. By contrast the affinity of BSA for Ni^{2+} is 11 decades lower (K_a=3×10 ^{5} M $^{-1}$) [36] which explains why Ni(II)-loaded surfaces are not affected. Additionally Kent et al. report that more extensive conformational changes and protein rearrangements may occur upon adsorption to Cu(II) than to Ni(II). This can lead to partial denaturation, decreased protein activity and thus lower assay signals [37].

For Zn(II) higher specificity accompanied by lower immobilisation capacity were reported [33]: This corresponds to the drop in H6-Protein G signal on Zn(II)-IDA slides by 44% in comparison with Ni(II)-IDA but also to the decreased response of nonspecifically adsorbed untagged Protein G.

For both Fe(III)-IDA and Fe(III)-CMA signals from H6-Protein G attain the same order of magnitude as on nickel-loaded slides. This is in line with the results of Run-Bo et al. [38] who used Fe(III)-charged hydroxyapatite and obtained protein loadings comparable to Ni-NTA adsorbents. Nevertheless unspecific signals from untagged protein G are 5 times higher on Fe(III)-loaded IDA slides than on Ni(II)-surfaces (Fig. 5a).

IDA substrates were also charged with ferrous ions. The decrease in the ion's valency leads to a significant drop in fluorescence signal of H6-Protein G and selectivity for his-tagged protein is virtually lost (Fig. 5a). This drastic change in properties again highlights the metal's paramount role in protein binding. To sum it up we demonstrate that the Ni(II)-ion is a selectivity conferring factor on the studied substrates and that Ni(II) confers highest signal strengths and best selectivity amongst investigated metal ions.

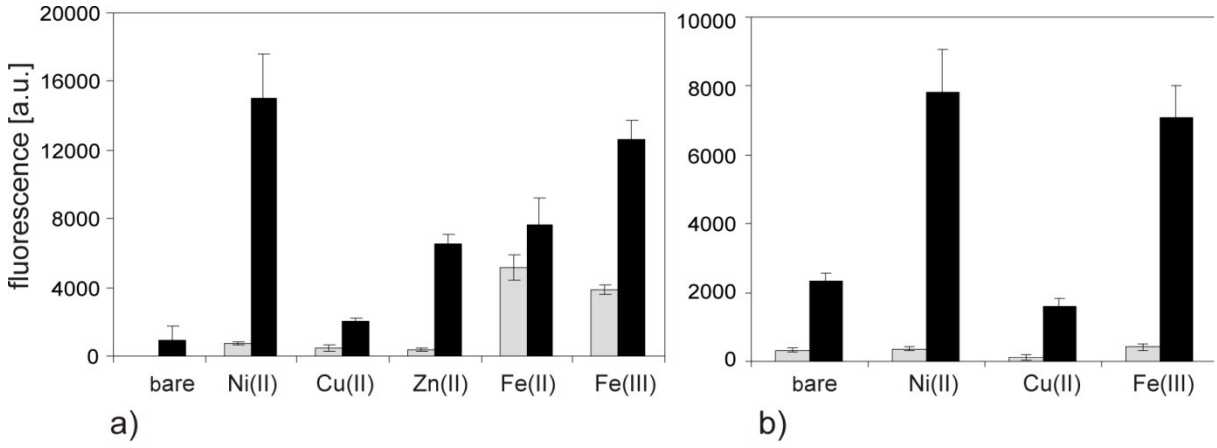

Fig. 5 Signal strengths of H6-Protein G (■) and untagged protein G (□) on (a) IDA and (b) CMA substrates. Substrates were either used uncharged or loaded with the respective metal ions.

3.3.3 Role of the aminoacid in N-(carboxymethyl) aminoacid derivates

Although structurally related we showed that IDA and CMA ligands exhibit very dissimilar characteristics concerning signal strengths and response to ionic strength. We speculated that this difference can be partly attributed to the additional charged carboxylate group of CMA. In an effort to retain the structure of a tetradendate chelator while using another uncharged donor atom instead of the carboxylic oxygen, the preparation of CMA was modified by substituting aspartate with methionine. This introduces a thioether group in the position of the

donor oxygen affording the ligand CMM. Though considered both poor σ-donor and poor π-acceptor ligands, neutral thioethers usually form strong bonds with *soft* metals through one of their lone pairs [39]. Regarding absolute hardness Ni^{2+} is a borderline ion that can behave as a soft ion. Structural investigations of Ni(II)-methionine complexes have revealed that the S atom is actually involved in coordination [40]. This does not only elucidate the tremendous increase of 140% in signal strength of H6-Protein G on Ni(II)-CMM slides in comparison to Ni(II)-CMA slides (Fig. 6) but also the distinct difference to Ni(II)-IDA. Depending on the NaCl concentration and pH signals of H6-Protein G on Ni(II)-CMM are up to 180 % higher than on Ni(II)-IDA (25% higher at pH 8, 100mM NaCl, Fig. 6).

To sum it up substitution of the amino acid in the *N*-(carboxymethyl) aminoacid synthesis can change substrate characteristics by modification of the metal ion's coordination sphere and by altering the chelating compound's overall charge. Obtained Ni(II)-CMM slides produce highest signals of all affinity slides in the study surpassing commercial hydrogel slides by 500%.

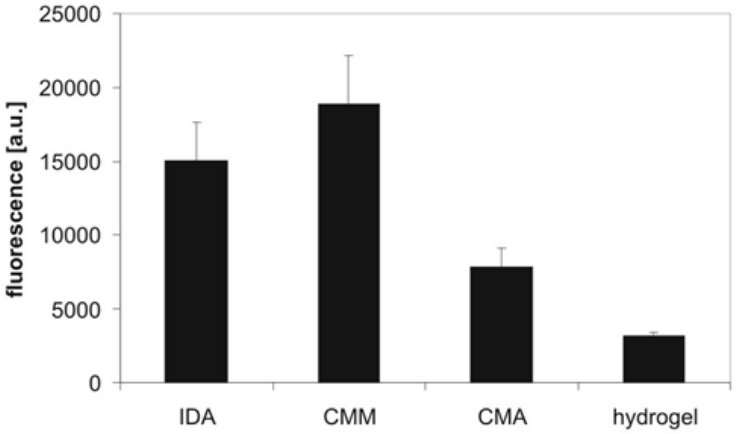

Fig. 6 Comparison of signal strength: H6-Protein G spotted in PBS/Tris/CHAPS/BSA/pH 8.0/40% glycerol on slides IDA, CMM, CMA and hyrogel slides.

4 Conclusions

A main objective of this study on nickel-chelate affinity slides for protein microarray fabrication was to assure binding equilibrium conditions while promoting signal strength and attachment specificity of proteins in nanoliter volume spots. We present three different surfaces featuring protein-repellent hydroxyl layers and grafted chelators IDA, CMA and CMM which prove to be effective alternatives to frequently applied NTA groups: In a microarray based binding assay high binding selectivities >95% were obtained without slide preblocking and signal strengths were higher than on commercial reference products (at least factor 2 up to factor 6).

Variation of the chelated ion further demonstrated that the surfaces' selectivity is considerably modified by the chemical identity of the central metal atom.

Ongoing research aims at characterizing local phenomena of interaction between his-tagged proteins and metal chelates including the modelling of surface-bound biomolecules. Presented affinity surfaces and protocols may serve as invaluable tools in the development of protein chips when tag specific binding and protein orientation are crucial.

5 Acknowledgement

The authors thank the Austrian Science Foundation for financial support through the Translational-Research-Programme (Project No. L415-N19).

6 References

1. Hirst, E.R., et al., *Bond-rupture immunosensors--A review.* Biosensors and Bioelectronics, 2008. **23**(12): p. 1759.
2. Nam, J.M., et al., *Bioactive Protein Nanoarrays on Nickel Oxide Surfaces Formed by Dip-Pen Nanolithography.* Angewandte Chemie, 2004. **116**(10): p. 1266-1269.
3. Gaberc-Porekar, V. and V. Menart, *Perspectives of immobilized-metal affinity chromatography.* Journal of Biochemical and Biophysical Methods, 2001. **49**(1-3): p. 335.
4. Ho, L.-F., et al., *Integrated enzyme purification and immobilization processes with immobilized metal affinity adsorbents.* Process Biochemistry, 2004. **39**(11): p. 1573.
5. Wu, Z., et al., *Immobilization of proteins on metal ion chelated polymer surfaces.* Colloids and Surfaces B: Biointerfaces, 2009. **69**(1): p. 71.
6. Nakaji-Hirabayashi, T., et al., *Oriented immobilization of epidermal growth factor onto culture substrates for the selective expansion of neural stem cells.* Biomaterials, 2007. **28**(24): p. 3517.

7. Kang, E., et al., *Specific Adsorption of Histidine-Tagged Proteins on Silica Surfaces Modified with Ni2+/NTA-Derivatized Poly(ethylene glycol).* Langmuir, 2007. **23**(11): p. 6281-6288.
8. Tinazli, A., et al., *High-Affinity Chelator Thiols for Switchable and Oriented Immobilization of Histidine-Tagged Proteins: A Generic Platform for Protein Chip Technologies.* Chemistry - A European Journal, 2005. **11**(18): p. 5249-5259.
9. Lata, S. and J. Piehler, *Stable and Functional Immobilization of Histidine-Tagged Proteins via Multivalent Chelator Headgroups on a Molecular Poly(ethylene glycol) Brush.* Analytical Chemistry, 2005. **77**(4): p. 1096-1105.
10. Akon, H., et al., *Serum protein adsorption and platelet adhesion on aspartic-acid-immobilized polysulfone membranes.* Journal of Biomaterials Science, Polymer Edition, 2004. **15**: p. 1051-1063.
11. Lepock, J.R., *Measurement of protein stability and protein denaturation in cells using differential scanning calorimetry.* Methods, 2005. **35**(2): p. 117.
12. Yang, C., et al., *Development of superparamagnetic functional carriers and application for affinity separation of subtilisin Carlsberg.* Polymer, 2006. **47**(7): p. 2299.
13. Caga, G., et al., *Natural poly-histidine affinity tag for purification of recombinant proteins on cobalt(II)-carboxymethylaspartate crosslinked agarose.* Journal of Chromatography A, 1999. **864**(2): p. 247.
14. Goward, C.R., et al., *Expression and purification of a truncated recombinant streptococcal protein G.* Biochem. J., 1990. **267**(1): p. 171-177.
15. Choi, J.-W., et al., *Regulation of anti-LDL immobilization on self-assembled protein G layer using CHAPS and its application to immunosensor.* Materials Science and Engineering: C, 2004. **24**(1-2): p. 241.
16. Bjorck, L. and G. Kronvall, *Purification and some properties of streptococcal protein G, a novel IgG-binding reagent.* J Immunol, 1984. **133**(2): p. 969-974.
17. Frank, M.B., *Antibody Binding to Protein A and Protein G beads*, in *Molecular Biology Protocols*, M.B. Frank, Editor. 1997: Oklahoma City.
18. Shen, J., et al., *Preparation and characterization of nitrilotriacetic-acid-terminated self-assembled monolayers on gold surfaces for matrix-assisted laser desorption ionization-time of flight-mass spectrometry analysis of proteins and peptides.* Analytical Biochemistry, 2005. **345**(2): p. 258.
19. Lee, J.K., et al., *Grafting Nitrilotriacetic Groups onto Carboxylic Acid-Terminated Self-Assembled Monolayers on Gold Surfaces for Immobilization of Histidine-Tagged Proteins.* The Journal of Physical Chemistry B, 2004. **108**(23): p. 7665-7673.
20. Jiang, W. and M.T.W. Hearn, *Protein Interaction with Immobilized Metal Ion Affinity Ligands under High Ionic Strength Conditions.* Analytical Biochemistry, 1996. **242**(1): p. 45.
21. Everhart, D.S., R.M. Kaylor, and K.M. Alpharetta, *Patterned binding of functionalized microspheres for optical diffraction-based biosensors*. 2003: US.
22. Glaser, R.W., *Antigen-Antibody Binding and Mass Transport by Convection and Diffusion to a Surface: A Two-Dimensional Computer Model of Binding and Dissociation Kinetics.* Analytical Biochemistry, 1993. **213**(1): p. 152.
23. Schuck, P. and A.P. Minton, *Analysis of Mass Transport-Limited Binding Kinetics in Evanescent Wave Biosensors.* Analytical Biochemistry, 1996. **240**(2): p. 262.
24. Preininger, C., *Fixed support for immobilizing biomolecules*. 2007, Oesterr Forsch Seibersdorf: AT 500669 B1.
25. Faucheux, N., et al., *Self-assembled monolayers with different terminating groups as model substrates for cell adhesion studies.* Biomaterials, 2004. **25**(14): p. 2721-2730.

26. Pultar, J., et al., *Aptamer-antibody on-chip sandwich immunoassay for detection of CRP in spiked serum.* Biosensors and Bioelectronics, 2009. **24**(5): p. 1456.
27. Tran, L.D., et al., *A polytyramine film for covalent immobilization of oligonucleotides and hybridization.* Synthetic Metals, 2003. **139**(2): p. 251.
28. MacBeath, G. and S.L. Schreiber, *Printing Proteins as Microarrays for High-Throughput Function Determination.* Science, 2000. **289**(5485): p. 1760-1763.
29. Sobral, P., et al., *Films Based on Biopolymer from Conventional and Non-Conventional Sources*, in *Food Engineering: Integrated Approaches*, G.F. Gutiérrez-Lopez, et al., Editors. 2008, Springer New York: New York. p. 193-223.
30. Birgit Guilleaume, A.B., Christian Schmidt, Fritz Klimek, Gerhard Moldenhauer, Wolfgang Huber, Dorit Arlt, Ulrike Korf, Stefan Wiemann, Annemarie Poustka,, *Systematic comparison of surface coatings for protein microarrays.* Proteomics, 2005. **5**(18): p. 4705-4712.
31. Steinhauer, C., et al., *Biocompatibility of surfaces for antibody microarrays: design of macroporous silicon substrates.* Analytical Biochemistry, 2005. **341**(2): p. 204-213.
32. Sharma, S. and G.P. Agarwal, *Interactions of Proteins with Immobilized Metal Ions: Role of Ionic Strength and pH.* Journal of Colloid and Interface Science, 2001. **243**(1): p. 61.
33. Porath, J., *Immobilized metal ion affinity chromatography.* Protein Expression and Purification, 1992. **3**(4): p. 263.
34. Camerman, N., A. Camerman, and B. Sarkar, *Molecular design to mimic the copper(II) transport site of human albumin. The crystal and molecular structure of copper(II) – glycylglycyl-L-histidine-N-methyl amide monoaquo complex.* Can. J. Chem., 1976. **54**(8): p. 1309-1316.
35. Nova, C.J.M., et al., *Elaboration, characterization and study of a new hybrid chitosan/ceramic membrane for affinity membrane chromatography.* Journal of Membrane Science, 2008. **321**(1): p. 81.
36. Lau, S.-J., T.P.A. Kruck, and B. Sarkar, *A Peptide Molecule Mimicking the Copper(II) Transport Site of Human Serum Albumin. A Comparative Study between the Synthetic Site and Albumin.* J. Biol. Chem., 1974. **249**(18): p. 5878-5884.
37. Kent, M.S., et al., *Adsorption of Myoglobin to Cu(II)-IDA and Ni(II)-IDA Functionalized Langmuir Monolayers: Study of the Protein Layer Structure during the Adsorption Process by Neutron and X-Ray Reflectivity.* Langmuir, 2005. **21**(15): p. 6815-6824.
38. Suen, R.-B., S.-C. Lin, and W.-H. Hsu, *Hydroxyapatite-based immobilized metal affinity adsorbents for protein purification.* Journal of Chromatography A, 2004. **1048**(1): p. 31.
39. Masdeu-Bultó, A.M., et al., *Chiral thioether ligands: coordination chemistry and asymmetric catalysis.* Coordination Chemistry Reviews, 2003. **242**(1-2): p. 159.
40. McAuliffe, C.A., J.V. Quagliano, and L.M. Vallarino, *Metal Complexes of the Amino Acid DL-Methionine.* Inorganic Chemistry, 1966. **5**(11): p. 1996-2003.

CHAPTER 5

Conference presentations

Parts of this thesis were presented as oral and poster presentations on international conferences. The abstracts of the contributions are sampled in this chapter.

Poster at the EUROPT(R)ODE IX, Mar. 31 – Apr. 2, 2008, Dublin

PROTEIN BIOMARKER CHIP FOR DIAGNOSIS OF MELANOMA

P. Domnanich, U. Sauer, J. Pultar, C. Preininger

Austrian Research Centers GmbH / ARC, Dep. Bioresources, 2444 Seibersdorf, Austria

patrick.domnanich@arcs.ac.at

The clinical course of malignant melanoma is notoriously variable. Current staging criteria including tumour thickness, invasion and metastasis formation allow assignment to risk categories but do not permit accurate assessment of prognosis. The detection of biomarkers reflecting disease stage and likelihood of progression can thus give raise to new, more effective and less toxic therapies on an individual patient basis.

The biomarker chip presented herein consists of antibodies against serum markers for melanoma immobilized covalently onto ARChip Epoxy slides. The melanoma specific prognostic and staging factors S100B and Vascular Endothelial Growth Factor A (VEGF-A) are analyzed as well as disease-related inflammatory and immunomodulatory parameters – C-reactive Protein (CRP), Tumor Necrosis Factor Alpha (TNFα) and interleukins IL6 and IL10 [1, 2]. The chip is implemented as a sandwich immunoassay with streptavidin-biotin chemistry and fluorescence detection.

Serum CRP concentrations can vary between 1 mg/L under normal to 1000 mg/L under inflammatory conditions. Cytokines, which have to be detected at the ng/L scale, span a three log range, whereas serum S100B and VEGF-A concentrations increase from below 75 ng/L to above 400 ng/L and from 300 ng/L to above 550 ng/L respectively during melanoma stage progression. In order to deal with the required low detection limits and broad working ranges optimized protocols for protein arrays have been developed. Investigated parameters include the array printing buffer, blocking conditions [3], the assay buffer and antigen incubation time. Optimizations resulted in enhanced signal-to-noise ratios and excellent dynamic detection ranges: e.g. 0.5 µg/L – 50 µg/L for TNFα and 0.05 µg/L – 50 µg/L for CRP and interleukins.

In comparison to conventional ELISA assays miniaturization and multiplexing with the presented melanoma protein chip allow a significant reduction of sample volume as well as an increase in the number of analytes that can be measured simultaneously. The platform's expandability permits the addition of new markers which are derived from a SELDI-TOF-MS screening (Department of Dermatology, Innsbruck Medical University) for novel marker proteins in sera of melanoma patients.

The system has therefore the potential of producing an unprecedented wealth of biological information which can lead to new ways in melanoma diagnostics and treatment.

[1] L. Brochez, J-M. Naeyaert, Serological markers for melanoma, Br. J. Dermatol., 143 (2000) 256–268
[2] F. Weber, N. Sepp, P. Fritsch, Vascular endothelial growth factor and basic fibroblast growth factor in melanoma, Br. J. Dermatol., 142 (2000) 392-4
[3] C. Preininger, U. Sauer, J. Dayteg, R. Pichler, Optimizing processing parameters of ARChip Epoxy for signal enhancement of oligonucleotide and protein arrays, Bioelectrochem., 67 (2005) 155-162

Short talk at the ESF-UB Conf. in Biomedicine, Sept. 19 – 24, 2008, Sant Feliu de Guixols

Development of a Protein Chip for the Analysis of Human Melanoma Biomarkers

P. Domnanich, U. Sauer, J. Pultar, C. Preininger

Austrian Research Centers GmbH - ARC, Dep. Bioresources, 2444 Seibersdorf, Austria

Melanoma is one of the most aggressive cancers in humans. A common problem of current staging criteria (e.g. tumour thickness, invasion, presence of lymph node and organ metastasis) is that tumours classified in the same category can still show highly variable clinical courses. Therefore, biomarkers reflecting disease stage and likelihood of progression could give raise to new, less toxic therapies on an individual patient's basis.
The biomarker chip presented herein consists of antibodies against melanoma serum markers immobilized covalently onto ARChip Epoxy slides. The melanoma specific prognostic and staging factors S100B and Vascular Endothelial Growth Factor A (VEGF-A) are analyzed as well as disease-related inflammatory and immunomodulatory parameters – C-reactive Protein (CRP) and interleukins IL-6 and IL-10. The chip is implemented as a sandwich immunoassay with streptavidin-biotin chemistry and fluorescence detection.
Serum concentration of CRP rises by a factor of 1000 in response to inflammatory stimulus (normal serum level: <3 mg/L). In contrast interleukins IL-6 and IL-10 have to be detected at the pg/mL scale. Biomarkers S100B and VEGF-A increase from below 200 pg/mL to above 200 pg/mL and from below 320 pg/mL to above 370 pg/mL respectively during melanoma stage progression [1, 2].
Using CRP as a model marker optimization of the chip in respect to printing buffer, antigen probe concentration (1 mg/mL), assay binding buffer and incubation time (120 min) is outlined. High reproducibility (CV < 20%), weak cross-reactivity (<0.5% with anti-IL-10) and low limit of detection were achieved. Fit of a four-parameter logistic quantification model to standard curves of the five on-chip assays shows excellent coefficients of determination ($R^2 \geq 0.966$). Achieved sensitivities (CRP: $1.88 \cdot 10^{-4}$ mg/L, IL-6: 3.1 ng/mL, IL-10: 2.4 pg/mL, S100B: 3.8 pg/mL, VEGF-A: 40.0 pg/mL) are perfectly comparable to classical ELISA kits and obtained working ranges allow discrimination between normal and literature-reported elevated serum levels of melanoma markers.
The platform's expandability permits the addition of new melanoma markers derived from a SELDI-TOF-MS screening (Department of Dermatology, Innsbruck Medical University).
The system has therefore the potential of producing an unprecedented wealth of biological information which can lead to new ways in melanoma diagnostics.

[1] R. Molina, J. Navarro, X. Filella, T. Castel, and A. Ballesta, S-100 protein serum levels in patients with benign and malignant diseases: false-positive results related to liver and renal function., Tumour Biol. 23 (2002) 39-44.
[2] S. Ugurel, [Serum markers for melanoma], Hautarzt 56 (2005) 173-184; 185-176.

Talk at the NANOSENS, Sept. 29 – 30, 2008, Vienna

Functional protein chip surfaces composed of Ni^{2+} chelating materials and microbial proteins

Patrick Domnanich, Kuheli Das Gupta, Ursula Sauer, Claudia Preininger

Austrian Research Centers GmbH – ARC, Department of Bioresources, 2444 Seibersdorf, Austria, Patrick.Domnanich@arcs.ac.at

The solid support for probe attachment holds a central role in the development of a diagnostic protein chip as the immobilization strategy applied influences sensitivity and specificity of the chip experiment. Strength of the binding, orientation and accessibility of the probes, density of bound probe molecules and the proportion of non-specific adsorption depend on the reaction chemistry.

Herein, two novel surface chemistries are compared with respect to the conventionally used ARChip Epoxy:

- microbial proteins, such as hydrophobins from *trichoderma reesei* and
- Nickel chelating matrices for binding his-tagged proteins

For the synthesis of Ni^{2+} -chelating surfaces 1) chitosan, 2) a 20-nt single stranded DNA tag to Ni^{2+} [1] and 3) carboxymethylaspartate and iminodiacetic acid coupled to ARChip Epoxy were used.

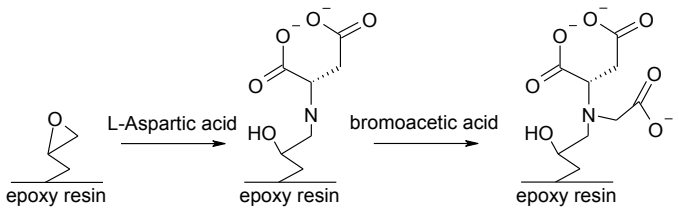

Fig. 1: Scheme of solid phase synthesis of Ni^{2+} chelator

Both hydrophobins and nickel chelating matrices were characterized with respect to surface topography and binding ability as well as chip performance using an on-chip immunoassay for diagnosis of sepsis-relevant biomarkers.

References

[1] Nastasijevic, B., N. A. Becker, et al. (2008). "Sequence-specific binding of DNA and RNA to immobilized Nickel ions". Biochemical and Biophysical Research Communications, 366(2): 420.

Poster at the 6. DBS Symposium, Mar. 29 – Apr. 1, 2009, Freiburg

IMINODIACETIC ACID AND CARBOXYMETHL-ASPARTATE AS METAL CHELATE AFFINITY LIGANDS IN PROTEIN MICROARRAYS

P. Domnanich[1], U. Sauer[1], R. Svagera[2], M. F. Ebel[2], C. Preininger[1]

[1] Austrian Research Centers GmbH – ARC, Dep. Bioresources, 2444 Seibersdorf, Austria

[2] Institute of Solid State Physics, Vienna University of Technology, 1040 Vienna, Austria

Solid-phase-based assays and protein microarrays are em-erging techniques in functional proteomics and medical diagnostics. They require an immobilisation method that minimizes structural perturbation and maximizes protein activity. Additionally structural and functional studies often demand uni-form orientation of imm-obilized proteins [1].

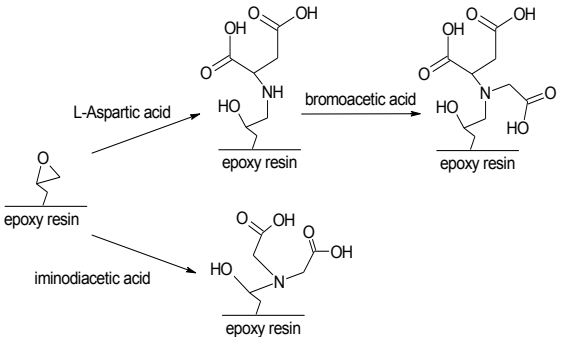

Figure 1: Solid phase synthesis of Ni^{2+} chelators

Formation of metal-chelate complexes is a strategy applied in affinity chromatography for the purification of proteins containing an engineered hexa-histidine tag (His-tag). Using this principle to address the immobilization requirements of solid-phase assays nickel chelating protein chip surfaces specific for his-protein binding were developed. Epoxy coated microarray chips were modified with either tridentate iminodiacetic acid (IDA) or with tetra-dentate carboxy-methylaspartate (CMA) (Figure 1). Surfaces were charged with Ni^{2+} and subjected to XPS analysis which revealed the Ni^{2+} characteristic Ni2p1 and Ni2p3 peaks.

In a functional binding assay in microarray format signal strengths and selectivity for his-tagged proteins were at least as high as on commercial surfaces. Furthermore pH and NaCl effects on protein binding were investigated: On the one hand side increasing NaCl concentration (0.1M up to 1.5M) resulted in a decrease in the concentration of bound his-tagged protein for both Ni^{2+}-CMA and Ni^{2+}-IDA affinity slides. On the other hand side increasing pH (pH 4 – pH 9) entailed augmenting binding affinity on Ni^{2+}-CMA (up to 180%) while the capacity of Ni^{2+}-IDA remained almost unaltered.

Additionally the influence of different chelate metal ions (Zn^{2+}, Ni^{2+}, Fe^{2+}, Fe^{3+}, Cu^{2+}, Ca^{2+}, uncharged) was studied. Each metal exhibits an unique salt and pH dependent protein binding profile.

Although most his-tag mediated immobilisation strategies rely on the chelator NTA we demonstrate that alternative ligands CMA and IDA lead to superior results in microarray chip fabrication and represent a promising tool for oriented protein immobilisation.

[1] A. Tinazli et al., Chemistry - A European Journal 11 (18):5249-5259.

Talk at the BBMEC 2009, Jun. 14 – 17, 2009, Montréal

Microarray Chip Technology for Multiplexed Detection of Diagnostic Markers

*Patrick Domnanich, Ursula Sauer, Johanna Pultar, Claudia Preininger**

Austrian Research Centers GmbH – ARC, Dept. Bioresources, 2444 Seibersdorf, Austria

Patrick.Domnanich@arcs.ac.at, Tel.: +43 (0) 50 550-3527, Fax: +43 (0) 50 550-3666

The diagnostic protein microarrays presented herein allow for the simultaneous and highly parallel analysis of biomarkers in patients' bodily fluids. These platforms are based on fluorescence detection and combine reduced analysis time with assay miniaturization. They thus permit rapid analysis in µL sample volumes.

Panels of biomarkers which play a role in the development of melanoma or in conditions like inflammation, sepsis or viral infections are assayed in complex sample matrices including serum, plasma, saliva and cell supernatants. Advanced chip design integrates sandwich format immunoassays side by side with binding inhibition based tests. This strategy accounts for the large heterogeneity in analyte molecules which requires the quantification of small and large, low abundant and highly concentrated proteins in parallel. Together with aptamers as alternative capture elements the approach meets the need for extended working ranges to cover some biomarkers' broad biologically relevant concentration intervals (e.g. C-reactive protein < 1 mg/L – 1000 mg/L).

Other analytes as the on-chip detected melanoma specific prognostic and staging factors S100 and Vascular Endothelial Growth Factor A act in picomolar concentrations. Thus sensitive detection is a key factor to chip design. To enhance signal strength integrated optical microlenses fabricated by contact-printing of photopolymerizable chemical materials are presented. Furthermore benefits and performance of new chip surfaces embracing planar as well as 3 dimensional immobilization matrices and associated immobilization principles (covalent, adsorptive, statistically orientated, site specific, affinity) are discussed.

J. Pultar, U. Sauer, P. Domnanich, and C. Preininger, Aptamer-antibody on-chip sandwich immunoassay for detection of CRP in spiked serum, Biosensors and Bioelectronics 24 (2009) 1456.
P. Domnanich, U. Sauer, J. Pultar, and C. Preininger, Protein microarray for the analysis of human melanoma biomarkers, Sensors and Actuators B: Chemical In Press, Corrected Proof

Part of this work has been performed within FP6 Integrated Project CARE-MAN, No NMP4-CT-2006-017333 and FWF Project L415-N19.

Poster at the EUROPT(R)ODE X, Mar. 28 – 31, 2010, Prague

PROTEIN MICROARRAY FOR DETECTION OF A MELANOMA MULTI-ANALYTE SERUM BIOMARKER PANEL

P. Domnanich [a,*], G. Weinlich [b], M. Schmuth [b], C. Preininger [a]

[a] *AIT Austrian Institute of Technology GmbH, Seibersdorf, Austria*
[b] *Innsbruck Medical University, Innsbruck, Austria*

Patrick.Domnanich@ait.ac.at

Melanoma is one of the most aggressive cancers in humans. Melanoma cells are prone to invade tissue and to metastasize which leads to a poor prognosis and a median survival of only 6-9 months.

Current staging criteria for melanoma used to determine the choice of treatment, include tumor thickness, invasion and presence of lymph node and organ metastasis. A common problem of those staging systems is that tumors classified in the same category can still show a highly variable clinical course. Therefore, analysis of a set of biomarkers reflecting disease stage and likelihood of progression could give raise to new, less toxic therapies on an individual patient's basis.

The reported protein microarray allows for the simultaneous and highly parallel analysis of seven melanoma biomarkers in patients' blood serum. Melanoma specific prognostic and staging factors S100B, Vascular Endothelial Growth Factor A (VEGF-A) and Secreted Protein Acidic and Rich in Cysteine (SPARC) are analyzed as well as disease-related inflammatory and immunomodulatory parameters – C-reactive Protein (CRP), Tumor Necrosis Factor Alpha (TNFα) and interleukins IL6 and IL10 [1,2].

ARChip Epoxy serves as a solid support for the covalent immobilization of antibodies and relevant antigens. Advanced chip design integrates sandwich format immunoassays and binding inhibition based tests on one platform. Signal readout is performed using fluorescence detection. The combination of two assay principles accounts for the large heterogeneity in analyte molecules and enables the quantification of small, large, low abundant and highly concentrated proteins in parallel. On the one hand side CRP and SPARC can be analyzed in the biologically relevant high concentration ranges of 0.5-50 mg/L and 0.2-2 µg/mL respectively. On the other hand side biomarkers as S100B and VEGF-A act in picomolar concentrations and the corresponding tests' detection limits are thus around 10 pg/mL and 100 pg/mL. For CRP it was demonstrated that antibody mediated antigen immobilization leads to increased assay signal intensities and a superior quantification model fit. Furthermore pretreatment of chips with crosslinker enhances precision and linearizes dose response curves in the studied concentration interval. Thus thorough optimization of immobilization chemistry and assay conditions resulted in overall sensitivities perfectly comparable to conventional tests as shown in validation studies with classical ELISA plate kits and a flow-cytometer based system. Finally the system's applicability is demonstrated in real patients' serum specimens sampled during disease follow up.

In comparison to conventional ELISA assays the presented melanoma protein chip allows for miniaturization and multiplexing coupled with a significant reduction in sample volume and processing time. The system has therefore the potential of producing an unprecedented wealth of biological information which can lead to new ways in melanoma diagnostics and treatment.

This work has been performed within the Austrian Science Foundation FWF Translational-Rearch-Programme (L415-N19).

[1] P. Domnanich, Protein microarray for the analysis of human melanoma biomarkers, Sensors and Acutators B: Chemical, (2009), 139, 2-8.
[2] J. Pultar, Aptamer-antibody on-chip sandwich immunoassay for detection of CRP in spiked serum, Biosensors and Bioelectronics, (2009), 24, 1456.

Poster at the SLONANO 2010, Oct. 20 – 22, 2010, Ljubljana

Xanthan/chitosan gold protein microarray for signal enhancement in melanoma biomarker detection

Patrick Domnanich, Dacimoneida Brito Peña, Claudia Preininger

AIT Austrian Institute of Technology GmbH, Health & Environment / Bioresources, 2444 Seibersdorf, Austria

Protein microarrays are poised to become one of the most powerful tools in clinical applications with diagnostic potential in many diseases such as melanoma [1]. However these systems face the challenge to accurately quantify analytes in the low pg/mL range. This task is hampered by weak signal strengths and too low detector sensitivity.

This issue becomes even more acute if miniaturized assays are to be integrated into a portable diagnostic device. There high sensitive laser scanners with tuneable photomultiplier tube cannot be used due to high costs, low scanning speeds and weight. Charge-coupled device cameras offer a robust alternative for signal detection, yet in practical terms, their limit of detection is significantly higher than in PMT based scanners.

To address this shortcoming, we present a platform that combines both a biocompatible polyelectrolyte multilayer (PEM) hydrogel for protein immobilisation and metal enhanced fluorescence signal amplification (Figure 1).

PEMs have proven to be favourable matrices as many immobilized proteins were reported to retain their activity for prolonged times. This effect was frequently attributed to the gel-like environment which keeps proteins hydrated and in a native conformation.

Among tested (semi)natural polysaccharides (xanthan, chitosan, carboxymethylcellulose, hyaluronic acid) PEMs composed of xanthan and chitosan performed best in terms of assay sensitivity, spot morphology, fluorescence background and variability (< 10%). Fluorescence signals on gold slides with a 75 nm coating of seven crosslinked polyelectrolyte double layers were up to 50 times higher than on bare glass slides.

The metal substrate associated amplification phenomenon can grossly be explained by the fact that emitted fluorescence light, which is normally scattered and lost through the glass substrate, is reflected back to the detector by the gold mirror. Both incident and emitted light independently interfere with their reflection from the mirror. In an optimized setup interference leads to signal amplification which is associated with shortened excitation lifetimes and increased quantum yields of the fluorophores [2].

In comparison to commercial microarray substrates the signal to noise ratio of the presented slides is enhanced by up to factor 11. Furthermore sandwich assays for interleukins 6, 8, 10, tumour necrosis factor alpha (TNFα), vascular endothelial growth factor A (VEGF-A) and S100B show working ranges which cover significantly lower concentrations (up to 38 fold).

Not limited to above assays the presented substrates, which combine a biocompatible interface with metal-based signal amplification, are a valuable tool in a variety of biosensor applications.

References: [1] Domnanich, P., U. Sauer, et al. (2009). "Protein microarray for the analysis of human melanoma biomarkers." Sensors and Actuators B-Chemical 139(1): 2-8.

[2] Lakowicz, J. R., K. Ray, et al. (2008). "Plasmon-controlled fluorescence: a new paradigm in fluorescence spectroscopy." Analyst 133(10): 1308-1346.

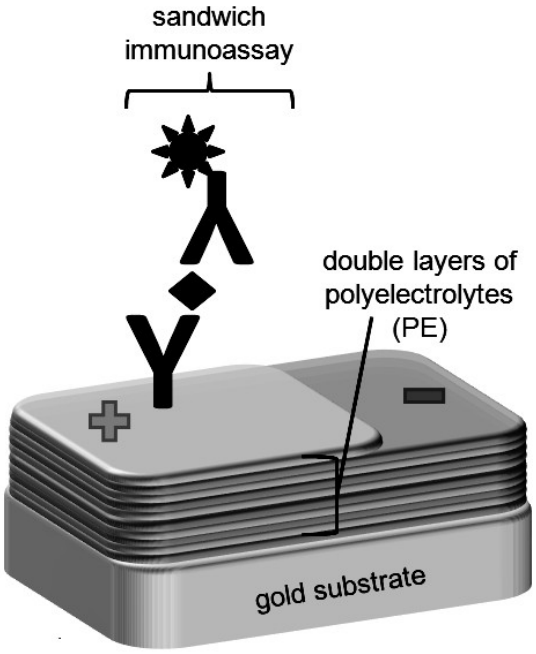

Figure 1: Scheme of the polyelectrolyte multilayer slides.

FINAL CONCLUSIONS

Protein microarrays, one emerging class of proteomic technologies, have broad applications in clinical research and medical diagnostics. Key attributes encompass parallelism, miniaturization and functional integration. Permitting routine multi-analyte detection of relevant biomarkers, protein microarrays promise a boost in knowledge about the different types and states of disease and pave the road to more personalized treatment approaches.

In this thesis a protein biomarker chip for the simultaneous quantification of five melanoma biomarkers in diluted serum is described. Specific prognostic and staging factors such as S100B and vascular endothelial growth factor A (VEGF-A) are analyzed in a panel with disease related inflammatory and immunoregulatory markers IL6, IL10 and CRP. For platform development an epoxy microarray surface was chosen and several assay parameters including antibody print buffer, probe concentration, assay buffer and incubation time were optimized. High test reproducibility (CV < 20%) and weak assay cross-reactivity were achieved. Reliable calibration curves ($R^2 \geq 0.966$) were obtained with an adequate predictive model and assay sensitivities were perfectly comparable to commercial microtiter plate ELISA kits. Advantages of the microarray system over the conventional ELISA test are reduced sample volume and processing time needed to obtain multiple results. The system qualifies as a cost effective and versatile tool as it requires less handling steps, features a decreased consumption of reagents and is readily extendable with additional marker tests.

Though extremely attractive and promising, protein microarrays are faced by a number of challenges. One factor that restricts the applicability of the technology is the limited availability of suitable antibodies for all potential biomarkers. Biomarkers encompass several types of molecules ranging from glycolipids to proteins. Assay recognition elements need to be both highly specific and stable in biological fluids. Although antibodies are the main studied receptors in protein microarray design, they feature some drawbacks: Firstly they tend to denature and lose their structure when heated or exposed to harsh conditions such as changes in pH. Secondly antibodies are produced using animal models through which many antibodies against key antigens are not accessible. Consequently RNA aptamers, which turned out to be both specific and stable in biological fluid, were studied as alternative receptors in this thesis. Both monoclonal antibodies and artificial aptamer receptors were immobilized on a microarray platform to detect CRP in diluted human serum. CRP was detected with high specificity and recoveries between 70% and 130%. In comparison to monoclonal antibodies

aptamers permitted an extended working range from 10 µg/L to 100 mg/L CRP. Furthermore CRP sample testing is simple as only one sample dilution covers the entire relevant analyte concentration range and enables CRP detection in serum samples of low risk patients (1-3 mg/L), high risk patients (> 500 mg/L), and elevated CRP levels (20-350 mg/L).

Another concern for protein microarray technology is sensitivity. Considerable effort is demanded to achieve the sensitivity adequate for routine analysis of relatively low abundance proteins. In this respect a variety of novel chip substrates as well as protein array labels and amplification schemes have been reported in literature. Improved assay performance as a result of superior surface materials was obtained on porous supports, surface enlarging nanostructures, dendrimers, hydrogels and polyelectrolyte multilayers. Amplification can be achieved by enzymatic reactions that lead to the accumulation of colorimetric, luminescent, and fluorescent substrates. Several methods employ coupling of nucleic acids to proteins, and thereby take advantage of the PCR method. Also proximity effects near metallic surfaces and metallic nanostructures were harnessed for signal amplification. In this work a platform is presented that combines a biocompatible polyelectrolyte multilayer for protein immobilisation with metal enhanced signal amplification.

Polyelectrolyte multilayer have proven to be favourable matrices as many immobilized proteins were reported to retain their activity for prolonged times. This effect was frequently attributed to the gel-like environment which keeps proteins hydrated and in a native conformation. Among tested (semi)natural polysaccharides (xanthan, chitosan, carboxymethylcellulose, hyaluronic acid) multilayers composed of xanthan and chitosan performed best in terms of assay sensitivity, spot morphology, fluorescence background and variability (< 10%). Fluorescence signals on gold slides with a 75 nm coating of seven crosslinked polyelectrolyte double layers were up to 50 times higher than on bare glass slides.

The metal substrate associated amplification phenomenon can grossly be explained by the fact that emitted fluorescence light, which is normally scattered and lost through the glass substrate, is reflected back to the detector by the gold mirror. Also both incident and emitted light independently interfere with their reflection from the mirror. In an optimized setup interference leads to signal amplification which is associated with shortened excitation lifetimes and increased quantum yields of the fluorophores.

In comparison to commercial microarray substrates the signal to noise ratio of the presented slides is enhanced by up to factor 11. Furthermore sandwich assays for interleukins 6, 8, 10,

tumour necrosis factor alpha (TNFα), VEGF-A and S100B show working ranges which cover significantly lower concentrations (up to 38 fold). Not limited to these assays, the developed substrates, which combine a biocompatible interface with metal-based signal amplification, are a valuable tool in a variety of biosensor applications.

In protein microarray development there is an increasing demand for selective and specific protein immobilization techniques. Especially small and delicate proteins require an approach that minimizes structural perturbation and maximizes activity. Also functional and structural studies often demand uniform orientation of immobilized probes. Affinity binding is an attractive strategy to reach these aims. The selection of functionalized substrates for affinity coupling includes streptavidin-coated slides, biotin-coated slides, DNA-modified substrates and Ni-slides. Ni-affinity substrates rely on the interaction between Ni^{2+} ions and poly-histidine tags which can be genetically engineered into protein probes at determined positions thus assuring defined protein orientation. The majority of microarray affinity substrates are based on nitrilotriacetic acid and its derivates as Ni^{2+} chelators. Gold surfaces modified with self-assembled monolayers (SAMs) are frequently employed in the preparation of the slides.

In contrast, in this work iminodiacetic acid and carboxymethyl amino acid-derivates are employed as alternative chelators in the fabrication of affinity substrates. The preparation process is based on simple chemical modification of polymeric coatings and thus avoids expensive SAM chemistry as well as the use of chemicals that have to be obtained via multistep organic synthesis. High binding selectivities >95% for hexa-histidine tagged proteins were obtained and signal strengths were higher than on commercial reference products (at least factor 2 up to factor 6).

Ongoing research in the field of protein biomarker arrays aims at combining different assay formats, e.g. sandwich immunoassays and binding inhibition immunoassays, on one chip platform. Different assay formats better account for the broad range of analyte characteristics and thus allow the simultaneous measurement of both small and large, low abundance and highly concentrated proteins. In implementing the new assays oriented probe immobilization can be a valuable tool to enhance test variability and sensitivity. Also new microarray tests may profit from the use of aptamers, as these highly stable and specific recognition elements can be obtained in a wide range of affinities for virtually any target molecule. Finally signal amplification strategies aid in measuring even lower protein concentrations and enable an early detection of pathological markers.

Curriculum Vitae

Persönliche Daten

Name	DI Patrick Domnanich
Anschrift	Arakawastr. 6/2/25, A-1220 Wien
Staatsbürgerschaft	Österreich
Geburtsort und -datum	Wien, 15.05.1983

Ausbildung

10/2007-	**Doktoratsstudium** der technischen Wissenschaften, Technische Universität Wien **Dissertation** (Dr. Claudia Preininger): "From Chip Surface to Signal Amplification: Protein Microarrays for Disease Biomarker Detection"
10/2001-09/2006	**Studium der Technischen Chemie**, Technische Universität Wien **Diplomarbeit** (Prof. Robert Mach): "Cloning and Characterisation of G-protein-coupled Receptors in *Trichoderma atroviride*" **Abschluss** mit ausgezeichnetem Erfolg: Diplom-Ingenieur
06/2001	**Matura** mit ausgezeichnetem Erfolg
1998-2001	**Bundesgymnasium und Gymnasium** Wien 23, Draschestr. 90-23, 1230 Wien

Auszeichnungen

9/2009	Best Student Project Award, Advanced Study Course on Optical Chemical Sensors (ASCOS) VII, Madrid, 26.08-3.09.2009
9/2008	Best Student Project Award, ASCOS VI, Graz, 31.08-6.09.2008
12/2007	Würdigungspreis des Bundesministers für Wissenschaft und Forschung für die besten Absolventen eines Jahrganges
11/2006, 2005, 2004, 2003, 2002	Leistungsstipendien der Fakultät für Technische Chemie
03/2005, 2006	Stiftungsstipendien des Universitätsdirektors (TU Wien)

Peer-reviewte Publikationen

P. Domnanich, U. Sauer, J. Pultar, C. Preininger, Protein Microarray for the Analysis of Human Melanoma Biomarkers, Sensors & Actuators B, 139 (2009), 2-8.

J. Pultar, U. Sauer. P. Domnanich, C. Preininger, Specific on-chip Detection of CRP using Aptamer Microarrays for Extended Working Range, Biosensors and Bioelectronics, 24 (2009), 1456-61.

K. Brunner, M. Omann, M.E. Pucher, M. Delic, S.M. Lehner, P. Domnanich, K. Kratochwill, I. Druzhinina, D. Denk, S. Zeilinger, Trichoderma G Protein-coupled Receptors: Functional Characterisation of a cAMP Receptor-like Protein from *Trichoderma atroviride*, Curr Genet., 54 (2008), 283-99.

September 2010